DANSK VANDBYGNINGSTEKNISK SELSKAB
DANISH SOCIETY OF HYDRAULIC ENGINEERING

v/ Helge Gravesen, Carl Bro as, Granskoven 8, 2600 Glostrup
Tlf. +45 4348 6328, Fax +45 4363 6567, email: hlg@carlbro.dk,
Home page: www.Dansk-vandbygning.dk

22.01.2003
HlG

Seminar on
Dynamic loads to stone bed foundations and soils
– from offshore wind turbines to earthquake
Organized by Danish Society of Hydraulic Engineering (DVS)
and Danish Geotechnical Society (DGF)

Time: Thursday 20 March 2003, 12.30 – 20.00 hrs
Language: English
Auditorium 81, Building 116, DTU, 2800 Lyngby

12.30 – 12.40	Helge Gravesen, Carl Bro and DTU: Introduction
Subject 1: Stone bed foundation of gravity structures exposed to dynamic loads	
12.40 – 13.10	Ole Steensen-Bach, Carl Bro: Stone beds at the wind turbine foundations at Middelgrunden
13.10 – 13.40	Jørgen Lorin Rasmussen, Rambøll: Brainstorming on potential foundation concepts to the foundations of the wind turbines at Nysted/Rødsand
13.40 – 14.10	Per Sandgaard Kristensen, Cowi: Experiences on stone beds at the East and West bridge of Storebælt
14.10 – 14.20	Jørgen Lisby, Per Aarsleff: Construction and quality control of the stone beds for the foundations of the wind turbines at Nysted/Rødsand
14.20 – 14.50	Coffee break
Subject 2: Pore pressure and liquefaction	
15.00 – 15.40	Mutlu Sumer and Jørgen Fredsøe, MEK, Coastal and River Engineering Section: Research on liquefaction around marine structures at DTU (incl a brief presentation of the LIMAS project,
15.40 – 16.20	H. F. Burcharth, Aalborg Universitet: Earthquake design for port structures
16.20 – 16.40	Break
16.40 – 17.20	Niels- Erik Ottesen Hansen, LicEngineering/Mutlu Sumer, MEK: Consequences to coastal structures of the 1999 Kocaelli, Turkey earthquake
17.20 – 18.00	Rasmus Miller / Niels- Erik Ottesen Hansen, LicEngineering: Bearing capacity of sand during partial drained conditions caused by impulsive loads (from ship impact to earthquake)
18.15 – 20.00	Dinner

Best regards

Helge Gravesen
chairman of DVS

Carsten Sørensen
chairman of DGF board

Selected articles and copies of overheads / power point presentations will be available in a binder to the participants.

Seminar : Dynamic loads 20 march 2003

DTU, Auditorium 81, Building 116

Nr	Fornavn	Efternavn	Company	Speaker
1	Helge	Gravesen	Carl Bro A/S	Yes
2	Ole	Steensen-Bach	Carl Bro A/S	Yes
3	Per Sandgaard	Christensen	Cowi A/S	Yes
4	Jørgen Lorin	Rasmussen	Rambøll	Yes
5	Niels-Erik	Ottesen Hansen	LicEngineering	Yes
6	Jørgen	Fredsøe	MEK, Coastal and river section	Yes
7	Mutlu	Sumer	MEK, Coastal and river section	Yes
8	Jørgen	Lisby	Per Aarsleff A/S	Yes
9	Hans Falk	Burchardt	Aalborg Universitet	Yes
10	Henrik S.	Hansen	Carl Bro A/S	
11	Frederik	Knudsen	Carl Bro A/S	
12	Arne Buhl	Petersen	Carl Bro A/S	
13	Casper	Paludan-Müller	Cowi A/S	
14	Jens Brink	Clausen	Geo	
15	Lindita	Kellezi	Geo	
16	Peter B.	Hasbo	Hasbo A/S	
17	Jes	Hardeman	Lesanco Aps	
18	Flemming	Hey	Lesanco Aps	
19	Kjartan	Gislason	LicEngineering	
20	René S	Lorenz	LicEngineering	
21	Bjarke	Pedersen	LicEngineering	
22	Kaan	Sumer	LicEngineering	
23	Hanne	Grindsted	Moe & Brødsgaard	
24	Henrik Lund	Rasmussen	NCC Danmark Anlæg	
25	Anders Tovsig	Andersen	Per Aarsleff A/S	
26	Jan	Boldsen	Per Aarsleff A/S	
27	Jesper Dyhrfjeld	Christensen	Per Aarsleff A/S	
28	Thomas	Gribsholt	Per Aarsleff A/S	
29	Hans Kristian	Havbro	Per Aarsleff A/S	
30	Jan	Hockerup	Per Aarsleff A/S	
31	Jesper K	Jacobsen	Per Aarsleff A/S	
32	René Mølgaard	Jensen	Per Aarsleff A/S	
33	Ole	Møller	Per Aarsleff A/S	
34	Jens Erik Ellergaard	Nielsen	Per Aarsleff A/S	
35	Ole	Rask	Per Aarsleff A/S	
36	John	Madsen	Peter Madsen Rederi A/S	
37	Jesper	Pedersen	Peter Madsen Rederi A/S	
38	Erik	Brenneche	Port of Esbjerg	
39	Kjeld Dahl	Sørensen	Port of Esbjerg	
40	Mikkel	Kjær Jensen	Rambøll	
41	Stefan	Carstensen	Studerende	
42	Thomas Lykke	Andersen	AAU, PhD	
43	Anders	Augustesen	AAU, PhD	
44	Einar	Helgason	AAU, PhD	

Nr	Fornavn	Efternavn	Company	Speaker
45	Lars Bo	Ibsen	AAU	
46	Morten	Kramer	AAU, PhD	
47	Morten	Liingaard	AAU, PhD	
48	Claus	Gormsen	NIRAS	
49	Svend	Krabbenhøft		
50	Erlan	Nanfeldt		
51	Ib	Sørensen		

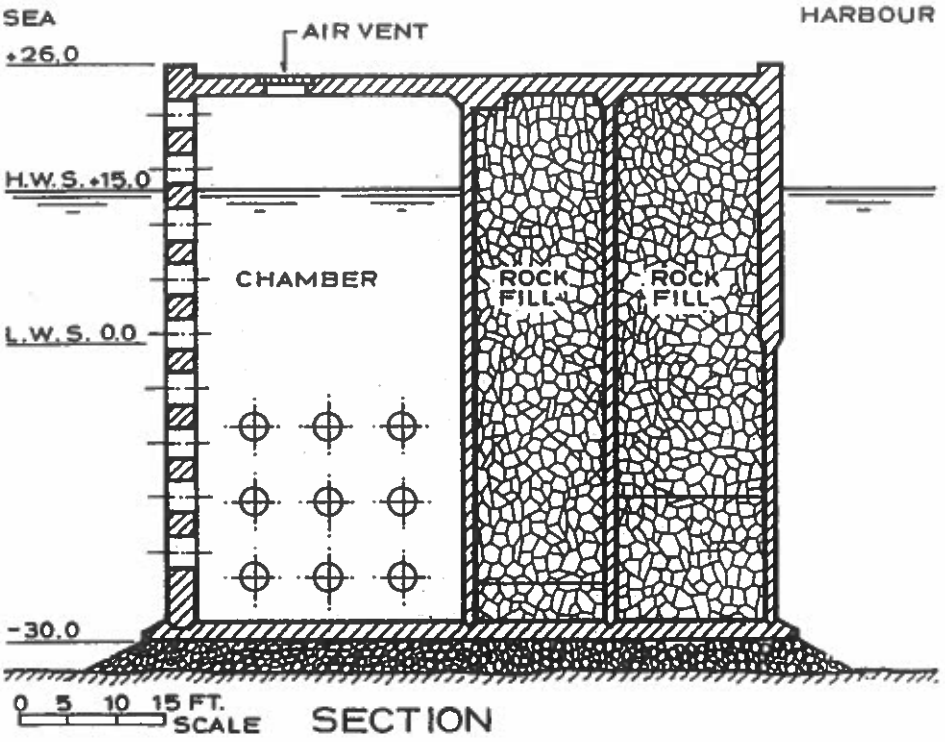

Fig. 1 Baie Comeau Breakwater

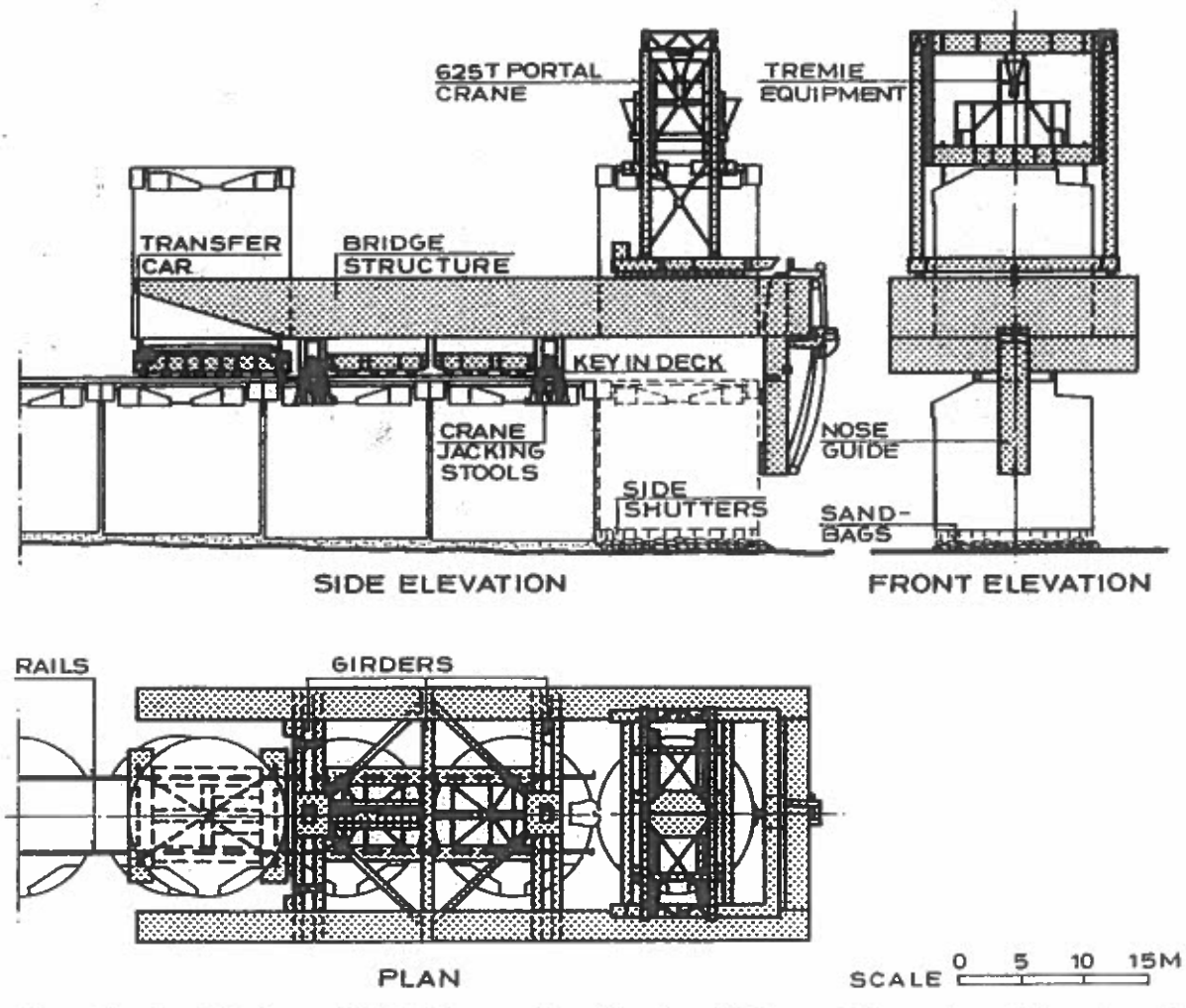

Fig. 2 Placing of 600-Tonne Nonfloating Caisson. Reproduced by permission of H. Vandervelden

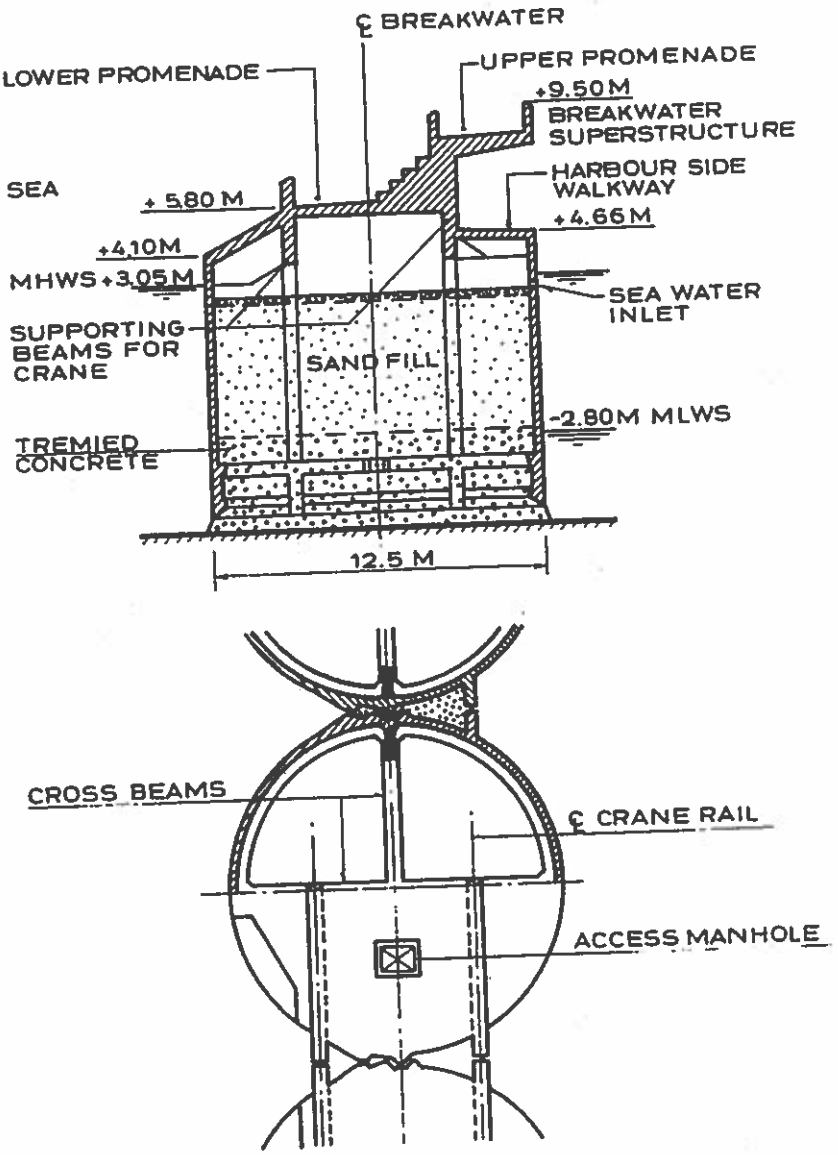

Fig. 3 Brighton Marina Breakwater

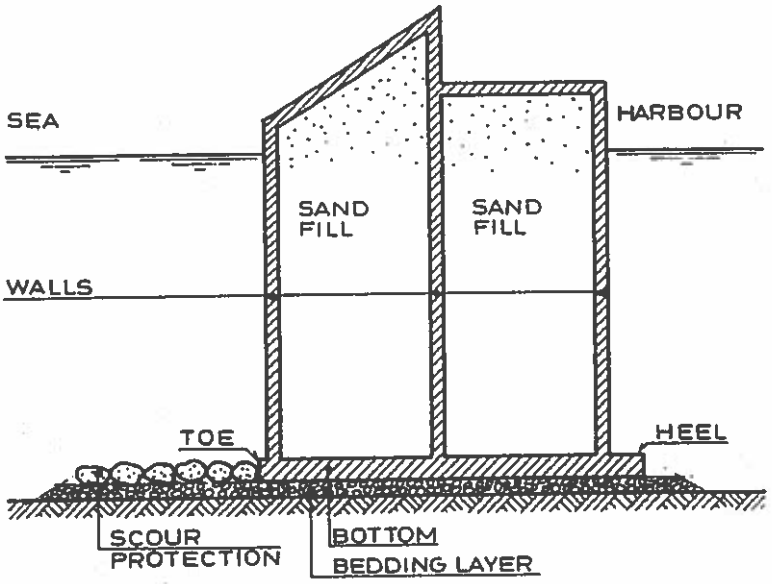

Fig. 4 Bedding Layer Foundation for Caisson

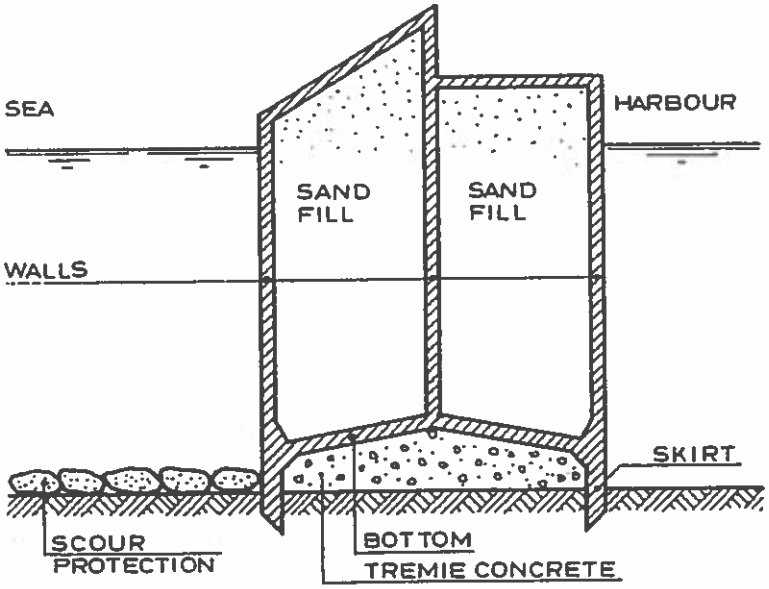

Fig. 5 Tremie Concrete Foundation for Caisson

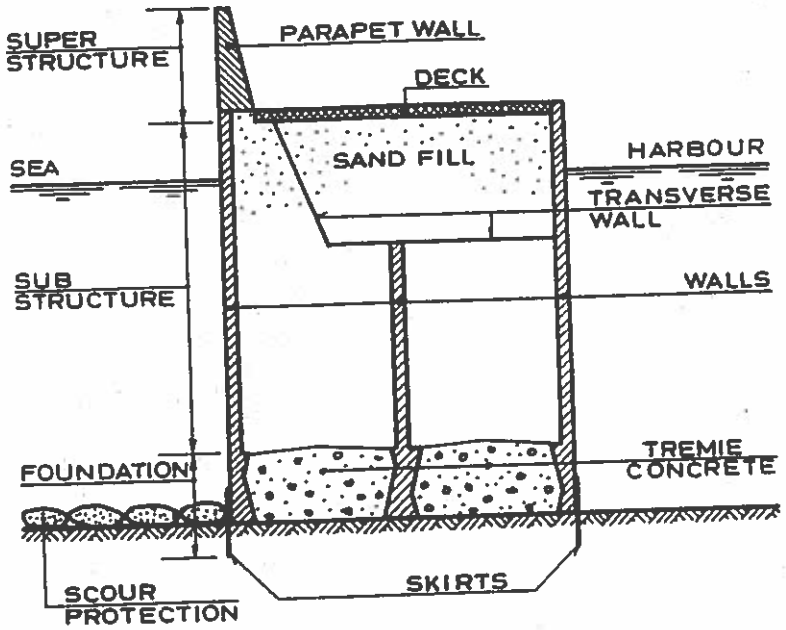

Fig. 6 (a) Typical Caisson Breakwater Cross Section

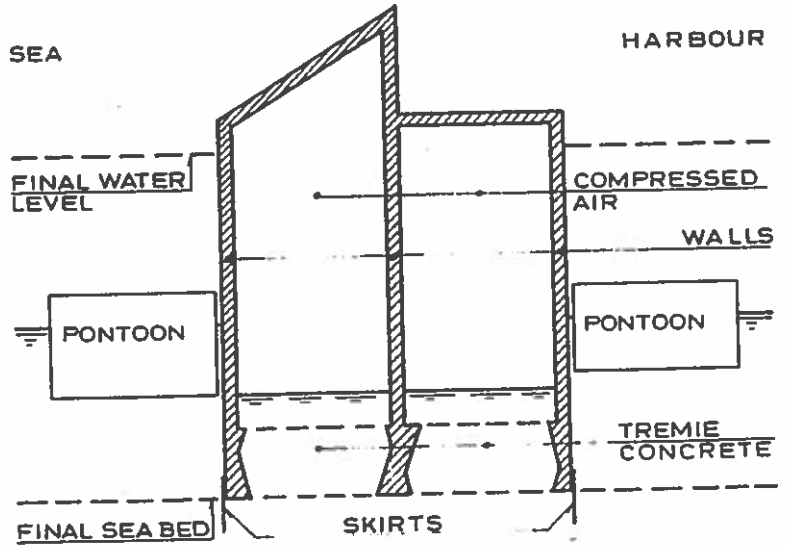

Fig. 7 (c) Caisson without Bottom. Flotation Provided by Pontoons

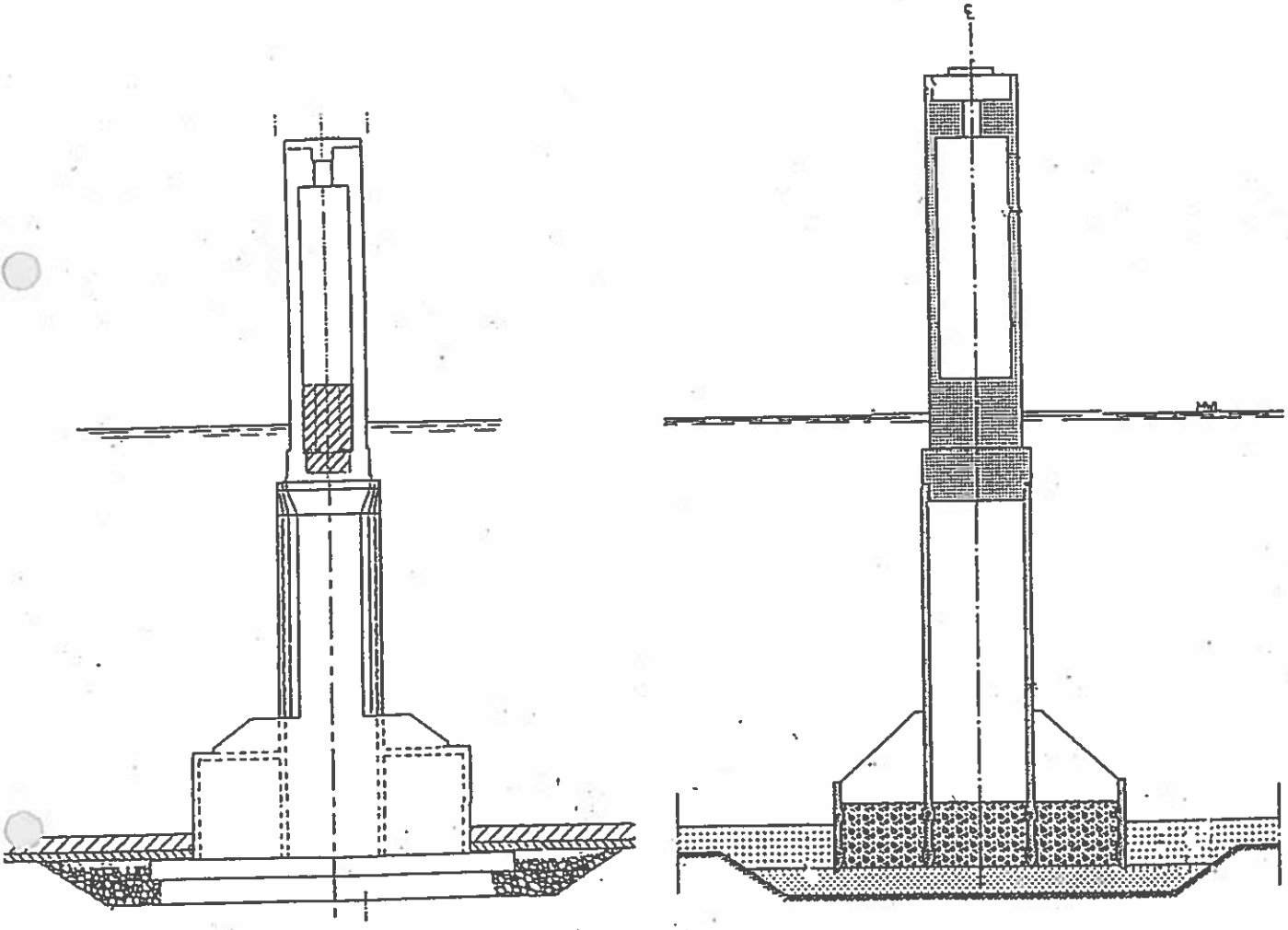

a) Plane base plate

b) Open caisson

Fig. 8 Caisson with plane base plate and open caisson with in-situ casting of tremie concrete

Storebælt West Bridge, Design alternatives

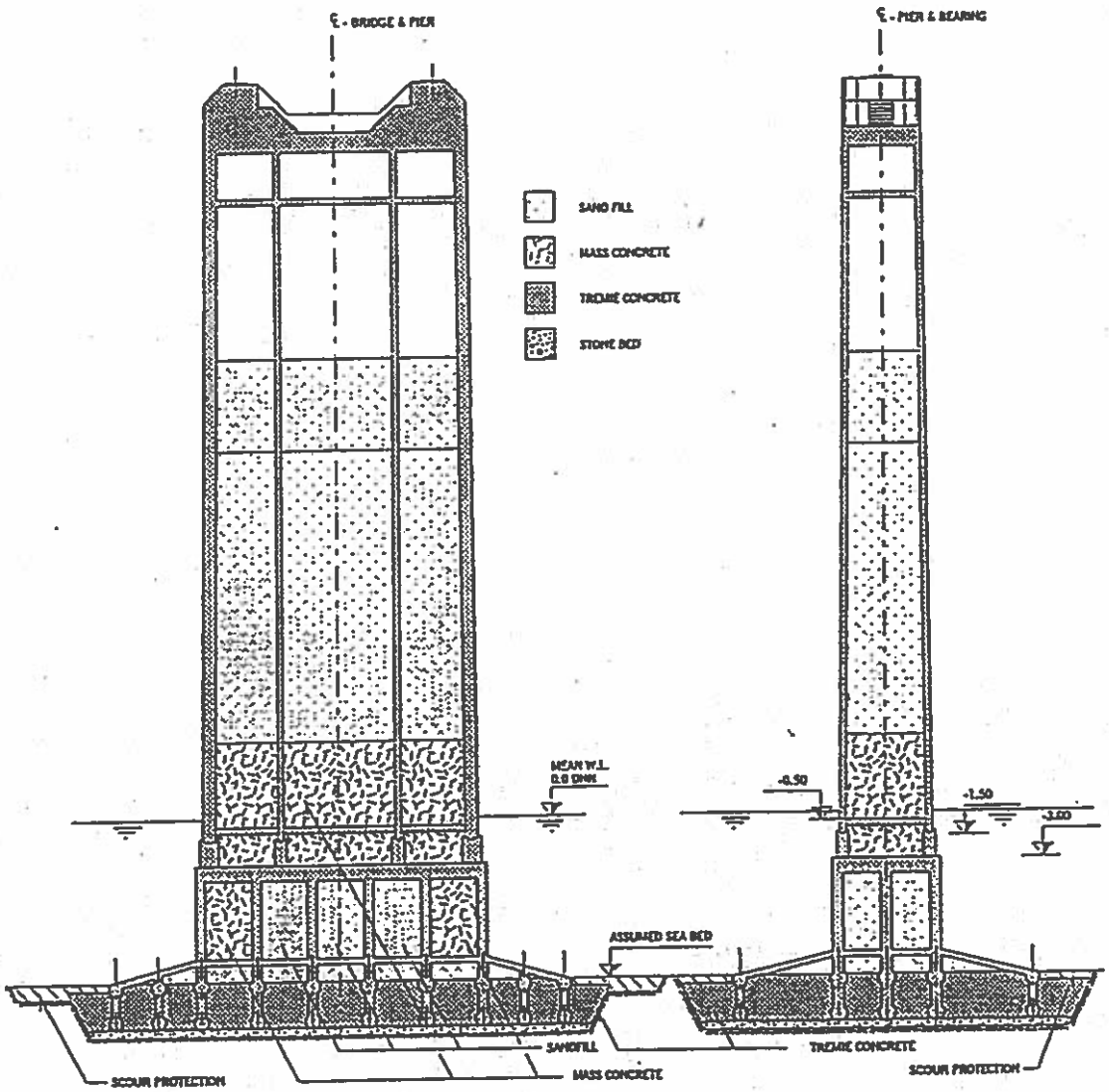

Fig. 9 Preliminary design of bridge pier for approach bridge
(Oresund, Tender)

Stone beds at the wind turbine foundations at Middelgrunden

Compaction Control of an Offshore Stone Bed

Jens Ole Steensen-Bach
Carl Bro as

Seminar on
Dynamic loads to stone bed foundations and soils
– from offshore wind turbines to earth quake

Danish Society of Hydraulic Engineering (DVS)
Danish Geotechnical Society (DGF)
20 March 2003

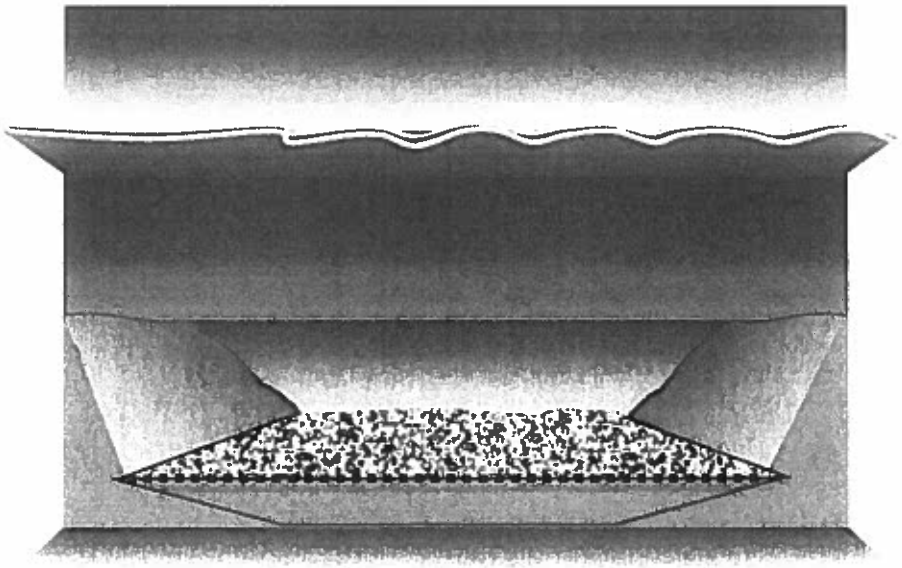

Compaction Control of an Offshore Stone Bed

Stone beds at the wind turbine foundations at Middelgrunden

Jens Ole Steensen-Bach
Carl Bro as

SUMMARY: The static and dynamic properties of crushed rock beneath the footings of offshore windmills have been investigated. After free-fall dumping, the crushed rock has been compacted by a large plate vibrator. The density of the uncompacted stone bed has been derived from measurements on a simulated stone bed and from plate load tests on an actual footing site. A simple model was established for the particular compaction equipment used, correlating void ratio after compaction to void ratio prior to compaction and settlement of the vibrating plate. Static strength and deformation parameters as function of void ratio and stress level have been obtained from large-scale triaxial tests. Accumulating deformations due to cyclic loading has been assessed using the results of cyclic consolidation tests. A simple model correlating void ratio and load amplitude to rate of strain increment was established. The obtained soil models comprised the primary basis for acceptance of the executed compacted stone beds.

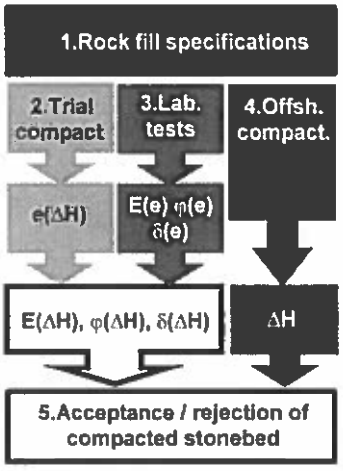

1. INTRODUCTION

For shallow water depths stone beds are often applied as base for footings. If properly designed, the stone beds may serve several useful purposes like soil improvement, levelling of seafloor, erosion protection etc.

In order to accept a stone bed for footing installation, the final stone bed shall have sufficient bearing capacity and accumulation of deformations due to cyclic loading shall be shown to be within acceptable limits. Requirements to the rock material may be formulated in terms of a grain size distribution interval and a relative density, as built-in, or in terms of engineering requirements like friction angle, φ', Young's Modulus, E' and plastic deformations. Due to the stress dependency of φ' and E' requirements are highly project specific.

As strength and deformation properties of crushed rock primarily depends on stress level and void ratio, the determination of the density of the compacted stone bed and the formulation of a mathematical model correlating void ratio and strength / deformation behaviour are vital elements for acceptance of the stone bed. Control of the density of a compacted rock layer of thickness 0.5-1.0 m may be difficult under offshore conditions. In order to be operational a simple technique is required that enables a quick acceptance or rejection of an executed compaction. This is the topic of this paper. It is important to bear in mind that the reported investigations aimed at obtaining an operational way to conservatively estimate the properties of the stone bed during construction, and will hence, include some shortcomings from a scientific point of view.

2. MIDDELGRUNDEN SOIL CONDITIONS

Soil investigations comprising geophysical survey, geotechnical borings, vibrocorings and CPT's revealed that the geology on the locations of the 20 windmills at Middelgrunden comprises typically 0-2.5m fill on top of very stiff clay/sand till with c_u=300kPa (7 mills) or intact/glacially disturbed Limestone H1 with unconfined shear strength q_{uc}=160-370kPa (13 mills).

Unfortunately the sample quality from the geotechnical borings was so poor that no material was found suitable for strength- and deformation testing in the laboratory.

Static and cyclic triaxial tests were limited to testing Limestone samples from vibro corings. Evaluation of the cyclic properties of the clay / sand tills was based on experience from other projects.

3. DESIGN REQUIREMENTS

The foundations were designed with respect to traditional bearing capacity, pure sliding and accumulated deformations in the form of tilt of the towers.

Design was carried out for each of the two soil cases (1) clay/sand till and (2) Limestone H1.

A maximum accumulated tilt of 0.5° after 50 years was acceptable. Of these α=0.25° was allowable to be due to 50 years of cyclic loading of the soil (α_{soil}) and stone bed (α_{rock}).

The remaining 0.25° was reserved as tolerance for the foundation installation.

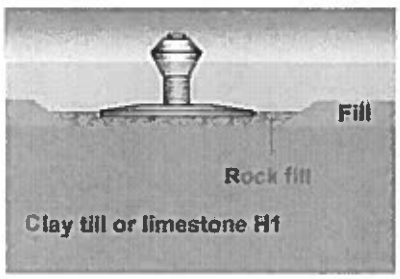

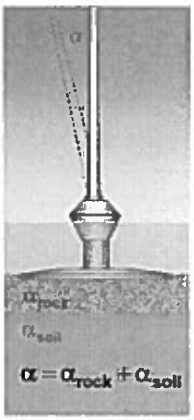

	Bearing	Sliding	Tilt
E (MPa)	40	40	-
φ' (°)	40	50	-
$\alpha_{50\ yrs}$ (°)	-	-	0.25

Reference (examples)	Triax.	Cons.	I_d (%)
Holtz et al (1956)	x		50-90
Marsal (1967)	x		65
Boughton (1970)	x		75-100
Marachi et al (1972)	x		77-85
Valstad et al (1975)	x	x	0-93
Al-Husaini (1983)	x		75-100
Idraratna et al (1993)	x		62-65
Idraratna et al (1998)	x		46-63
Steenfelt et al (1994)	x		40-77
Horn et al (1995)	x		50-100
Yasuda et al (1997)	x		26-70

4. ROCK FILL SPECIFICATION

4.1 Desk study

Initially a desk study of available data on rock fill properties was initiated in order to formulate simple requirements for the rock fill to be used below the wind turbine foundations. In the literature many references provides data regarding stiffness, E, and the angle of friction, φ'. on coarse grained materials like rock fill. Although discussions has been (and still may be) ongoing regarding the use of relative density as a parameter governing the engineering properties of rock fill, relative density is commonly used:

$$I_d = \frac{e_{max} - e}{e_{max} - e_{min}}$$

Using the triaxial data presented by Valstad & Strøm (1975) for Svartevann Damm rock fill the Young's modulus for compacted rock fill seems to be conservatively described by:

$$E_r = 15MPa \cdot I_d \cdot \sqrt{\frac{\sigma'_{cell}}{1kPa}}$$

where σ'_{cell} is the cell pressure in triaxial compression tests.

Analysing 182 triaxial compression tests reported in the literature (the six test series numbered in the above table weighted equally) yields the following relationship between friction angle, φ', relative density, I_d and triaxial cell pressure, σ'_{cell}:

$$\varphi'_{s,max} = 36.2° + 3.5° \cdot I_d \cdot \left(10 - \ln\left(\frac{\sigma'_{cell}}{1kPa}\right)\right)$$

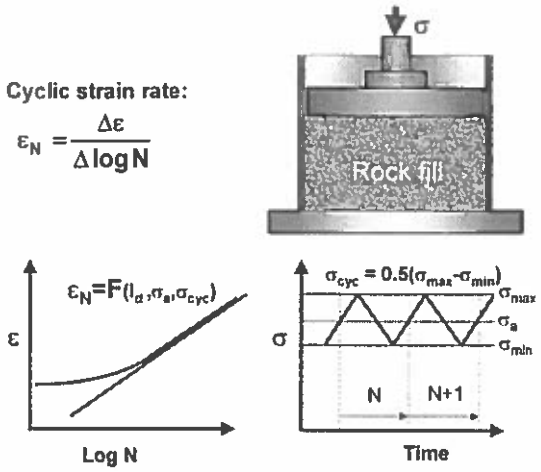

When it comes to cyclic properties of rock fill, literature is significantly more limited. Dynamic/cyclic tests have primarily been aimed at investigation of liquefaction, damping and dynamic G-modulus. For evaluation of accumulation of deformations only data for Storebælt East Bridge rock fill (Horn & Christensen, 1995) was found useful. The present analysis of these data indicate that for $I_d \geq 0.6$ (corresponding to the lowest relative densities investigated) strain accumulation during cyclic loading may be described by:

For $\sigma_a \leq 600\text{kPa}$:

$$\varepsilon_N \leq \left(k_1 + k_2 \frac{\sigma_a}{1\text{kPa}}\right)(1 - I_d)\sqrt{\frac{\sigma_{cyc}}{1\text{kPa}}}$$

$k_1 = 0{,}05\%, k_2 = 0.00018\%$

For $\sigma_a > 600\text{kPa}$:

$$\varepsilon_N \leq 0.16\% \cdot (1 - I_d)\sqrt{\frac{\sigma_{cyc}}{1\text{kPa}}}$$

4.2 Specifications

Using the above models for E, φ' and ε_N the design requirements was found fulfilled for $I_d \geq 0.6$ The specifications for the rock fill to be used in the stone beds below the wind turbine foundations at Middelgrunden was thus formulated in terms of

- end-specification $I_d \geq 0.6$
- a range of allowable grain size distribution curves
- grain shapes (L/B>0.5 and H/B>0.5)

All the above requirements are comparable with rock fill used for Storebælt Eastbridge.

5. MIDDELGRUNDEN ROCK MATERIAL

5.1 Grain size, density and shape

The parent rock of the investigated crushed rock is granite. The rock fill comprises 0-80 mm angular, equant shaped grains.

The specific gravity of the rock fill is G_s=2.65.

The rock comprised two batches of which the first batch contained a significant amount of sand and clay (not rock flour) adhering to the rock grains. The "dirty" rock was split into two portions: one portion with removal of soil-cake by washing (denoted material 2), and one portion of unaltered material (material 1). Material from the second batch is denoted material 3.

During the course of construction several specimens of the materials 1,2 and 3 were sampled and sieved.

5.2 Maximum and minimum void ratio

The minimum and maximum void ratios have been determined using a modified version of BS 1377 Part 4 (density index). A 500 mm high, 480mm diameter rigid steel cylinder was used for the density determinations.

For determination of maximum void ratio no energy has been applied, whereas minimum void ratio have been obtained by preparing the specimen in six layers each tamped in 3 minutes by a 350N drop hammer (6 tests). In two cases maximum density was determined by vibratory compaction.

On average the minimum and maximum void ratios were found to

e_{min}= 0.394 and e_{max} =0.732

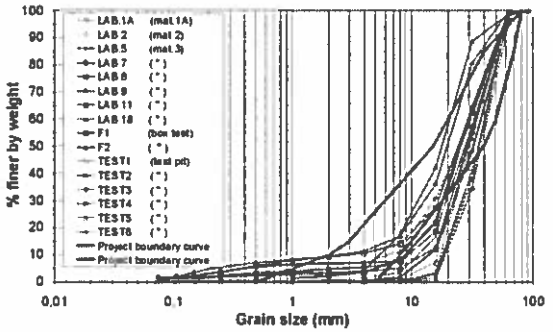

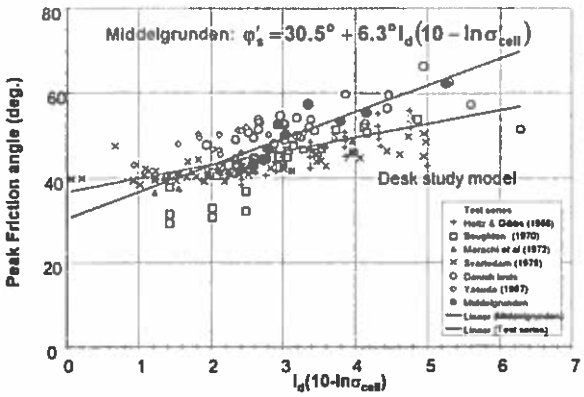

5.3 Friction angle, φ'

Triaxial tests were carried out in the large-scale triaxial equipment at the Danish Geotechnical Institute The apparatus handles cylindrical specimens of height to diameter ratio H/D=0.5m/0.5m = 1 with smooth ends.

Three multiple triaxial tests have been carried out, each having a shear phase at σ_3 = 10, 50 and 100 kPa. The mobilized strength in each shear tests has been determined corresponding to a strain increment of 1% and at peak (maximum).

The secant angle of friction has been found, in terms of the "Kerisel parameter = etanφ_s" as function of the confining stress. In the evaluation of the compacted rock fill the 1% strain increment equation has been used:

$$e\tan\varphi'_{1\%} = 0.87\left(\frac{\sigma'_{cell}}{1kPa}\right)^{-0.12}$$

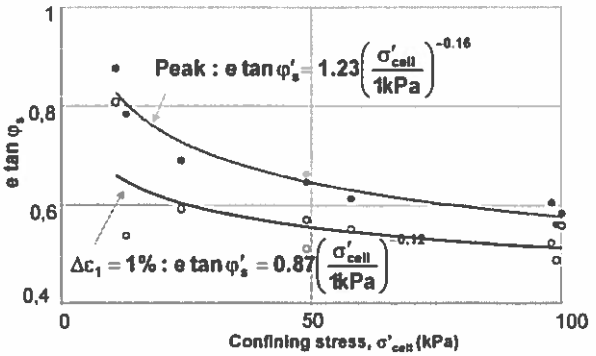

5.4 Cyclic strain rate, ε_N

The cyclic consolidation tests were carried out in the large-scale oedometer equipment at the Danish Geotechnical Institute (H/D = 0.5m/0.5m). The apparatus is particularly suited for monotonic or cyclic loading of coarse materials.

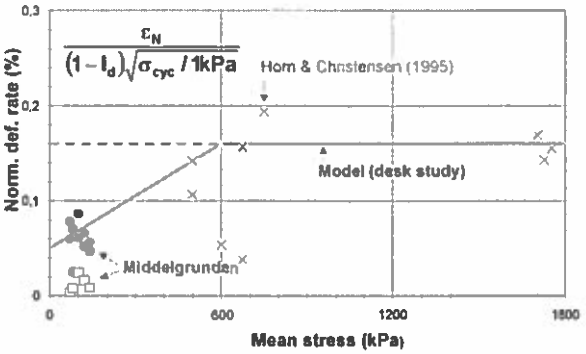

Three cyclic consolidation tests have been carried out on specimens of material 1 and 3.

Regression analysis results in the following equation to predict rate of strain increment as function of maximum cyclic stress and start void ratio of each cyclic test level.

For $\sigma_{max} = 60 - 140kPa$ & $\sigma_{min} = 60kPa$:

$$\varepsilon_N = \left(\frac{\sigma_{cyc}}{1kPa}\right)\cdot 3\cdot 10^{-5}\% \cdot \exp(12\cdot[e-0.31])$$

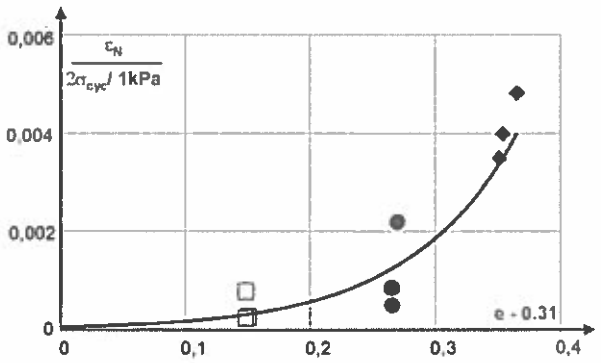

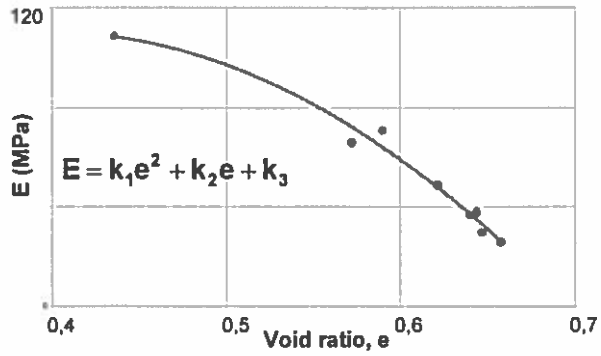

5.5 Stiffness, E

The Youngs Modulus, E, was determined by plate load tests in trial compactions (described subsequently) using B=0.36m.

$$E = -1245e^2 + 988e - 85.5 \quad \text{(MPa)}$$

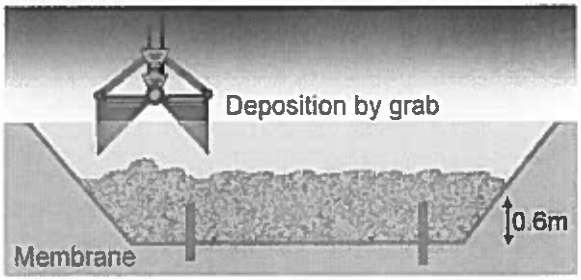

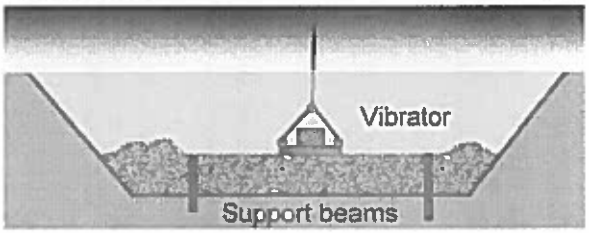

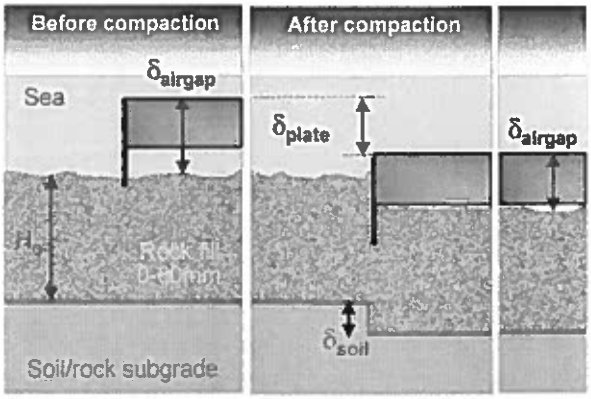

6. TRIAL COMPACTIONS

6.1 Trial pit – density measurement

The stone beds are to be formed by dumping the rock fill from a grab at a height of 0.5-1.0 m above the excavated seafloor. Trial dumpings using Material 3 were made in the harbour and in a submerged test pit on land.

In two trial dumpings in the harbor, the crushed rock was dumped into a rectangular text box LxBxH = 2.2mx1.4mx0.65m and the top leveled by a diver. Measurements of the density of the total sample in the box indicated a very loose deposit, I_d = 0.15-0.2.

In order to obtain a better estimate on the void ratio of the uncompacted rock fill two trial dumpings were made in a submerged trial pit area LxB = 25mx15m.

The trial stone bed was leveled off leaving a thickness 0.5-0.7m. A total of 10 measurements were carried using the "water method" (a membrane is placed in the excavated hole a filled with water). The mean value and standard deviation for material 3 was found to be:

$$e_{om} \pm s(e_o) = 0.654 \pm 0.068$$

6.2 Trial pit – compaction tests

It was decided to accept/reject compactions based on an assessment of the void ratio from the settlement of the vibrator plate after termination of compaction. For this purpose trial tests were initiated leading to a simple estimation of the void ratio,e_c, after compaction.

The settlement of the vibrator plate during compaction was assumed to comprise of three contributions (1) vertical compaction of the rock cushion, (2) horizontal compaction of rock material surrounding the vertical column below the compaction equipment due to forced-out material from the column, and (3) punching of the subsoil, δ_{soil}.

Compaction tests were performed in the test pit trial dumping using 1.5m by 2.1m and 2.1m by 2.6m rectangular plates, as well as other less effective (and hence discarded) compactors, tested at various frequencies.

During compaction the plate settlement was recorded and after compaction a double determination of the void ratio was carried out within the compacted area. Measurement of the surface of the stone bed outside the compacted area showed no change (i.e. no heave or settlement of the original uncompacted rock). The punching effect into the natural soil of the test pit below the stone bed was also measured by careful removal of the stone bed after testing.

It was found that after 10 seconds additional compaction time only lead to increasing punching into the subsoil. As punching effects may destroy the properties of the subsoil, it was decided to use a compaction time of 10 seconds. The following model was developed to predict void ratio after compaction. $e_{c,}$.

$$e_c = e_o - \frac{\Delta H}{H_o}(1+e_o) - (k_1 e_o - k_2)\Delta H$$

$$\Delta H = \delta_{plate} - \delta_{soil} - \Delta\delta_{airgap}$$

For 2.1mx2.6m plate compacting at 1400rpm in 10 seconds k_1= 0.046 and k_2=0.044.

The model requires information regarding the initial void ratio, e_o, the initial thickness of the uncompacted layer, H_o, and the settlement of the compactor, ΔH, corrected for airgap and punching of rock fill into the subsoil.

The compaction tests showed that for 2.1m x2.6m plate compacting at 1400rpm in 10 seconds, the punching of the rock fill into subsoil stiffer than tested in the trial pit (which is the case for Middelgrunden) will be less than $\delta_{soil} \leq 1$cm.

The airgap measured before and after compaction. The difference in the measurements defines $\Delta\delta_{airgap.}$

7. FIELD COMPACTION

7.1 Post excavation

After excavation to the target depths (below the fill) control investigations was carried out in order to verify that the soil conditions (geology and strength) were as anticipated in design.

The thickness of the mud/sand layer on top of the intact soil was measured as well and in the cases where it exceeded a thickness of 5cm the bottom was cleaned up.

Prior to dumping of rock fill by grab, the bottom levels of each excavation was measured

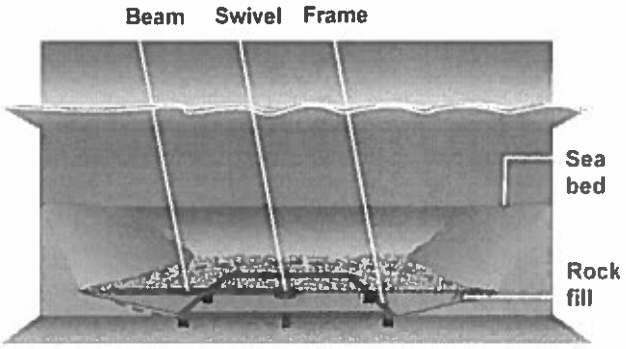

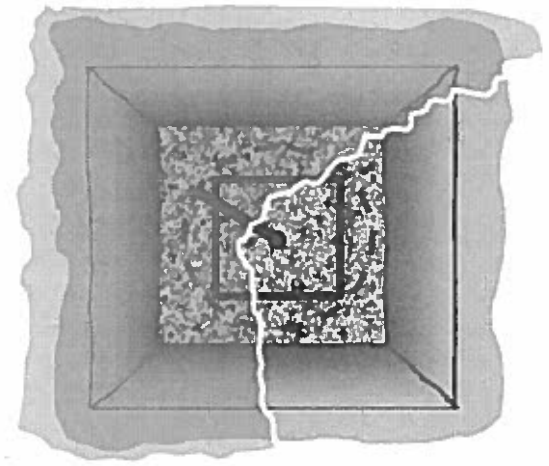

In order to level the uncompacted rock fill prior to compaction, a system comprising a 11mx11m steel frame supporting a 20m long leveling beam rotating on a central swivel was installed in the rock fill.

7.2 Compaction

Compaction was carried out for the rock fill covering the outer 4m ring below the footing, using the 2.1mx2.6m plate.

The outer 4m ring was split into two rings, each comprising 16 compaction fields. In each compacted rock fill ring approximately the settlement of the vibrator plate after compaction was carried out in approximately 10 of the 16 fields.

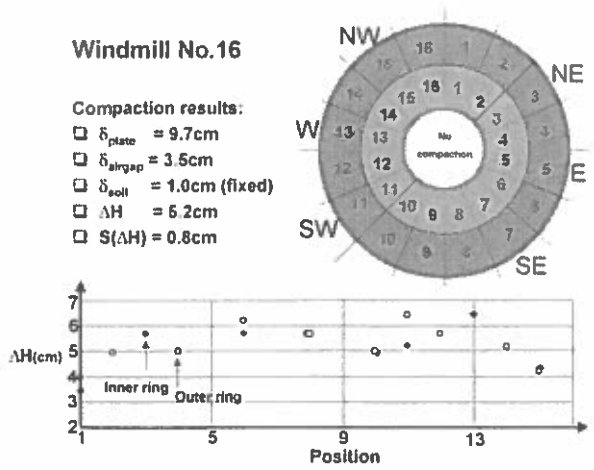

The mean settlement, ΔH_m, and the standard deviation, s(ΔH) , was calculated for each site using all site field measurements. The final thickness of the 20 stone beds (all compacted in rings) below the foundations varies from 0.55m to 1.72m with an average of 0.82m and a standard deviation of 0.25m.

7.3 Acceptance of compaction

The compacted stone beds were accepted or rejected on basis of the conformity with the design requirements of the static and dynamic properties as calculated by the models for E, φ and accumulated deformations using $(e_o)_c$ and the relevant stress level for the coming structure.

A conservative approach was adopted by using modified input values the compaction model:

$$(e_o)_c = e_{om} + s(e_o)$$
$$\Delta H_c = \Delta H_m - s(\Delta H)$$

e_o+s(e_o) (input)	ΔH-s(ΔH) (input)	e_c (calc.)	$\Sigma\delta_{50\,yrs}$ (calc.)	φ'_s (calc.)	E (calc.)
0.722	4.4cm	0.590	5cm	44.3°	62MPa
			ok	ok	ok
Design			<5.6cm	>40°	>40MPa

	$\delta_{4\text{-}32mm}$	$\delta_{0\text{-}80mm}$	$\delta_{clay\ t.}$	$\delta_{limest.}$	$\Sigma\delta_{50\,yrs}$
Clay T.	1cm	0.9cm	3.1cm	0	5cm
Limest.	-	-	-	-	-

Example. Windmill No.16

7.4 Refilling of compaction voids

After compaction of each field the vibrator plate was removed and a steel frame placed on top of the void left by the plate.

The frame rests on all four sides at the original rock fill level (corresponding to final level) and is fixed to a central swivel allowing the frame to be rotated around the foundation center for easy positioning. The frame allows for refilling rock material into the compaction void. Subsequent leveling of the refill is performed within the frame.

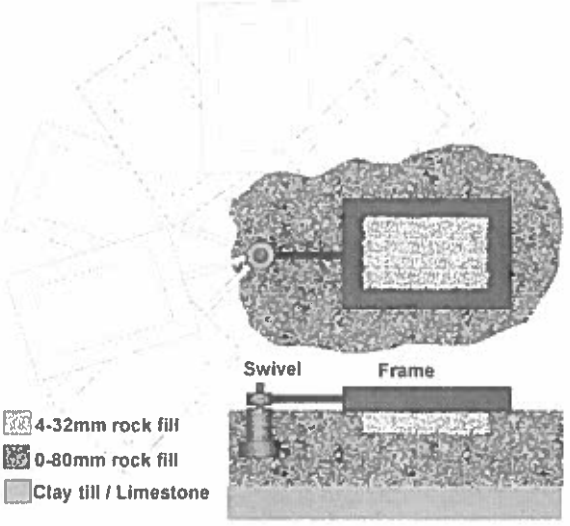

Compaction is continued at the next field after completion of the refilling operation in the previously compacted field. The refilling rock material has a grading 4-32mm. The refilled material is not compacted. Accumulated strain contribution of a refilled layer up to 10cm thickness has been assessed to be $\delta_{4\text{-}32mm} \leq 1cm$.

After the refilling of the compaction voids the surface of the stone beds was video filmed as a final control measure. After acceptance (review of film) the compaction control of the stone bed (as covered by this paper) was completed and the foundation allowed to be placed on top of the stone bed.On top of the stone bed outside the foundation area a filter layer of coarser stones was dumped. Finally, erosion protection was dumped on top of the filter layer.

8. CONCLUSION

Based on very limited investigation program the attempt to establish a simple operational way to verify that the compacted stone beds fulfill the static and dynamic design requirements, was successful.

RAMBØLL

Brainstorming on Potential Foundation Concepts for the Foundation of the Wind Turbines at Nysted/Rødsand

Jørgen Lorin Rasmussen

Geological Model

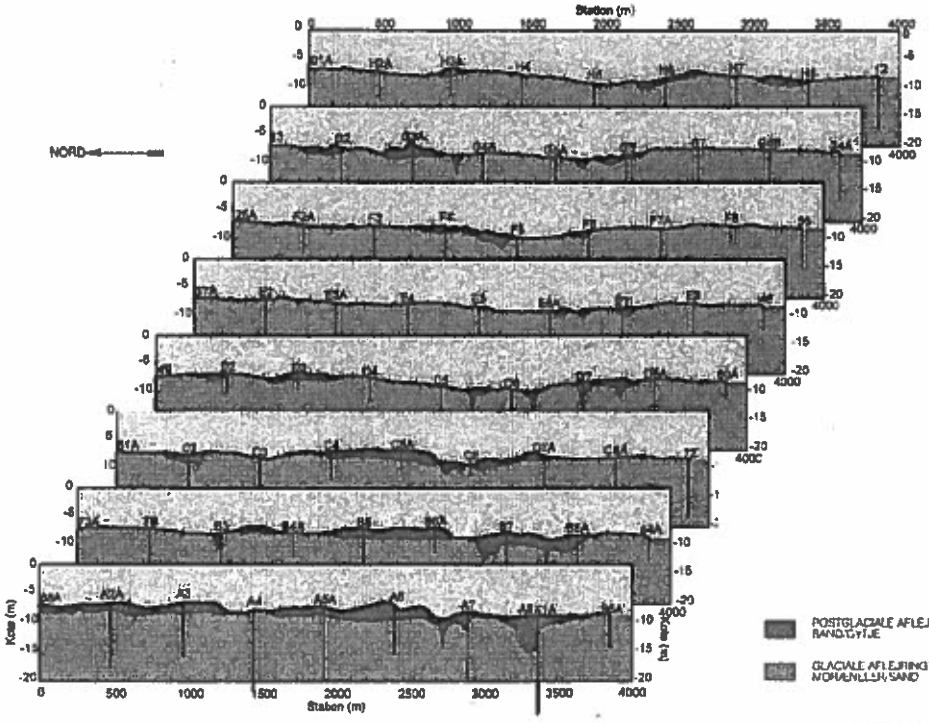

RAMBØLL

Foundation Concepts

- Very Stiff to Hard Clay Till
- Minor Areas with Soft Post Glacial Deposits
- Shallow Water

↓

- Gravity Base Foundation

↓

- Steel Caisson
- Concrete, Solid
- Concrete Caisson

Geotechnical Problems to be Considered

- Penetration Resistance of Skirts
- Local Contact Pressure on Base Slab
- Settlements of Structure
- Stability of Structure
- Displacement
- Cyclic Loading, Cyclic Degradation of Soil
- Scour
- Removal of Foundation Base

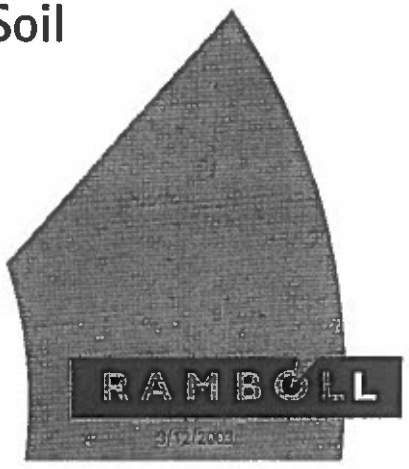

Foundation Concepts

- Skirts or no Skirts ?
- Stone Bed or no Stone Bed ?
- Filter Stability between Stone Bed and Natural Soil?
- Grouting of Stone Bed or no Grouting of Stone Bed ?
- Soil Contact Pressure.

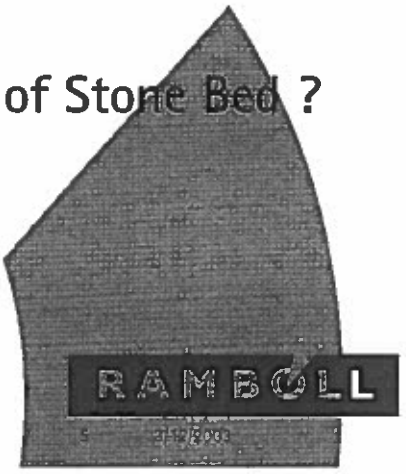

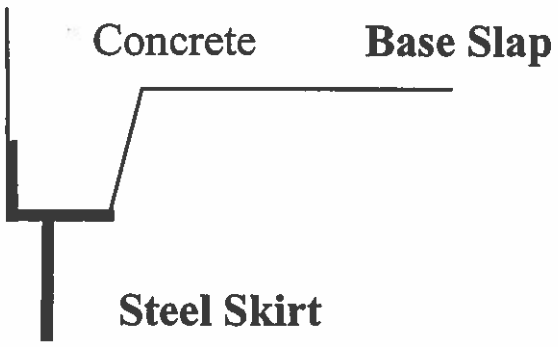

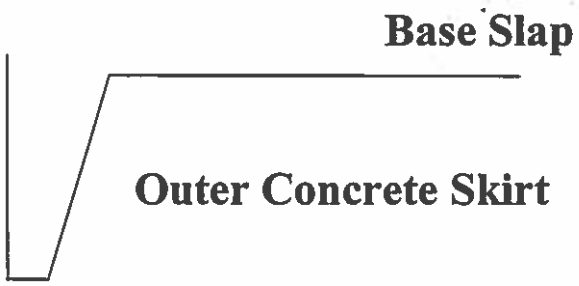

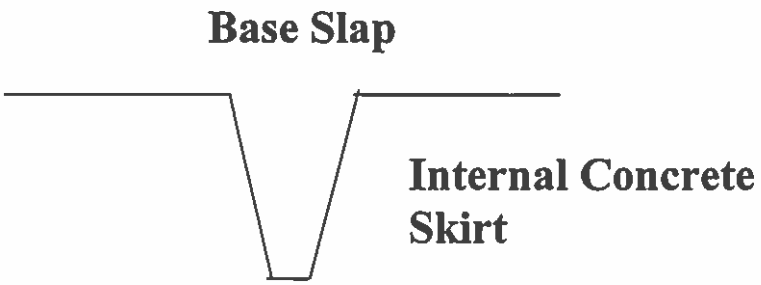

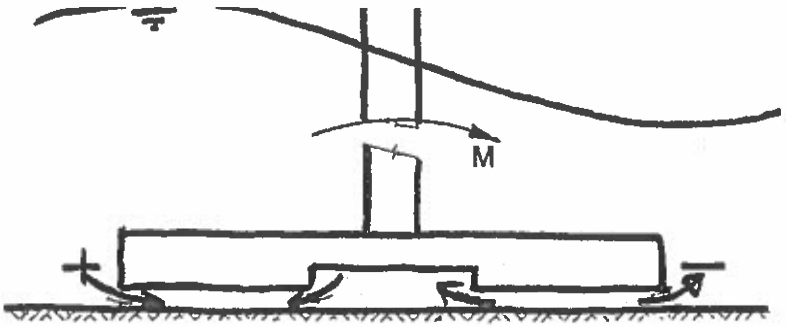

(a) Open gap

NO SKIRTS

+ INCREASE IN WATER PRESSURE.

— DECREASE IN WATER PRESSURE.

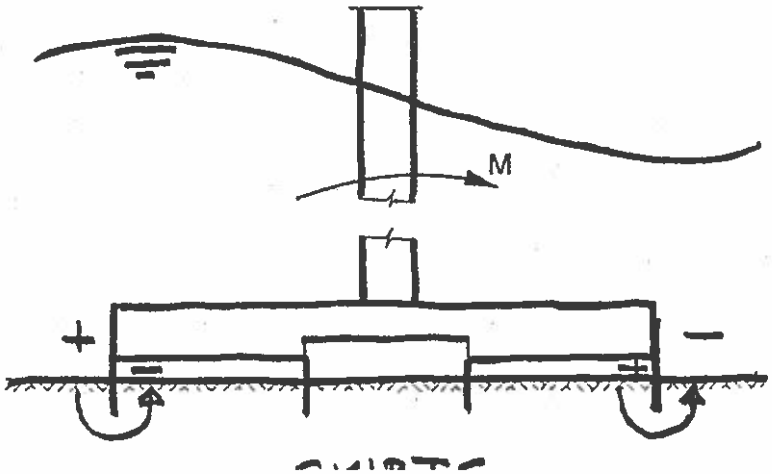

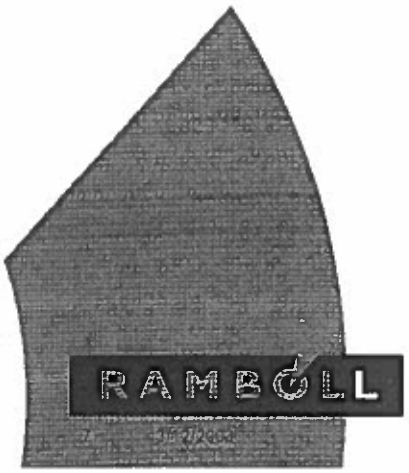

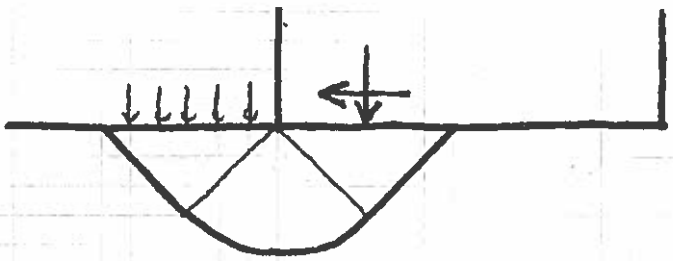

VERTICAL FAILURE MODE

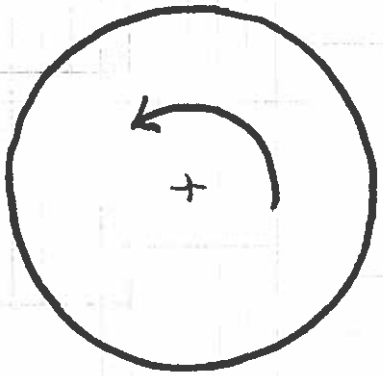

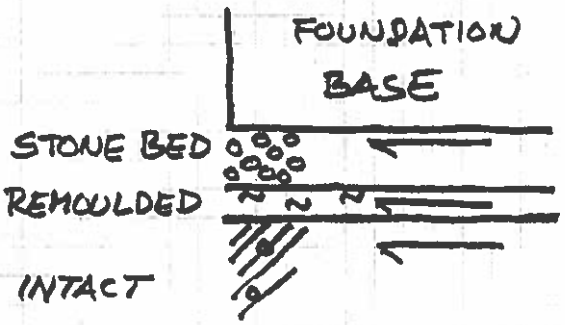

TORSION FAILURE MODE

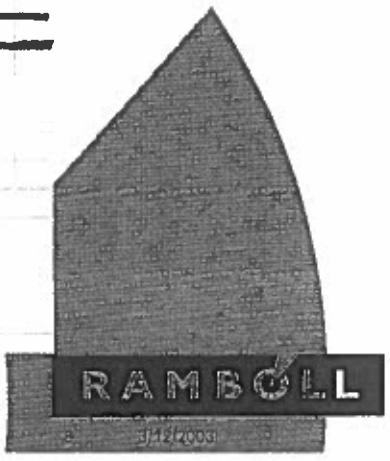

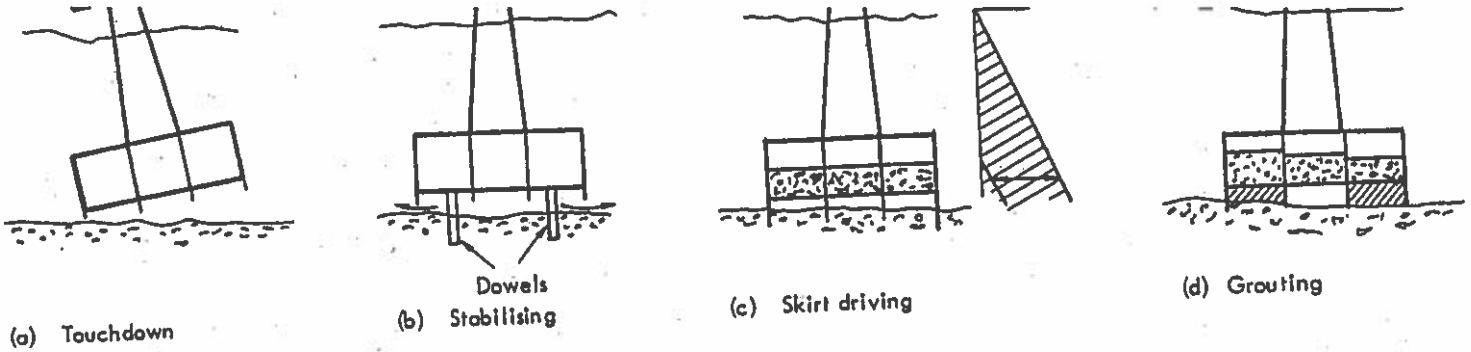

Soil Contact Pressure

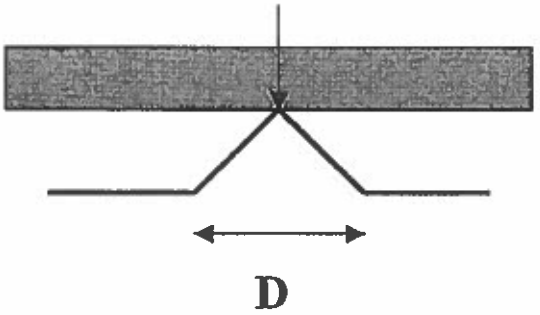

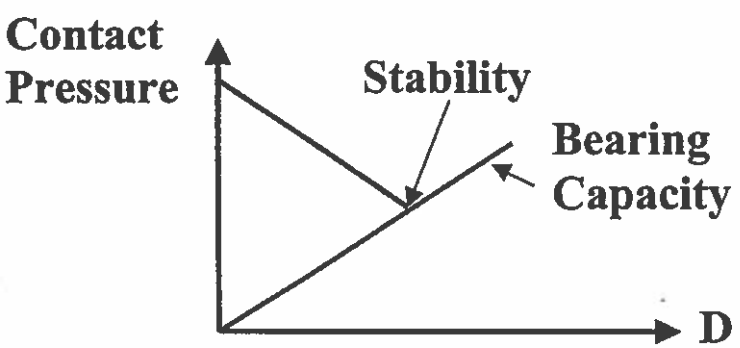

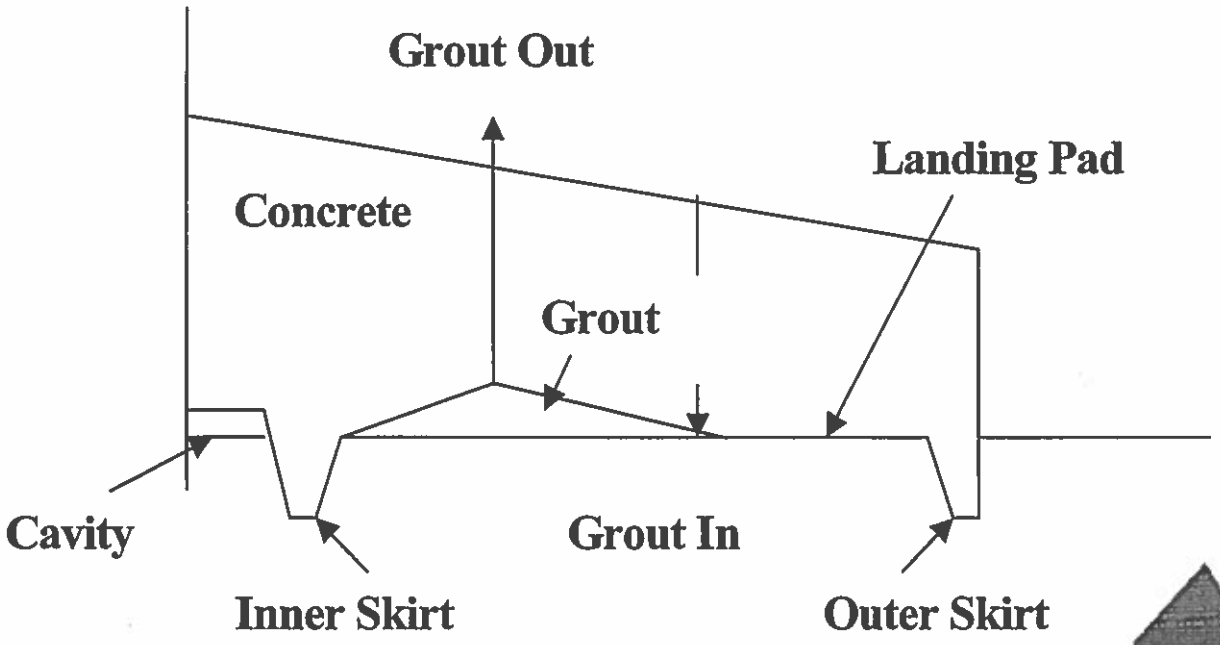

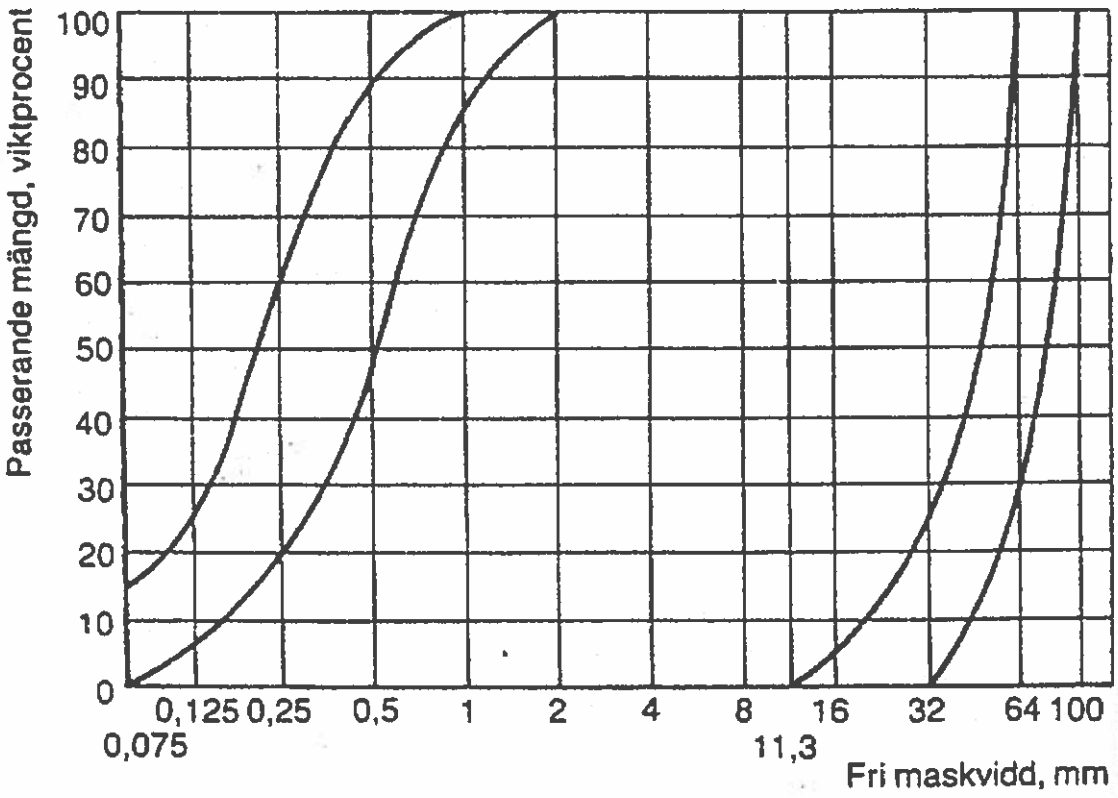

Figur 28.3:1. Gränskurvor för ballastmaterial till injekteringsbetong.

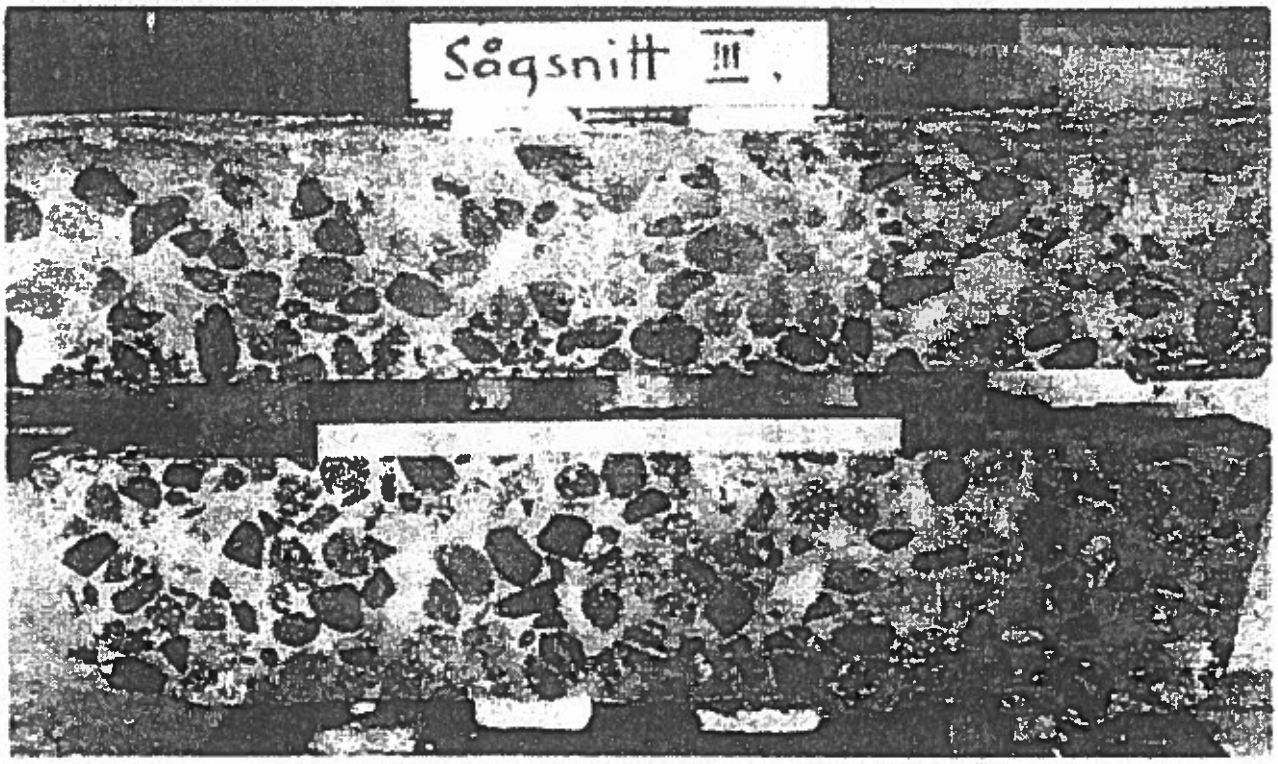

Figur 28.3:2. Betongreparation med injekteringsbetong.

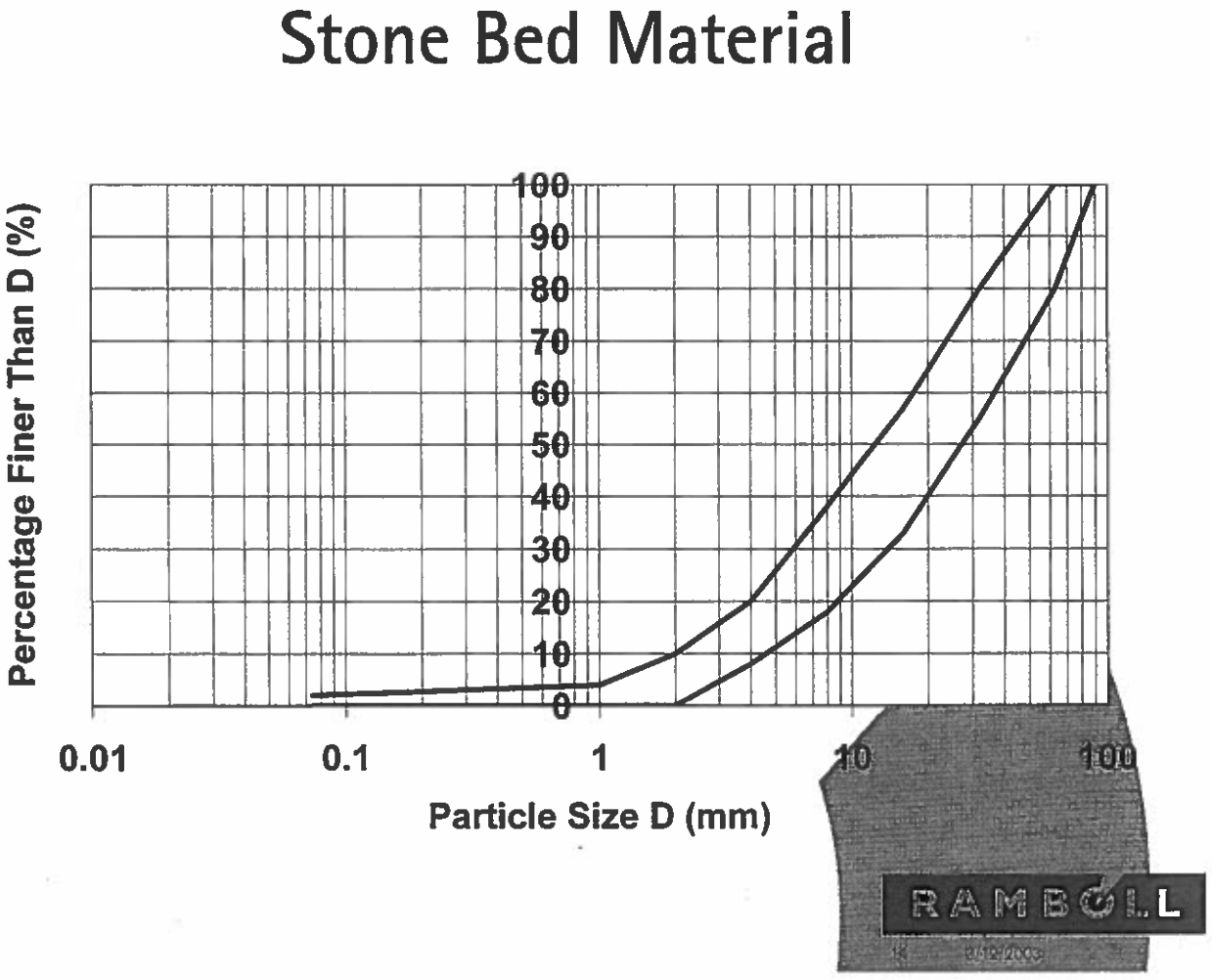

Stone Bed Material

Installation

- Scour in Stone Bed , Evacuvation of Water
- Damage of Stone Bed , Oscillation of Gravity Base
- Inclination of Gravity Base
- Scour Protection

Scour on Top of Stone Bed

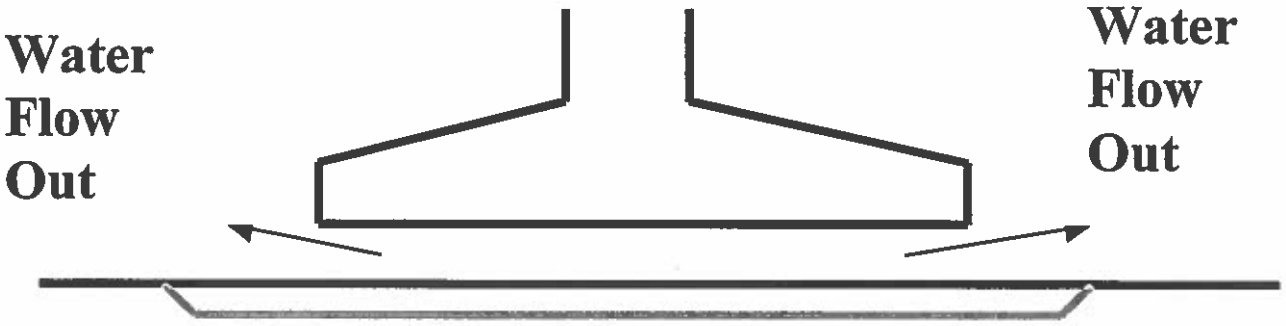

Critical Shear Stress on Stone Bed

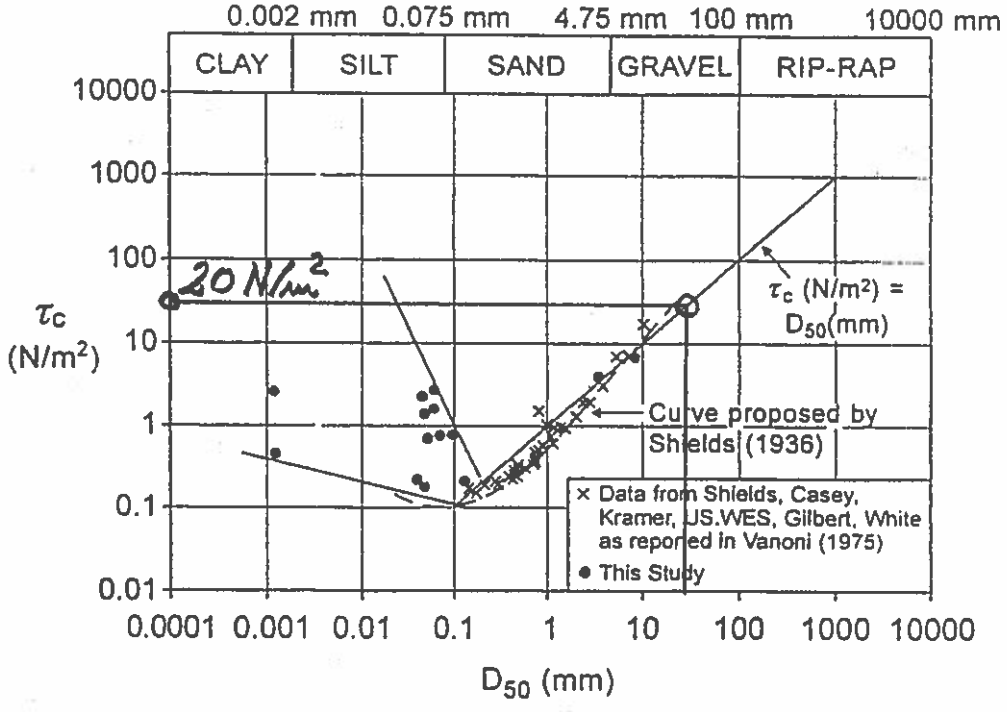

FIG. 3. Critical Shear Stress versus Mean Soil Grain Diameter

Evacuvasion of Water Beneath the Base Slap

- Critical Shear Stress appox. 20 Pa
- Friction Coefficient 0.01 to 0.02
- Critical Velocity 0.4 to 0.6 m/sec.

↓

- Crane Velocity shall be less than 0.4 m/sec

Nysted Havmøllepark ved Rødsand

- Ref. COWI

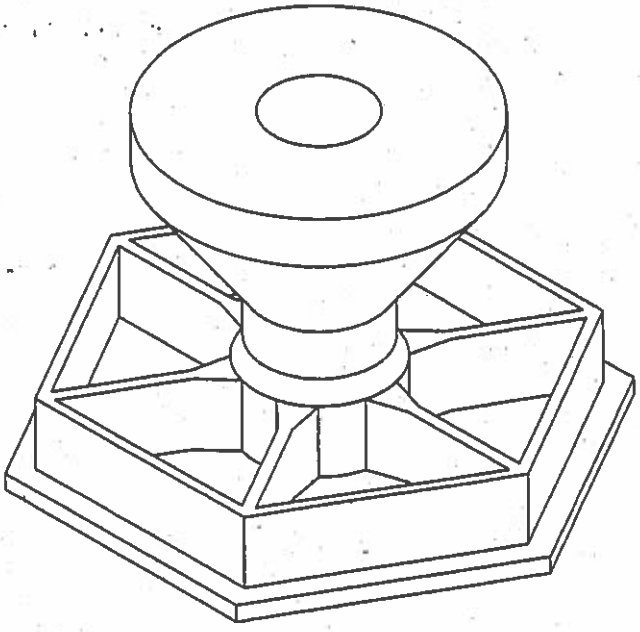

COWI's Foundation Design

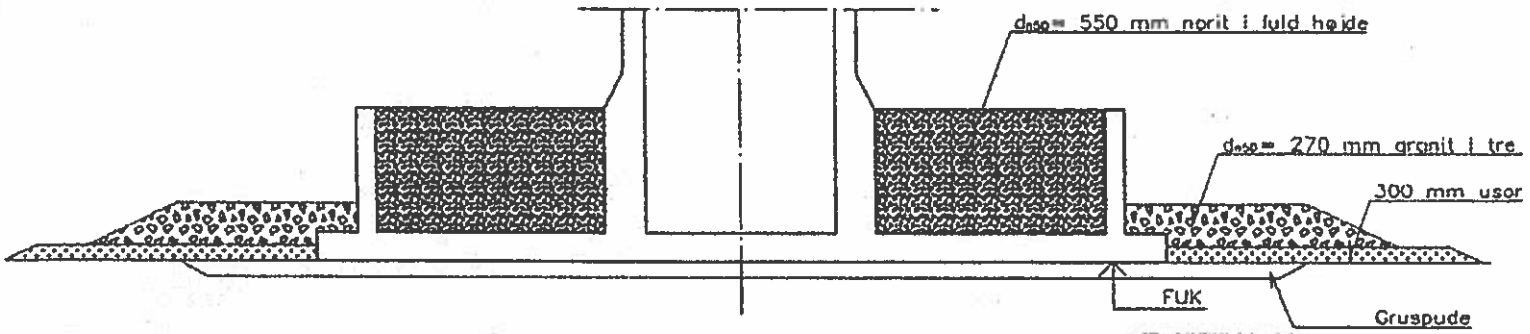

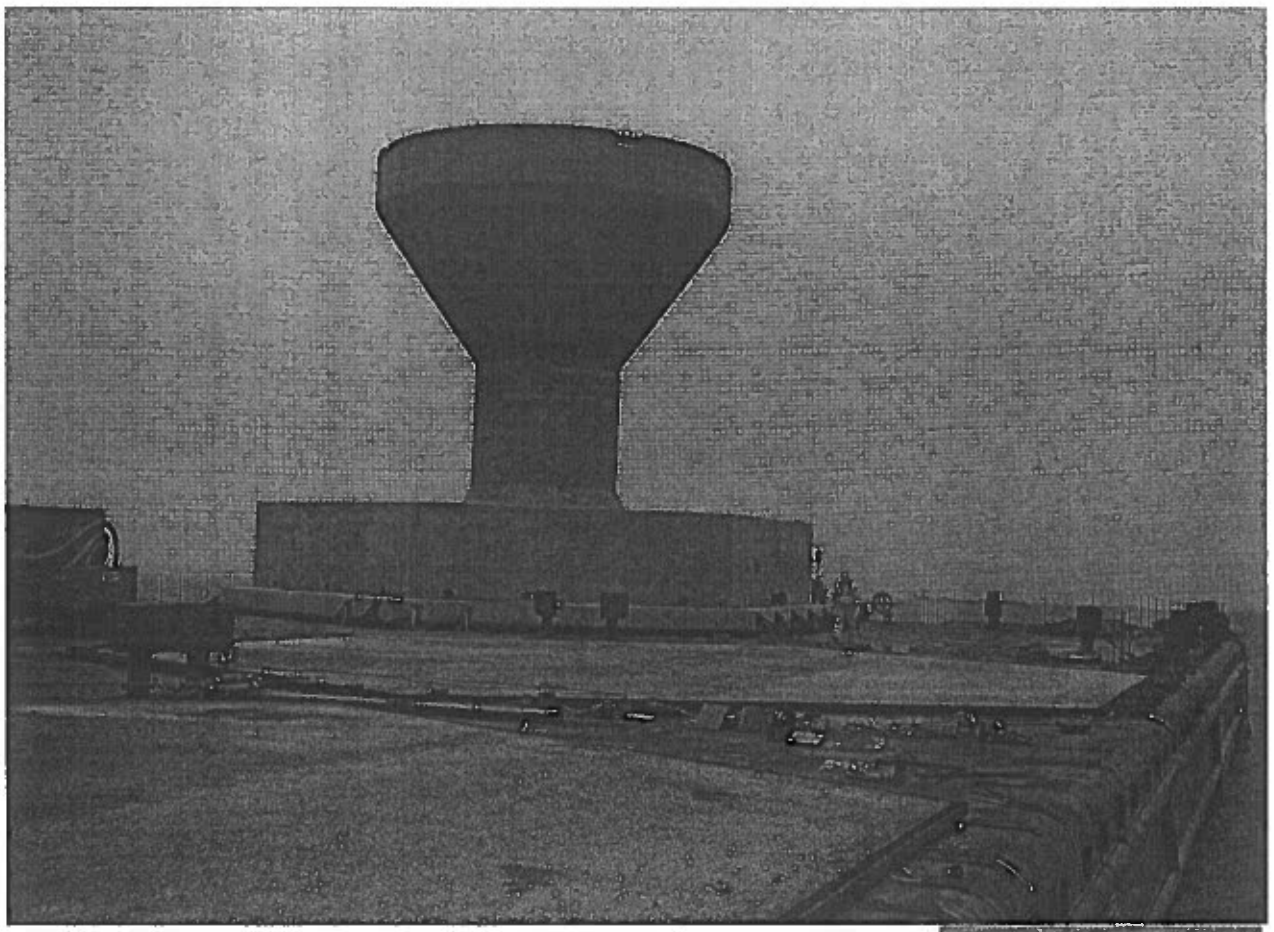

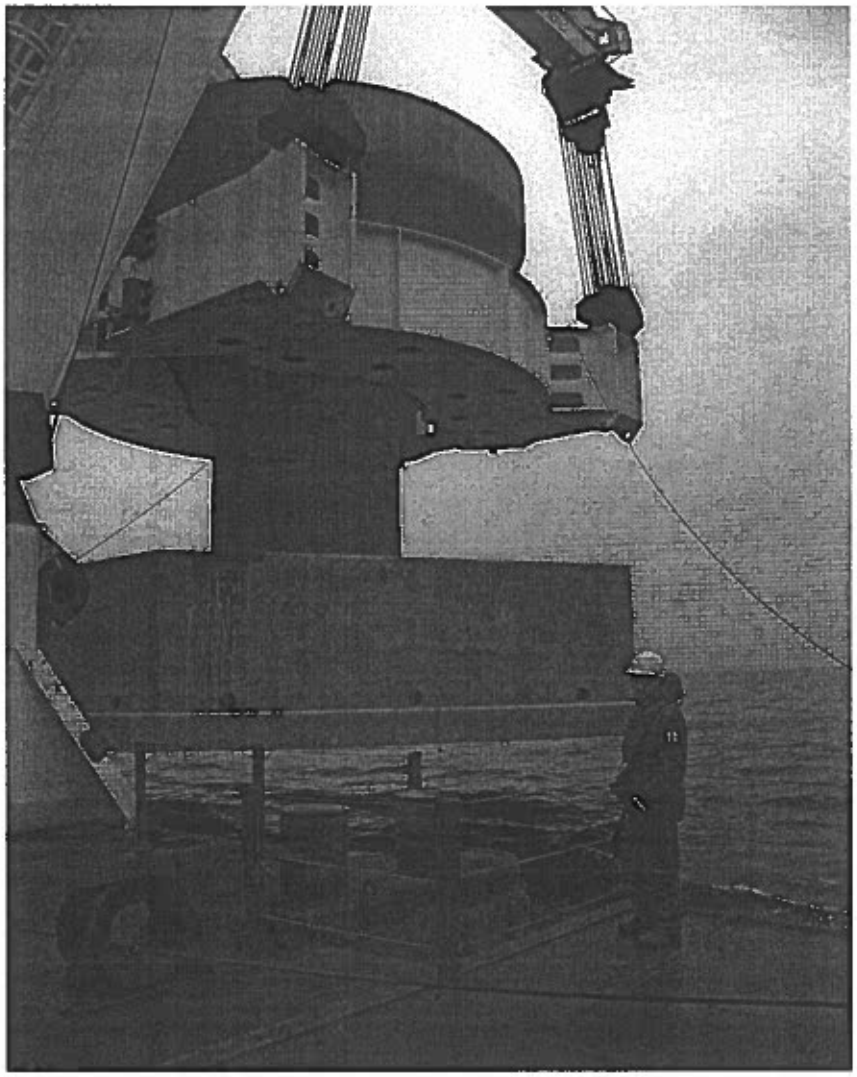

RAMBØLL

23 3/12/2004

Questions ?

RAMBØLL

26 3/12/2004

Per Sandgaard Kristensen

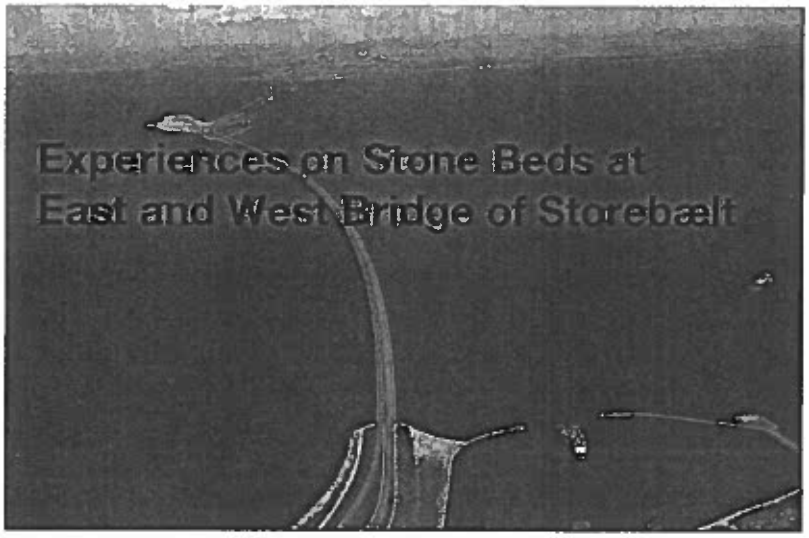

Stonebeds at Storebælt. Headlines

- Function
- Subsoil
- Equipment for preparation, placing and compaction
- Stonebed materials
- Compaction tests
- Working method
- Compaction requirements and control
- Geometrical requirements and control
- Were requirements fulfilled?
- Special items
- Conclusions

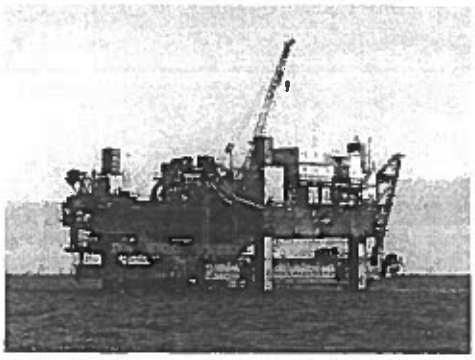

Storebælt. Function of Stonebeds

- Transfer of stresses from bottom plate of caisson to subsoil

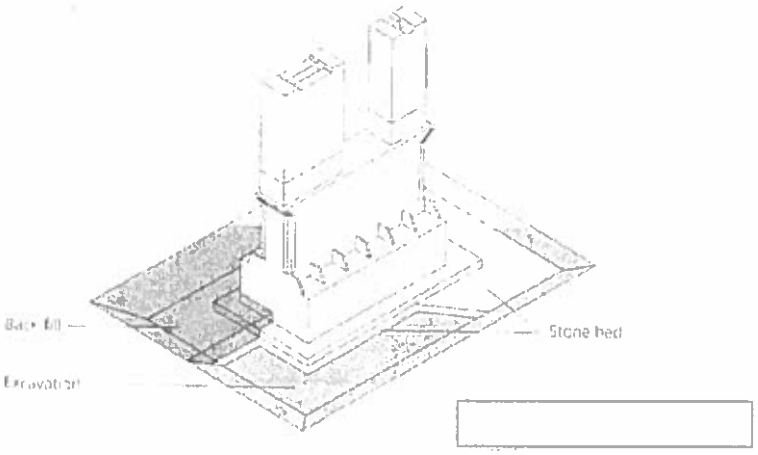

Storebælt. Subsoils West Bridge

Stiff and Strong Subsoils:

- Bryozoan Limestone
- Kerteminde Marl
- Calcarenite/Calcisiltite (Lellinge Greensand)
- Knudshoved Till
- Lower Till
- Upper Till
- Occationally Meltwater Sand

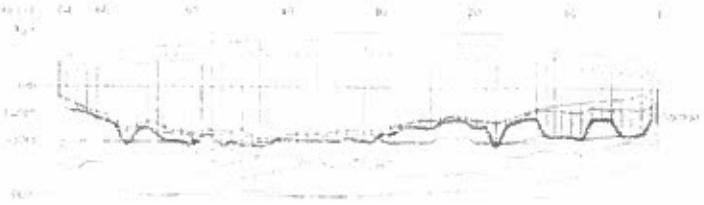

Storebælt. Equipment, West Bridge 1

- Buzzard

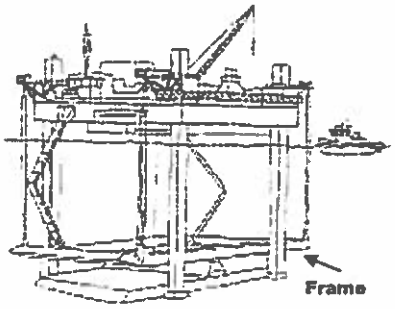

- Cleaning Pan

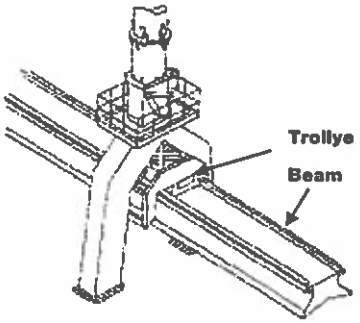

COWI

Storebælt. Equipment West Bridge 2

- Pouring Pipe

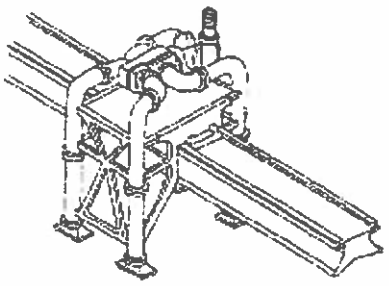

- Compaction Unit

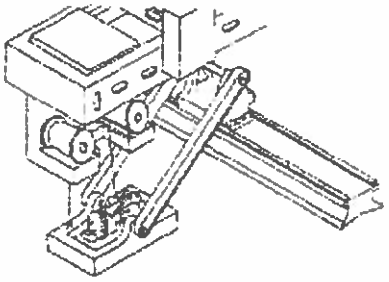

COWI

Storebælt. Stonebed Materials, West Bridge

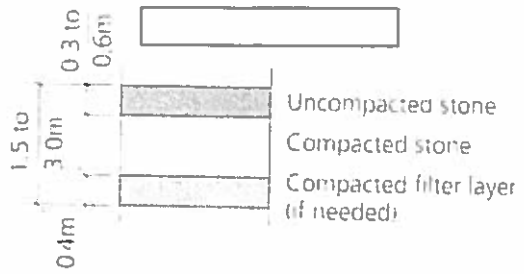

- Uncompacted Stone, Screeding Layer, #40 -120 mm
- Compacted Stonebed, #5 - 60 mm
- Filter Layer, Sand for Concrete, Aker #0 - 8 mm

Storebælt. Compaction Tests 1

- West Bridge: Test, February 1990 in Utrecht. Lay-out:

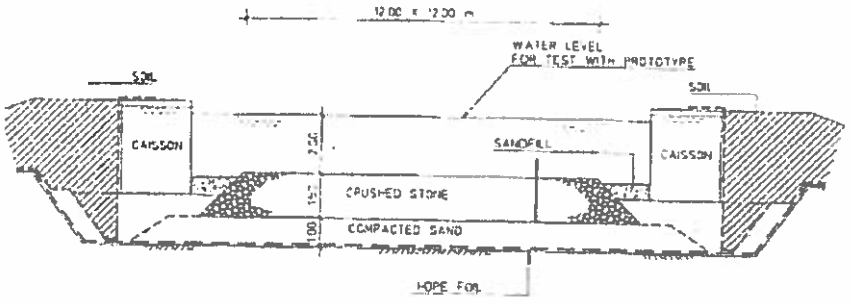

TEST PIT CROSS SECTION

Storebælt. Compaction Test 2

Equipment, West Bridge

- 3.5 × 4.6 m² plate
- Static mass 37,000 kg
- Dynamic mass 26,000 kg
- Vibrator: 2 pc. Müller-Vibrator Type MS-50 H
- (First, trials with a smaller plate)

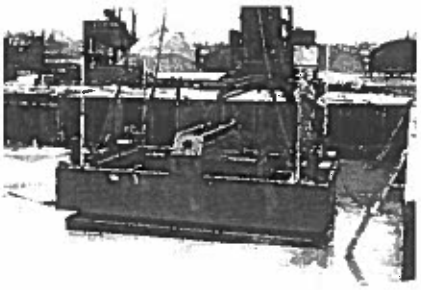

Storebælt. Compaction Test 3

- West Bridge Equipment in Detail 1. The Compaction Equipment

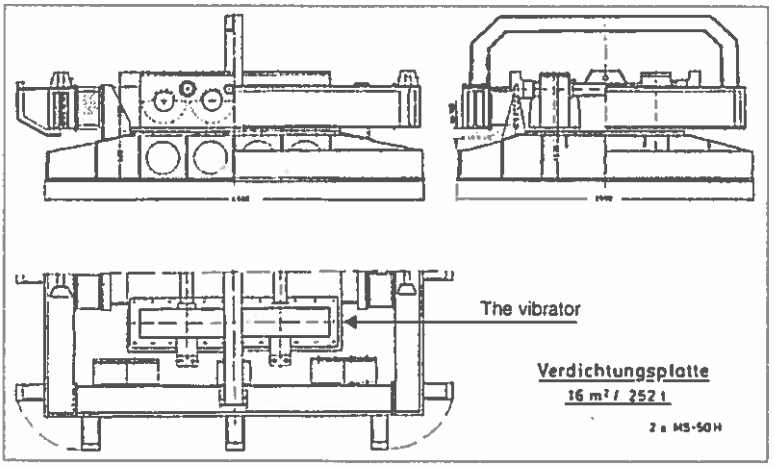

Storebælt. Compaction Test 4

West Bridge Equipment in Detail 2

- The Müller Vibrator
- Holes in Bottom Plate

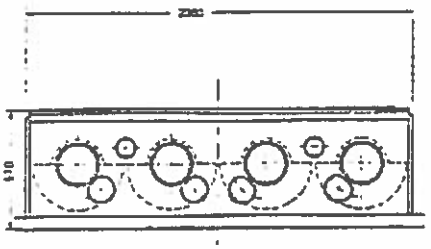

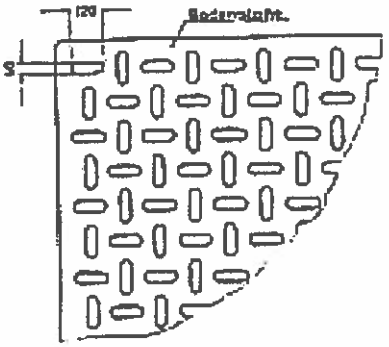

COWI

Storebælt. Compaction Test 5

Bottom of Compaction Unit

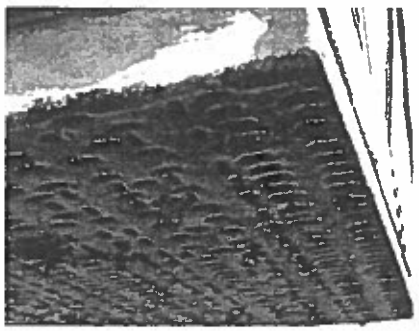

The Compaction Unit at Work

COWI

Storebælt. Compaction Test 6

Harmonic Oscillations:

- $F(t) = mr\omega^2\sin(\omega t)+F_0$

Here, Superharmonic Oscillations, which Increase the Compaction Effects

Superharmonic Oscillations, Example

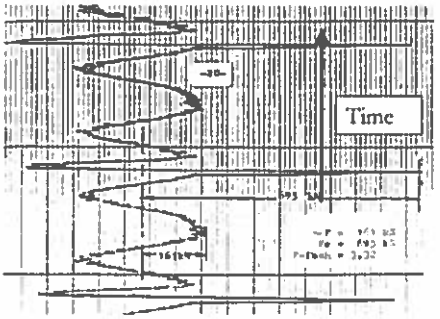

Storebælt. Compaction Test 7

The Execution of the Test for West Bridge

- First, 1 minute with the frequency 13-15 Hz
- Then, 3 minutes with the frequency 18-20 Hz

Storebælt. Compaction Test (West Bridge) 8

- The Surface after Test

- In situ Density Determination by use of Gypsum

Storebælt. Compaction Test 9

Compaction obtained

West Bridge, at Ütricht

Depth below Surface [m]	% Relative Density
0.0 – 0.3	178
0.6 – 0.9	100
1.05 – 1.35	104

East Bridge, at Kalundborg

Depth below Surface [m]	% Relative Density
0.0 - 0.3	206
0.5 – 1.3	110
1.5 – 2.3	125
2.5 – 3.3	155

Storebælt. Working Method, West Bridge 1

- Cleaning of bottom
- Control of excavation by divers (knife test)
- Survey
- (Placing of 0,4 m filter layer, where necessary)
- Placing of #5-60 mm stonebed material
- Evening the surface by screeding
- Compaction 1 minute. 13-15 Hz
- Compaction 3 minutes 18-20 Hz
- Survey
- Placing of #40-120 mm screeding layer
- Evening the surface by screeding
- Survey

Storebælt. Working Method, West Bridge 2

Compaction:

- Phase 1: 1 minute compaction of the whole area in a chess board pattern
- Phase 2: 3 minutes compaction of the whole area in a chess board pattern

Chess Board Pattern:

1	3	1	3	1
4	2	4	2	4
1	3	1	3	1
4	2	4	2	4

Storebælt. West Bridge
Compaction Requirements and Basis for Acceptance

Requirement:

- Compacted layers: Minimum 65 % relative density

Basis for acceptance:

- Verification of 1 minute compaction with 13-15 Hz followed by 3 minutes compaction with 20-22 Hz
- Minimum value for maximum superharmonic stress force measured by accelerometer
- Minimum value for measurement of settlement of surface during compaction

Measured maximum Superharmonic Stress, Example:

Storebælt. West Bridge
Geometrical Requirements and Basis for Acceptance 1

Geometrical Requirements to final surface 1:

- Divide the foundation area into about 70 numbers of 3 x 3 m^2 cells
- Determine average level of cell based on 100 to 150 values from echo soundings
- Determine best fit parabolic surface of the average values:
- $z = Ax^2+By^2+Cxy+Dx+Ey+F$
- Thus, A and B were related to depression, C to twist, D and E to inclination and F to absolute level

Storebælt. West Bridge
Geometrical Requirements and Basis for Acceptance 2

Requirements 1

- Average level relative to theoretical: ±100 mm

- Max. level difference between two corner cells: 100 mm

- Depression between 0 and +50 mm (corners were to be higher than center)
- Twist, T, to be between -12 and +12 mm:
  $T = z_1 - z_2 + z_3 - z_4$
  z_1, z_2, z_3 and z_4 levels of corner cells numbered clockwise

Storebælt. West Bridge
Geometrical Requirements and Basis for Acceptance 3

Requirements 2

- Roughness = difference between individual cell average and best fit parabolic surface: Between -25 mm and + 25 mm

- Under special circumstances these limits could be increased to between -50 mm and +50 mm

Storebælt. West Bridge. Were Requirements Fulfilled?

Yes

- Compaction: No problem at all. The equipment worked well
- Geometrical requirements: Some times additional screeding was necessary

Storebælt. West Bridge. Special Items

Survey

- The strict requirements to levels of final layer resulted in a comprehensive determination of the movements and deflections of the frame, beam and trolley

Filter layer

- Introduction of simultaneous compaction of #4-60 mm material and underlying #0-8 mm material had not been tested on beforehand, but was based on theoretical considerations only. The movement of the compacting unit showed that it went well

Storebælt. Conclusion

- No problems with placing and compaction of the stonebed
- Strict requirements to the shape of the final surface were fulfilled by conscientious calibration of the equipment and occasional re-screeding
- Introduction of a granular filter layer did not create special problems

NYSTED OFFSHORE WINDFARM

AT RØDSAND

Construction and quality control of the stone beds for the foundations of the wind turbines at Nysted / Rødsand

Presentation 20 March 2003 on

Seminar on Dynamic loads to stone bed foundations and soils – from offshore wind turbines to earth quake.

Danish Society of Hydraulic Engineering (DVS)

And Danish Geotechnical Society (DGF)

Jørgen Lisby

Project Development and Design

Dredging for foundations

For the 73 foundations dredging is performed to reach bearing capacity on the clay till surface. In most of the positions an undrained shear strength of cu = 300 kN/m2 is reached with relatively small dredging volume.

A total dredging volume of 52450 m3 is found based on geotechnical investigations.

The main part of dredging is executed by a backhoe dredger (Grethe Fighter). The ship has 3 anchor spuds and the dredging depth is 12m.

In a few positions dredging depth is more than 12m. Here a hydraulic excavator with extended arm mounted on a barge is used.

Dredged materials are transported and dumped from the hopper of the same ship.

Diver controls the dredged surface and 5 short CPT tests shall prove, that no soft materials are left and that soil properties has been reached.

Stone Bed Foundations

The stone bed is 300 mm thick and it is laid out without compaction. A vessel mounted with crane does the execution of the stone bed (type as Peter Madsen). The vessel also has a diving team.

A centre foundation is placed and levelled. A steel frame is placed and levelled. On the centre foundation a rotating beam with mounted with a small jetting vehicle is placed. The divers controls the placing and quantity of stones giving instructions to the crane operator while the levelling beam and the jetting vehicle is rotating an covering the total surface of the stone bed.

Deep Stone Bed Foundations

If the necessary soil properties are reached at a deeper level than expected or other reasons a thicker stone bed becomes actual.

If the bearing stone bed layer shall be extended the lower part is compacted while the upper 300 mm is executed as described above.

Deep stone beds are placed in layers not exceeding 2.5 – 3m. Each layer is compacted on the surface by a plate vibrator (2.6 x 2.1m plate and vibrator ICE 416). Trials before the works were performed in a test pit at Gedser.

Test on Normal Stone Bed

- Gradation curves
- Surface test for level tolerances
- Plate bearing test in the first bed

Test on Deep Stone Bed

Purpose

Tender Document demands on deep stone beds were tested in a pit close to the beach at Gedser.

A deep stone bed was laid out below water surface in the test pit under same circumstances as actual foundations.

Densities before and after compaction and plate bearing tests were performed.

Design Properties

- Angle of friction $\varphi'_{tr,s}>40^{o}$
- Youngs modulus by 50% brudgrad $E_{50}>20$ MPa

For normal 300 mm stone beds design properties used was:

- Total density $\gamma_m = 19$ kN/m3
- Effective density $\gamma_m = 9$ kN/m3
- Plane angle of friction $\varphi_{pl,k} = 40°$
- Parameters of deformation G = 6MPa , E = 15 MPa , K = 18 MPa

For deep stone beds design properties used was:

- Total density $\gamma_m = 20$ kN/m3
- Effective density $\gamma_m = 20$ kN/m3
- Plane angle of friction $\varphi_{pl,k} = 45°$
- Parameters of deformation G = 25MPa , E = 62 MPa , K = 75 MPa

Testpit Execution

A circular sheet pile cofferdam with diameter 16m with top level +3.0m and toe level –7.0m was installed. Inside was dredged to level –2.75m.

Levels and diameters were measured and a plate for measuring settlements was installed. 5 pipes for later density measurements trough the stone bed were also installed.

The pit was filled with water to level 0.0m and the stones were placed under water.

Aluminium pipes were installed in the streel pipes and densities through the layer was measured.

Water was filled to level +3.0m and compaction was performed according to the procedure mentioned later.

After compaction the water level was lowered to stone surface and densities through the layer was measured as well as diameters of the pit.

After tests the pit was emptied and geometry and settlements was measured.

Stone quantities used were also measured in the ship (950Tons).

Compaction Equipment

ICE 416 vibrator with free varying frequencies mounted on a 2.6 x 2.1 x 0.075m plate was used. The vibrator was operated hanging in a mobile crane.

Compaction Procedure

The surface was compacted in 2 rounds.

First time in one minute with a frequency of 12Hz. After covering the total surface a second round was performed with a frequency of 18 Hz in 4 minutes.

Control easurements

Plate bearing tests

3 tests on the stone surface with ground water level in the surface was performed.

- One test on 300 mm non compacted stone bed.
- One test directly on compacted surface
- One test one m below compacted surface

All tests is performed with plate diameter 0,6m. Offloading and reloading was performed at 20, 40 and 60 kN.

Test results:

- In test no. 1 loading was 108 kN without rupture giving a $\varphi_{pl,k} > 45°$.
- In test no. 3 loading was 145 kN without rupture giving a $\varphi_{pl,k} > 47°$.
- E-modulus in test no. 1 in all reloadings are 64 MN/m2
- E-modulus in test no. 2 and 3 in all reloadings are 79,5 – 227 MN/m2 MN/m2

Density tests

Density tests was executed with a "Depth Moisture / Density Probe".

Results can be seen in enclosure 11. A raise in density from 1,948 to 2,054 ton/m3 is measured.

Compaction has worked in all levels of the stone bed.

By measuring the volume of the stone bed before and after compaction a raise in density from 2.077 to 2.278 ton/m3 is measured (enclosure 12).

By vibration compaction in the laboraty a dry density 2.094 t/m3 and a saturated density of 2,324 t/m3 is measured. The obtained compaction measured on dry density of compacted material compared to laboraty measurements is 96,5%.

It can be concluded, that the measurements by the "Depth Moisture / Density Probe" is not reliable in this rough stone material, but it shows a good and uniform effect trough the layer.

Afgravning

Grovudgravning:

- **Grethe Fighter / Margrethe Fighter**
- **Hydraulisk gravemaskiner**
- **Kan grave med stor præcision**
- **Forankrer på ben**
- **Positioneringsudstyr med RTK D-GPS nøjagtighed**
- **Med IHC gravemoniteringssystem type XPM**
- **Udgravningsmængde total 52436 m3**

Oprensning og eventuel opgravning af lokal blød bund

- **Merete Chris / Aase Madsen**
- **Fladgrab uden tænder**
- **Sikre mindst mulig opblanding af havbunden på funderingsniveau**
- **Antennen til positioneringssystemet er placeret i toppen af bommen**

Vejrligsbegrænsning

- **Uddybningsarbejde: bølgehøjde > 1 meter**
- **Afsluttende oprensning: bølgehøjde > 0,5 meter.**

Klapning

- **De opgravede materialer sejles i skibenes lastrum til *klappladsen* hvor de losses med skibets gravemaskine.**

Kontrol

- **Dykkerinspektion**
- **Beskrivelse af udgravningsunderlaget**
- **Prøvetagning**
- **Korte CPT forsøg**

Skærvepuder

- **Center fundament og stålramme placeres**
- **Højde og placering kontrolleres ved måling til fast stadie over vandspejl**
- **Hældningen på rammen med min. 4 målinger med trykmåler**
- **Stenmaterialer leveres i selvlossende fartøjer**
- **Lokalt depot for sten på opankrede pramme på 2000 tons**
- **Ca. 75% af stenmængderne til skærvepuden grovreguleres med grab**
- **De sidste ca. 25% af skærverne udlægges løbende samtidig med fin afretningen**
- **Afretterskinne trækkes hen over stålrammen**
- **Højtryksspulevogn flytter overskuds skærver således af skinnen konstant skubber en ca. 10 cm høj vold af sten foran sig**
- **Afretningen dokumenteres med UV kameraer på spulevognen og optages på video**
- **Afretterskinne, centerfundament og stålramme løftes op og ar i overfladen på skærvepuden repareres med dykker**
- **Afsluttende dokumentation af rethed på overfladen foretages med retskede**

Komprimeret skærvepude

- **Anvendes, hvor der sker bundudskiftning (bærelag > 300mm)**
- **I nedre del af gruspude anvendes materiale, som er filterstabilt mod såvel underbund som mod skærvepude (eventuel geotextil)**
- **Afrettes alene fra vandoverfladen med en tolerance på ± 100 mm**
- **Komprimeres med pladevibrator på overfladen**
- **Stålplade med dimensioner 2 x 3m monteret på en ICE 416 vibrator ophængt i kran**
- **Densiteten belyses ved forsøg i testpit**
- **Øverste 300 mm af bærelaget udføres som normal skærvepude**
- **Styrke- og deformationsegenskaber søges belyst ved pladebelastningsforsøg.**
- **Kravene til skærvepuder må ses i lyset af, at fundamentskonceptet er baseret på lave fundamentsspændinger**

Erosionssikring

- **Stenmaterialer leveres i selvlossende fartøjer**
- **Lokalt depot for sten på opankrede pramme på 2000 tons**
- **Sten lastes i udlægningsskibets lastrum fra stendepot**
- **I møllepositionen losses med grab**
- **Udlægningen foretages efter positioneringsskærmen, hvor grabbens position vises i forhold til det indtegnede fundament**

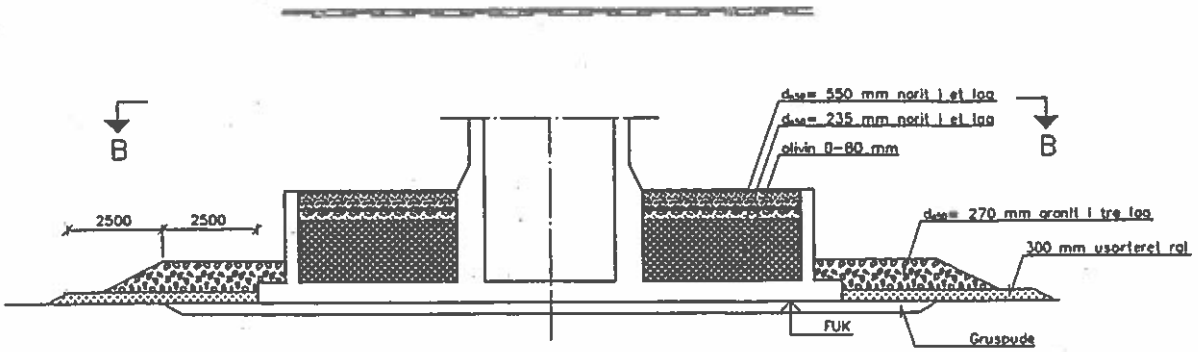

Ballast type 1, Snit A–A, 1:100

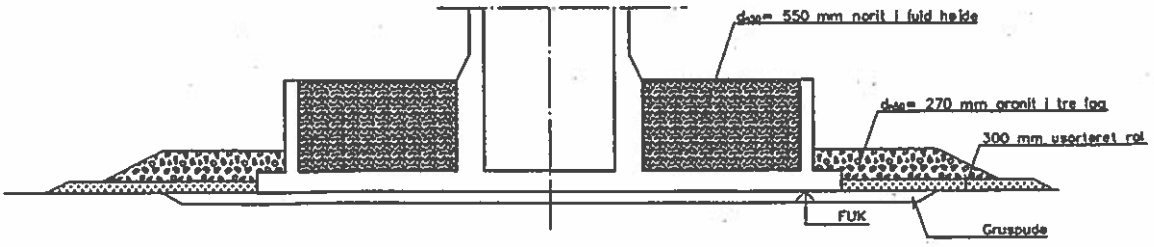

Ballast type 2, Snit A–A, 1:100

m.v. "GRETE FIGHTER"

Dredger and contracting vessel

Telephone	+45 20 21 83 96
Fax	+45 20 26 92 17

Crew	4
Accommodation	11
Life-saving equip.	6
Tonnage	BT 582 NT 174
Classification	Bureau Veritas class I 3/3 (E) – Dredger
Built	1980
Length	46.5 m
Breadth	12.0 m
Draught	unloaded: 2.2 m Loaded: 3.5 m
Capacity	630 tonnes or 390 m^3 (load 12.0 x 9.0 x 3.6 m)
Propulsion	2 no. Scania DS 14.2 x 355 hp
Speed	unloaded: 9.0 knots loaded: 7.0 knots

Working Equipment:

DEMAG H95 backhoe excavator.
Standard equipment: Boom 10.5m. Stick 7.0m. Dredging depth 12.0m with a 3.0m^3 bucket. 16" sand pump, Deutz 748hp, option for trailing suction dredging up to 17m depths

IHC excavator monitoring system type XPM with positioning equipment connected
Positioning equipment: Trimble RS 4000 DGPS and Robertson RGC 11 gyro

3 anchor spuds for depths up to 12m.
4 point mooring, 5 tonnes winches.
Bar sweeping equipment for both vessel and workboat.
Steel workboat for anchor handling, 75hp.
Deck crane, 7 tonnes.

Option: barges and tug boat.

m.v. "GRETE FIGHTER" is suitable for:

- Dredging works in hard material
- Major dredging contracts, - the vessel has a large digging capacity.
- Sand suction and pumping material
- Manoeuvring / working within busy harbours and narrow channels – the vessel can anchor with spuds
- Stone laying to breakwaters, scour protection and other stone works.
- Trench excavation for cables, pipelines etc.
- Various other forms of contracting work

PETER MADSEN REDERI A/S
Søren Nymarksvej 8 DK-8270 Højbjerg Telephone +45 8629 0100 Fax +45 8629 4333

m.v. "PETER MADSEN"

Diving and contracting vessel

Telephone	+45 20 21 53 99
Fax	+45 21 62 54 93

Crew	3
Accommodation	4
Life-saving equip.	6
Tonnage	BRT 159 NRT 44
Classification	Danish Maritime Authority
Built	1968 / 1998 / 2001
Length	30.20 m
Breadth	7.50 m
Draught	Unloaded: 2.00 m Loaded: 2.30 m
Capacity	150 tonne or 100 m^3 (load 9 x 5.5 x 2.5 m)
Propulsion	Scania DS11, 261 hp
Speed	Unloaded: 7.0 knots Loaded: 6.0 knots

m.v. "PETER MADSEN" is suitable for:

- Breakwater construction and stone works
- Dredging and scour protection
- Levelling and underwater foundation works
- Pipe laying and diving works
- Various other forms of contracting work

Working Equipment:

Sennebogen 625 R-HD 30 tonne crane
Standard equipment: Boom 16.0 m. Dredging depth 35.0 m.
Grab equipment for rock & stone handling and excavation.

2 anchor spuds for depths up to 11.5 m
2 capstans astern, 2 tonne winches.
Steel workboat for anchor handling, 30 hp

Option: electronic positioning with
RTK GPS and PMS positioning software

PETER MADSEN REDERI A/S
Søren Nymarksvej 8 DK-8270 Højbjerg Telephone +45 8629 0100 Fax +45 8629 4333
Homepage: www.peter-madsen.com E-mail: info@peter-madsen.dk

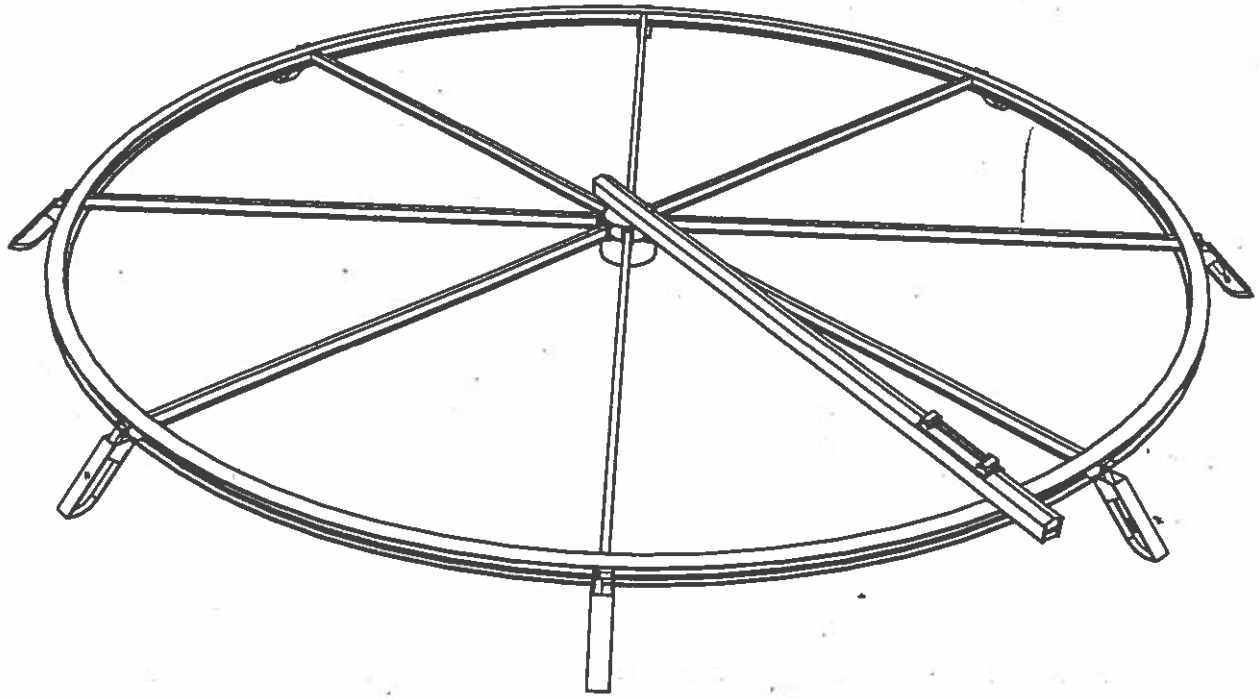

Ramme for afretning
af skærvepude.

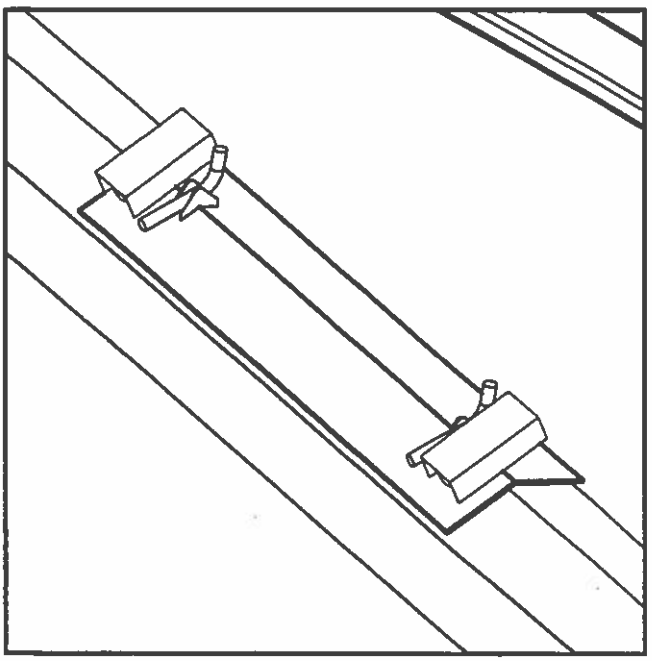

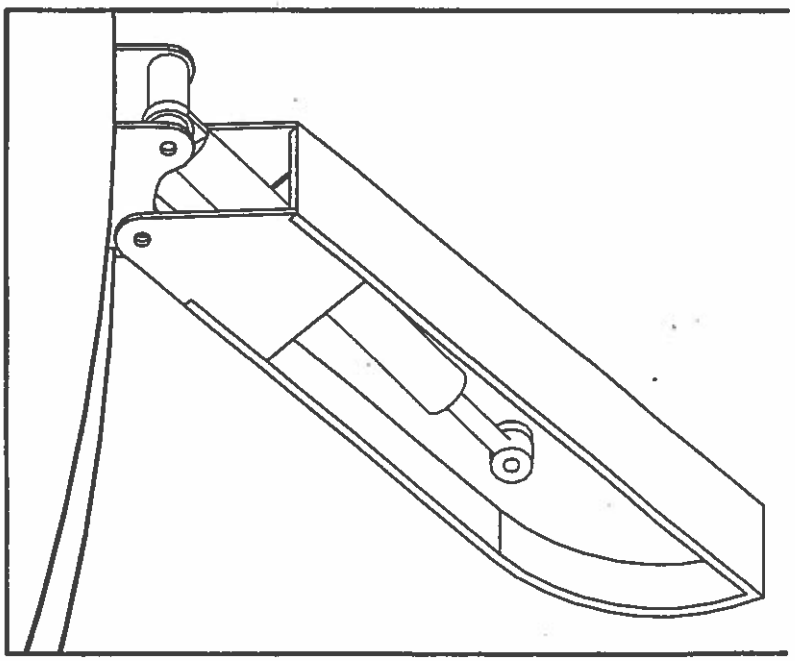

AARSLEFF-BALLAST NEDAM INTERNATIONAL JOINT VENTURE
RDSI, NYSTED HAVNEMØLLEPARK VED RØDSAND – FUNDAMENTSLEVERANCEN
TILBUD

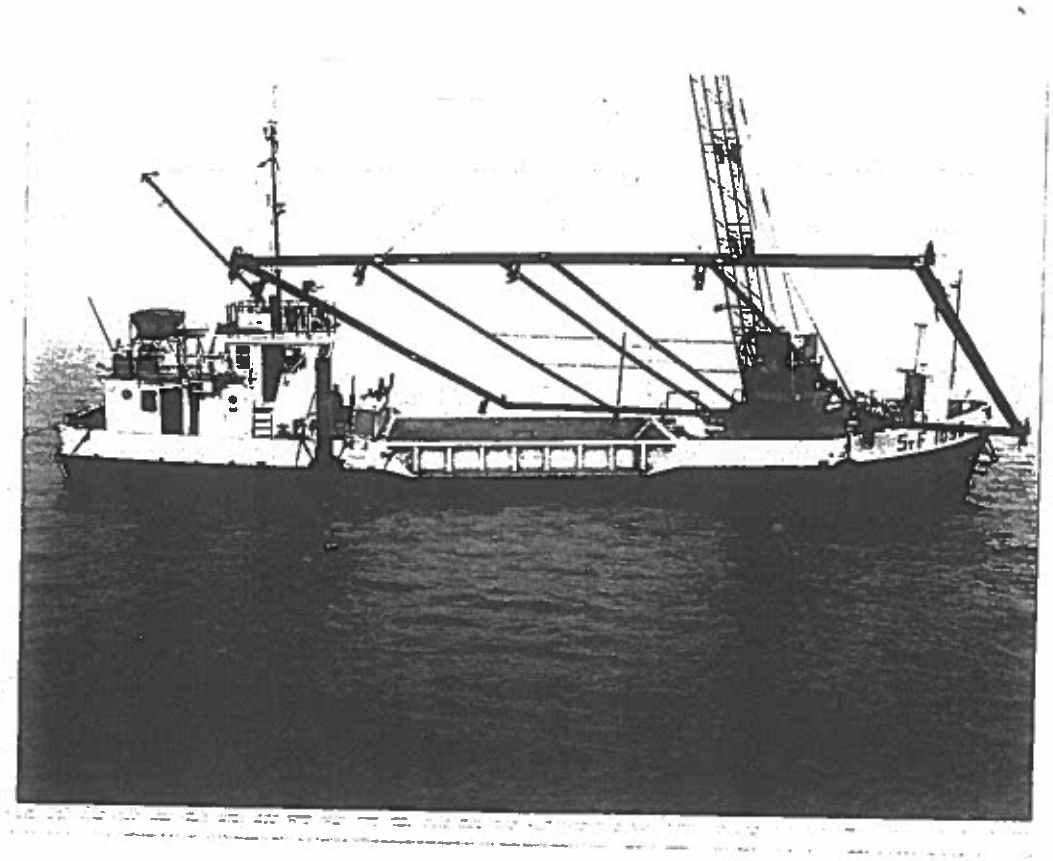

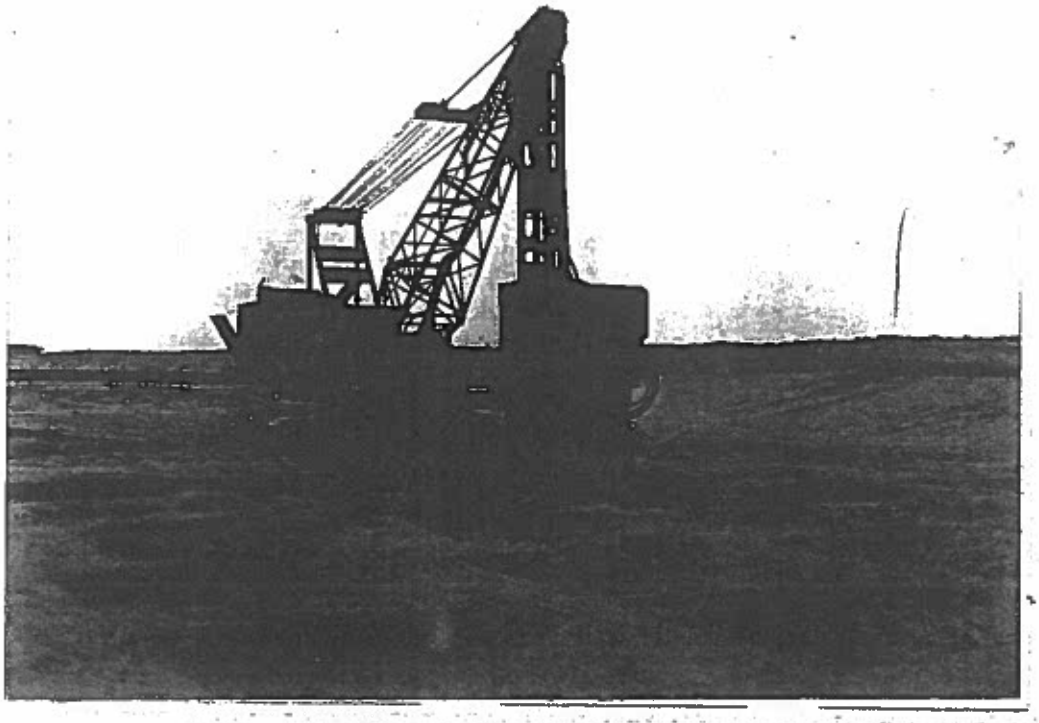

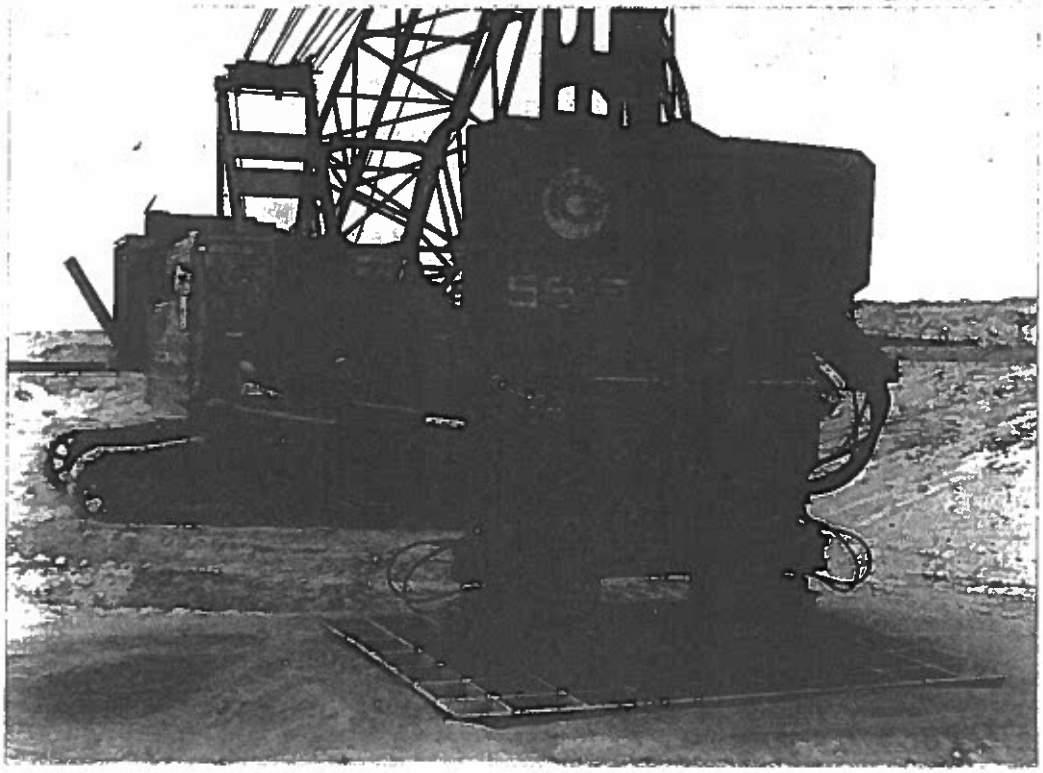

AARSLEFF

NYSTED HAVMØLLEPARK VED RØDSAND

RESULTATER FRA KOMPRIMERINGSFORSØG I TESTPIT VED GEDSER

september 2002

FORELØBIG UDGAVE

Formål

For at teste udbudsmaterialets krav til udførelse af nedre komprimerede skærvepuder etableredes i Gedser ved lystbådehavnen tæt på strandkanten en testpit (bilag 1).

I testpitten blev udlagt en skærvepude, hvor såvel udlægning som komprimering blev foretaget under vand for at forsøget skulle ske under samme betingelser som udførelse ved de aktuelle fundamenter.

Der er testet densiteter før og efter kompimering og der er udført pladebelastningsforsøg på puden.

Krav til skærvepude

Udover designkravene skal følgende minimumskrav til effektiv friktionsvinkel og Youngs modul opfyldes ved de designrelevante spændinger og acceptable deformationer:

- Triaksial sekant friktionsvinkel $\varphi'_{tr,s}>40^{\circ}$
- Youngs modul ved 50% brudgrad $E_{50}>20$ MPa

For ikke komprimeret skærvepude er designforudsætningerne:

- Rumvægt total $\gamma_m = 19$ kN/m3
- Rumvægt effektiv $\gamma' = 9$ kN/m3
- Karakteristisk plan friktionsvinkel $\varphi_{pl,k} = 40^{\circ}$
- Deformationsparametre G = 6MPa , E = 15 MPa , K = 18 MPa

For komprimeret nedre skærvepude er designforudsætningerne:

- Rumvægt total $\gamma_m = 20$ kN/m3
- Rumvægt effektiv $\gamma' = 10$ kN/m3
- Karakteristisk plan friktionsvinkel $\varphi_{pl,k} = 45^{\circ}$
- Deformationsparametre G = 25MPa , E = 62 MPa , K = 75 MPa

Udførelse af testpit

Der blev udført en cirkulær spunset fangedæmning med diameter ca. 16m med topkote ca. 3,0m og spidskote ca. –7,0m. Jordbunden bestod af sand. For adgang til cellefangedæmningen blev spunsen skåret i terrænniveau i kote ca. 1m i en åbning på ca. 4m. Herefter blev der udgravet inde i cellen til kote ca. –2,75m samtidig med sænkning af vandstanden til udgravningskoten.

Der blev udført et måleprogram inden indfyldning af skærver bestående af nivellement af udgravningsbund samt måling af celldiameteren i såvel udgravningskote som i kote ca. 0m.

Der blev på bunden udlagt en 1x1m 20 mm tyk stålplade svejset på et 3" rør (for styring og måling) (bilag 2).

Der blev nedsat 5 stk 3" rør i bunden ragende op til kote ca. 0m for senere måling af densiteter igennem skærveopfyldningen (bilag 2).

Pitten fyldtes med vand til kote ca. 0m og skærver blev udlagt under vand op til kote ca. 0m og rettet af.

Aluminiumsrør (hvori densiteter måles) blev monteret i 3" stålrør, hvorefter disse blev trukket op.

Densiteten gennem laget før komprimering blev målt i de 5 rør.

Åbningen i spunsen blev lukket og der indfyldtes vand til spunstop og komprimering blev foretaget i henhold til proceduren herfor.

Vandet sænkedes til skærveoverfladen og pladebelastningsforsøgene udførtes. Densiteten gennem laget efter komprimering blev målt i de 5 rør. Celldiametre efter komprimering blev opmålt.

Cellen blev tømt for skærver og sætningspladen nivelleret. Celldiametre ved udgravningsbund blev opmålt.

Skærvepude

Skærveleverancen kommer fra Rønne på Bornholm. Materialet er granit og kornkurven ligger inden for grænserne vist på bilag 3.

Skærvepuden udlægges og komprimeres i lag af 3m eller derunder.

Der blev efter anmning af skib med skærveleverancen målt en indfyldt skærvemængde på 950 tons.

Komprimeringsmateriel

Der anvendtes en ICE-416 vibrator med trinløs frekvensregulering påmonteret en perforeret stålplade 2,6 x 2,1 x 0,075 m. Data for vibrator og stålplade fremgår af bilag 4 og 5. Vibrator blev ophængt i en mobilkran.

Komprimeringsprocedure

Hele overfladen komprimeres af 2 omgange.

I første runde komprimeres over en periode på ca. 1 minut hvert sted, idet komprimering over yderligere tid ikke medfører forbedringer af materialet af relevant betydning.

Som resultat af første runde er det udlagte lags styrke og stivhed forøget tilstrækkeligt til, at der kan foretages en effektiv komprimering i anden runde.

Efter at hele voluminet af det udlagte lag er komprimeret i første runde, komprimeres hele voluminet af et lag igen i anden runde, men nu med en større frekvens.

Hensigten med anden runde er at opnå, at jordoverflade og plade i et vist omfang kommer i modfase, med det resultat, at der nu sker en effektiv komprimering.

Modfase betyder, at de effektive spidsbelastninger stiger voldsomt med øget frekvens. Der tilstræbes, at lastintensiteten i anden fase er af størrelsesordenen 3 gange lastintensiteten anvendt i første fase. Dette vil formentlig kunne opnås ved en frekvens som er af størrelsesordenen 1,5 større end den, der anvendtes i første runde.

Den præcise frekvens fastlægges indledningsvis ved forsøg.

I anden runde tilstræbes en så god komprimering som muligt. Derfor komprimeres hvert sted i 4 minutter, idet der er erfaring for, at der ikke sker en forøgelse af tætheden af gruspuden efter 3-5 minutters komprimering.

For hver placering af pladen foregik selve komprimeringen, som følger.

- Pladen placeres på den ukomprimerede overflade
- Vibrationen sættes i gang med frekvens på 12Hz
- Efter 1 minut (første runde) komprimering stoppes vibratoren og flyttes til næste komprimeringsposition og således dækkes hele overfladen
- Dernæst komprimeres overfladen efter samme procedure i 4 minutter i hver position med frekvens 18 Hz (anden runde)

Kontrolmålinger

Pladebelastningsforsøg

Der blev udført 3 pladebelastningsforsøg på skærvepuden med grundvandsspejl i skærveoverfladen (bilag 6):

Pladebelastningsforsøg nr. 1 udførtes på 300mm løs udlagt skærvepude ovenpå den komprimerede overflade svarende til projektets løst udlagte pude, hvorpå fundamentet placeres.

Pladebelastningsforsøg nr. 2 udførtes direkte på den komprimerede overflade.

Pladebelastningsforsøg nr. 3 udførtes på udgravet overflade 1m under komprimeret overflade.

Forsøgene er alle udført med diameter 0,6m plade. Der blev aflastet og genbelastet ved 20, 40 og 60 kN.

Forsøgsresultaterne fremgår af bilag 7, 8 og 9.

- I forsøg nr. 1 er belastning oppe på 108 kN uden brud, hvilket kan omregnes til, at $\varphi_{pl,k}$ er større end 45°.
- I forsøg nr. 3 er belastning oppe på 145 kN uden brud, hvilket kan omregnes til, at $\varphi_{pl,k}$ er større end 47°. Der er heller ikke opnået brud i de øvrige forsøg, så kravene til friktionsvinkel er opfyldt.
- E-modul er for løst udlagt skærvepude i forsøg nr. 1 i alle genbelastningsgrene (64 MN/m2) over de 20 MN/m2, som var kravet i udbudsmaterialet. På komprimeret skærvepude i forsøg nr. 2 og 3 er E-modulet i alle genbelastningsgrene (79,5 – 227 MN/m2) over de 62MN/m2, som var forudsat i beregninger.

Densitetsmålinger

Densitetsmålinger udførtes med en "Depth Moisture / Density Probe" som beskrevet i bilag 10.

Resultaterne fra de 5 nedsatte rør ses af bilag 11.

Det ses, at densiteten er ret ensartet ned gennem laget både før og efter komprimeringen. Der er målt en stigning i densiteten fra gennemsnitlig 1,948 til 2,054 ton/m3.

Komprimeringen har virket over hele lagets tykkelse.

Ved opmåling af volumen af skærvelaget før og efter komprimering kan beregnes en densitetsstigning fra 2,077 (beregnet efter indfyldt mængde) til 2,278 ton/m3 (bilag 12).

Ved vibrationsindstampning er målt en tørdensitet på 2,094 t/m3 og en vandmættet densitet på 2,324 t/m3. Den opnåede komprimeringsgrad beregnet som tørdensitet af komprimeret materiale i forhold til tørdensitet af den vibrationsindstampede prøve er 96,5% regnet over hele lagets tykkelse.

Det kan konkluderes at der må være en fejl i kalibreringen af densitetsmåleren, men at resultaterne viser at komprimeringen har haft god og ensartet effekt gennem hele laget.

Testpit i Gedser

Bilag 1

Sætningsplade

Rør for densitetsmåling

Testpit i Gedser

Bilag 2

Bilag 3

NCC

BLÅ RØNNE

RÅSTOFFER

PRODUKTTEKNISKE SPECIFIKATIONER

RØNNE GRANITVÆRK

Granitten Blå Rønne er siden 1873 blevet brudt på Snorrebakken ved Rønne, Bornholm.
Blå Rønne er kendt vidt omkring på grund af granittens tekniske egenskaber: høj styrke og holdbarhed.

Blå Rønne er meget velegnet til beton, asfaltfremstilling samt andre anlægsopgaver, idet parametre som styrke, stabilitet og vedhæftningsevne er helt i top.

Til betonfremstilling har Blå Rønne også vist sit værd – blandt andet er tunnelen og pylonerne på Storebæltsbroen støbt med denne granit.

Blå Rønne er godkendt i Danmark af Dansk Grus Certificering til højeste miljøklasse: kl. E iht. DS 481.

Dansk Grus Certificering

Egenskaber
Bjergart: Rønne Granit

Farve	Blå-sort
Densitet	2,72 g/m³
Kubisitet	88%
Absorbtion	0,70%
ASTM C 1260-94	0,01%
Lette korn < 2.500 kg/m³	0,01%
Chloridindhold	0,00%
Flisethed	1,35
Sprødhedstal	30

Alle værdier er tilnærmede og deklarationer kan rekvireres.

ISO 14001

Miljøcertificeret efter ISO 14001

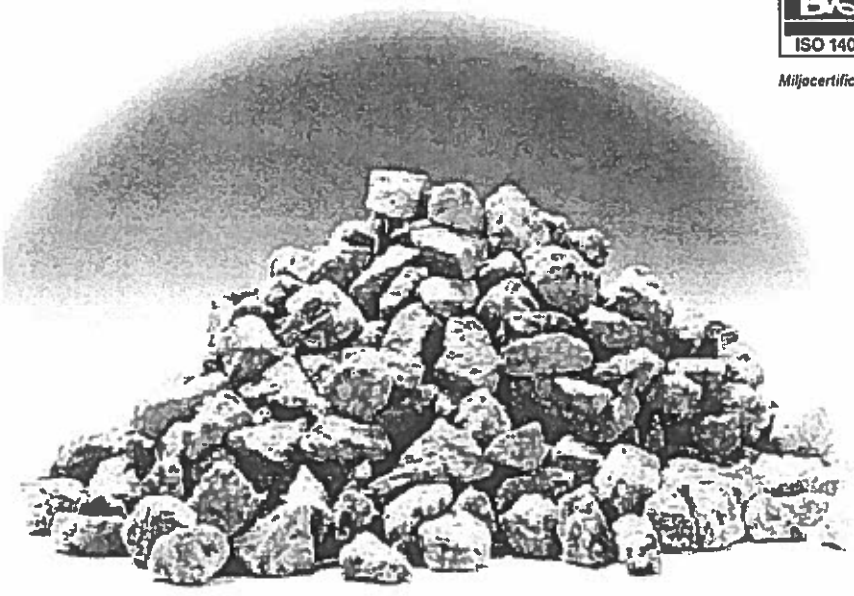

NCC

Kornstørrelse (mm)	Vægtprocent (%)
90	100
63	80-100
32	55-80
16	33-57
8	18-38
4	8-20
2	0-10
1	0-4
0,074	0-2

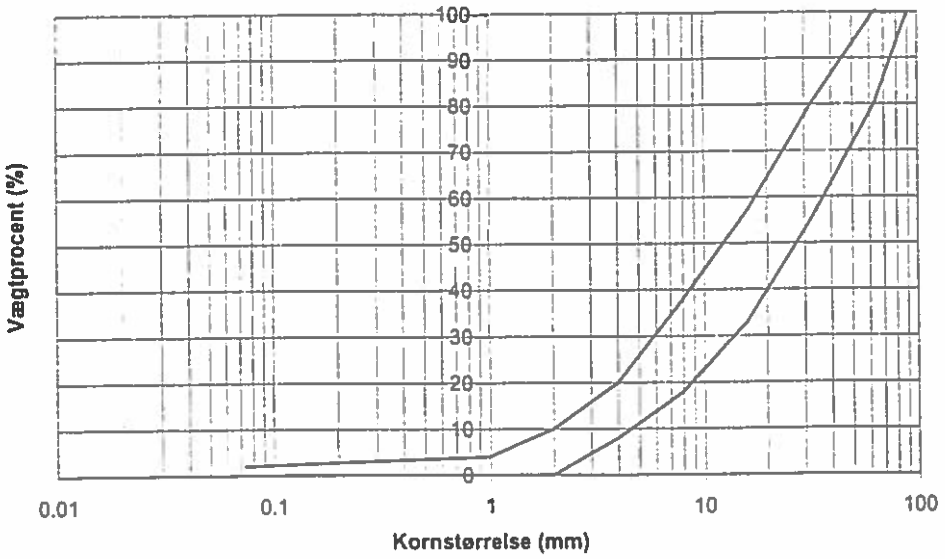

Bilag 3

Hefbrugweg 6 (De Vaart)
1332 AN ALMERE, Holland
Tel. : 036-5320560
Telex: 47162 ICE NL
Fax : 036-5320401

info

INFO416.E/0894

ICE-416

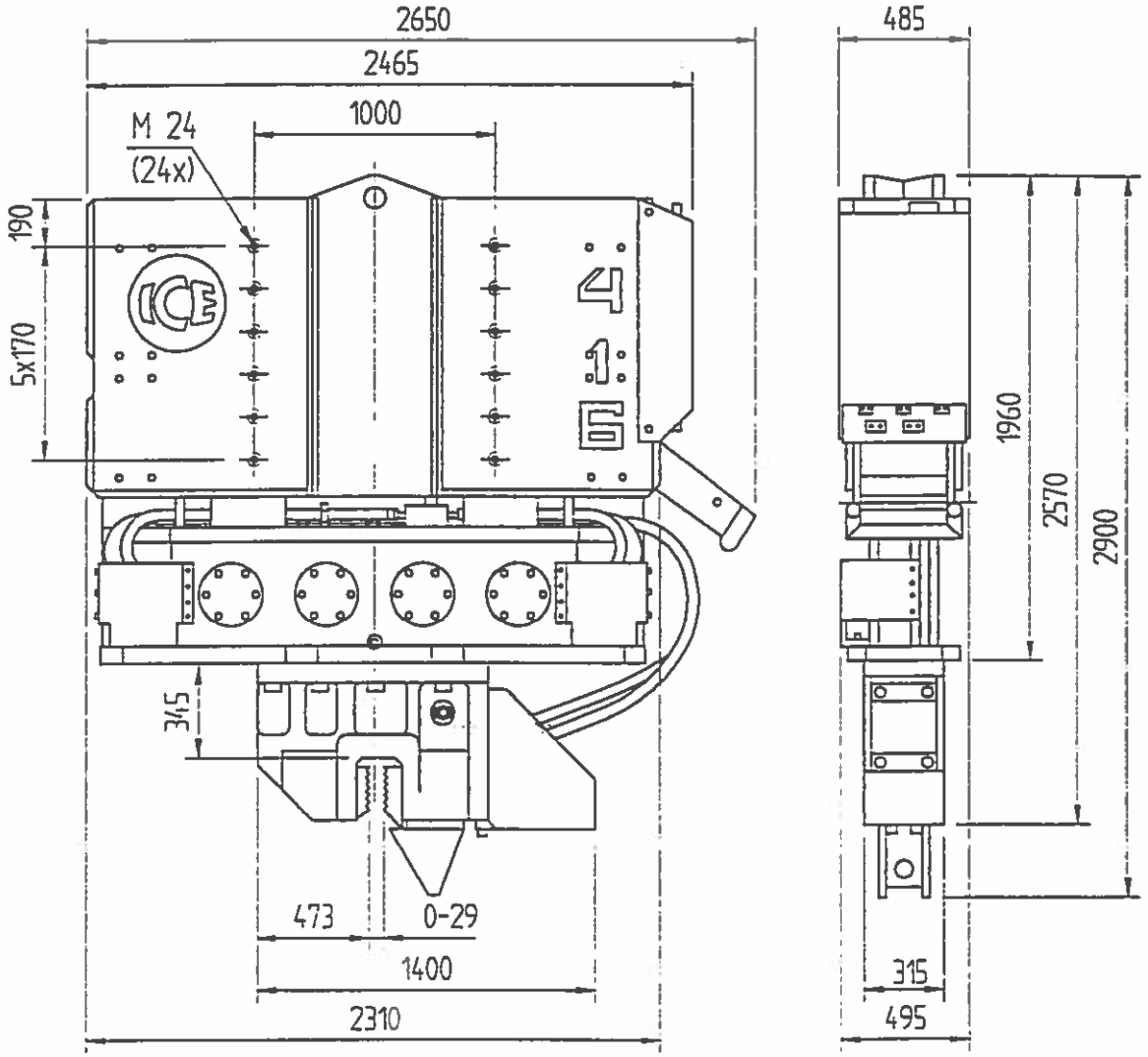

Specifications:			
Eccentric moment	:	23	kgm
Max. centrifugal force	:	645	kN
Max. frequency	:	1600	RPM
Max. amplitude excl. 126TU	:	18	mm
Max. amplitude incl. 126TU	:	13	mm
Max. static linepull	:	400	kN
Max. hydraulic power	:	193/262	kW/HP
Max. operating pressure	:	340	bar
Max. oil flow	:	340	l/min
Dyn. weight excl. 126TU	:	2500	kg
Dyn. weight incl. 126TU	:	3450	kg
Total weight incl.126TU	:	5950	kg
Transportation weight	:	6300	kg

Clamps:	
Universal	: 126 TU
Weight	: 950 kg
Caisson cl.	:2x80 TC
Weight	:1350 kg

Powerpack:	
Model	:ICE 300
Power kW/HP	:224/305
Weight	:4700 kg

Bilag 4

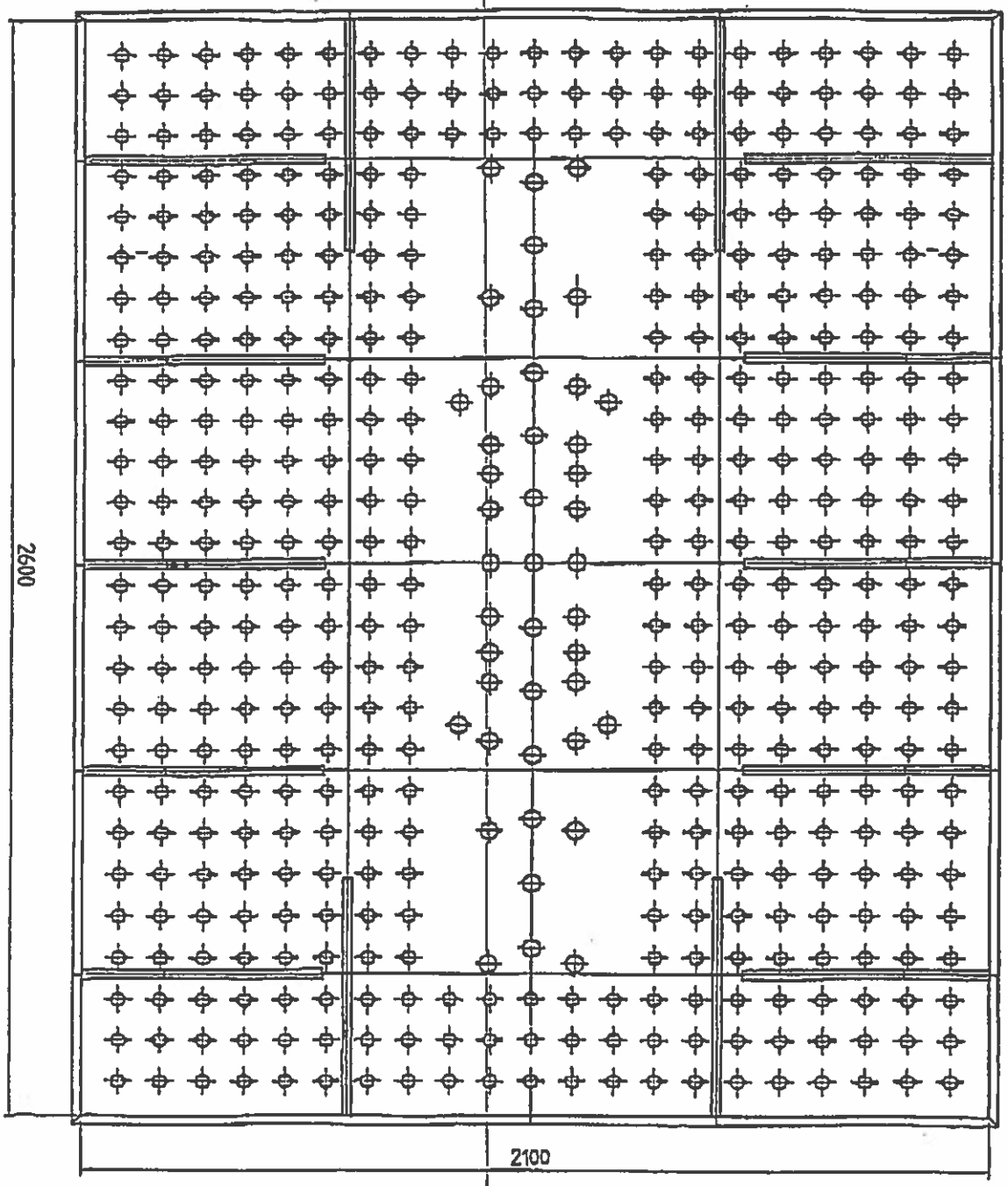

Bilag 5

Pladebelastningsforsøg på overfladen

Pladebelastningsforsøg 1m under overflade

Vibrator ophængt i kran

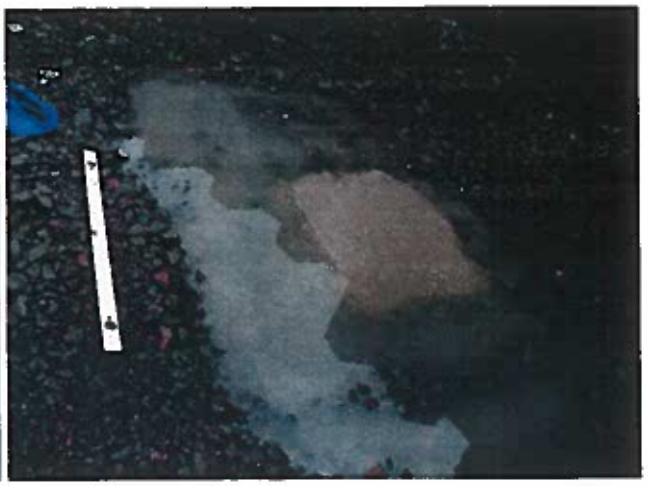

Overflade klargjort til pladebelastningsforsøg

Pladebelastningsforsøg i testpit

Bilag 6

Pladebelastningsforsøg i tespit ved Gedser

Formel: E0 = 1,5 * sigma * r / s0

sigma	pladetryk
r	pladeradius
s0	flytning

Forsøg 1 på løst udlagt 0,3m skærvepude på komprimeret nedre skærvepude

	r	P	sigma	s0	E0
Begyndelses E	0,3	0,02	0,070736	0,0035	**9,094568**
1. Genbelastn. E	0,3	0,02	0,070736	0,0005	**63,66198**
2. Genbelastn. E	0,3	0,04	0,141471	0,001	**63,66198**
3. Genbelastn. E	0,3	0,06	0,212207	0,0013	**73,45613**

Forsøg 2 på overflade komprimeret skærvepude

	r	P	sigma	s0	E0
Begyndelses E	0,3	0,02	0,070736	0,0014	**22,73642**
1. Genbelastn. E	0,3	0,02	0,070736	0,00014	**227,3642**
2. Genbelastn. E	0,3	0,04	0,141471	0,00035	**181,8914**
3. Genbelastn. E	0,3	0,06	0,212207	0,00051	**187,2411**

Forsøg 3 på overflade 1m under top af komprimeret skærvepude

	r	P	sigma	s0	E0
Begyndelses E	0,3	0,02	0,070736	0,0016	**19,89437**
1. Genbelastn. E	0,3	0,02	0,070736	0,0004	**79,57747**
2. Genbelastn. E	0,3	0,04	0,141471	0,0006	**106,1033**
3. Genbelastn. E	0,3	0,06	0,212207	0,0009	**106,1033**

Bilag 6

Pladebelastningsforsøg nr. 1

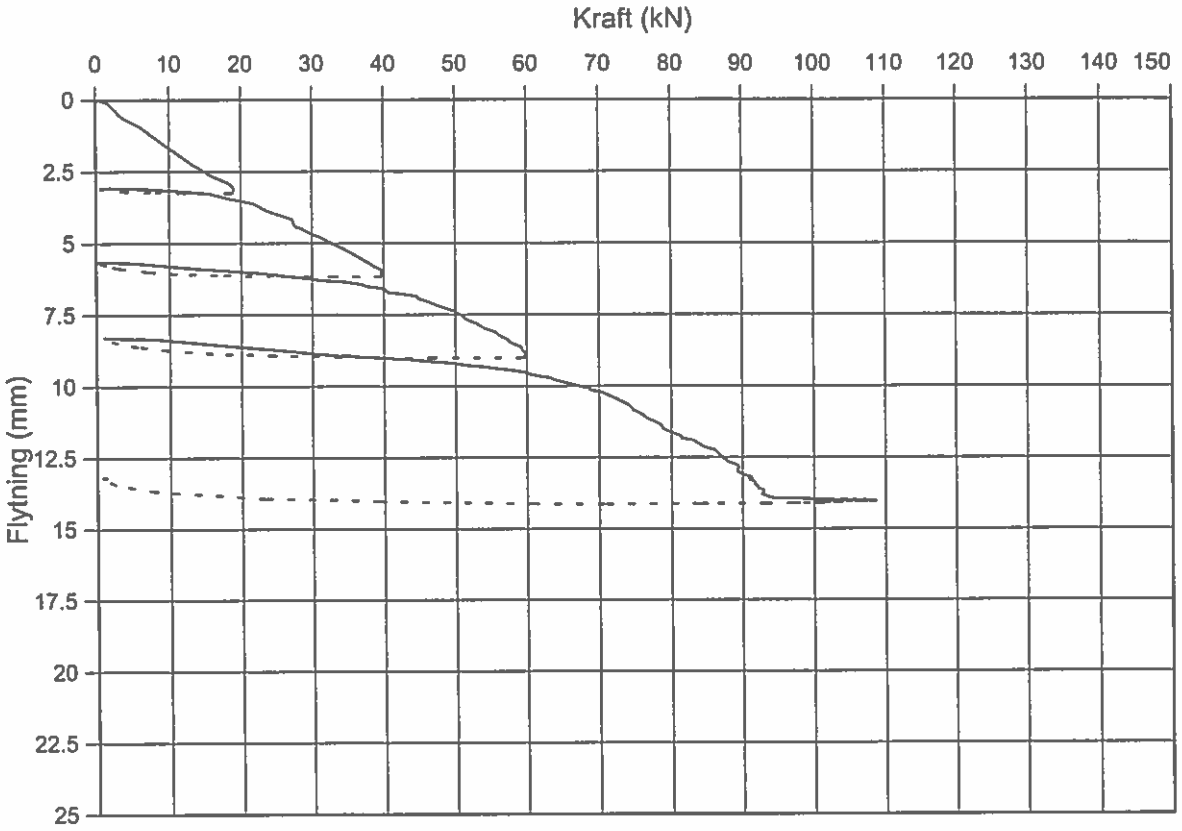

Fundament : L-	Udført af : BON-LEJ
Pladediameter : 600 mm	Dato : 2002-08-26

GEO Geoteknisk Institut — Projekt : 22741.50.1 Rødsand

Udført	: bon	Dato: 26-08-02	Emne : Belastningsforsøg L-01		
Kontrolleret	: HGR	Dato:			Side 1 / 1
Godkendt	: JBC	Dato:	Rapport: 1	Bilag 1	Rev.

Bilag 7

Pladebelastningsforsøg nr. 2

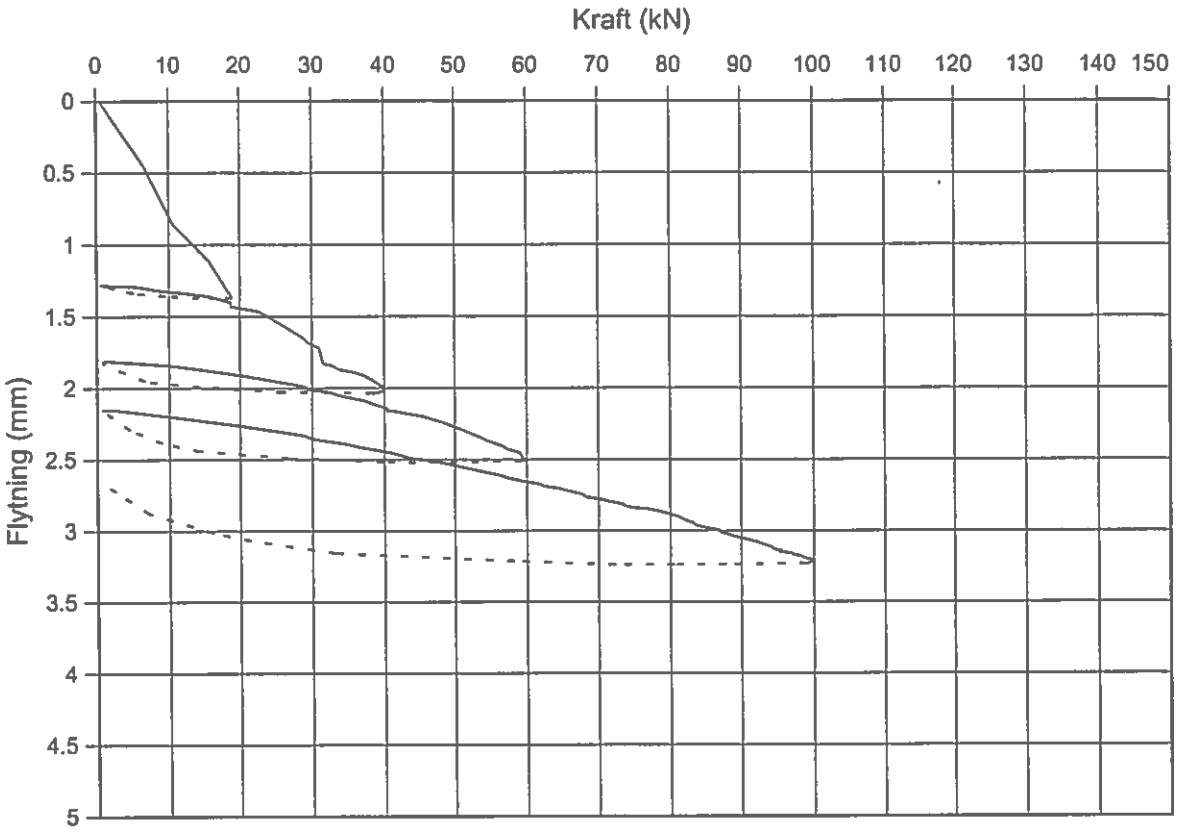

Fundament : L-	Udført af : BON-LEJ
Pladediameter : 600 mm	Dato : 2002-08-26

GEO Geoteknisk Institut — Projekt : 22741.50.1 Rødsand

Udført	: bon	Dato: 26-08-02	Emne : Belastningsforsøg L-02		
Kontrolleret	: HGR	Dato:			Side 1 / 1
Godkendt	: JBC	Dato:	Rapport: 1	Bilag 2	Rev.

Bilag 8

Pladebelastningsforsøg nr. 3

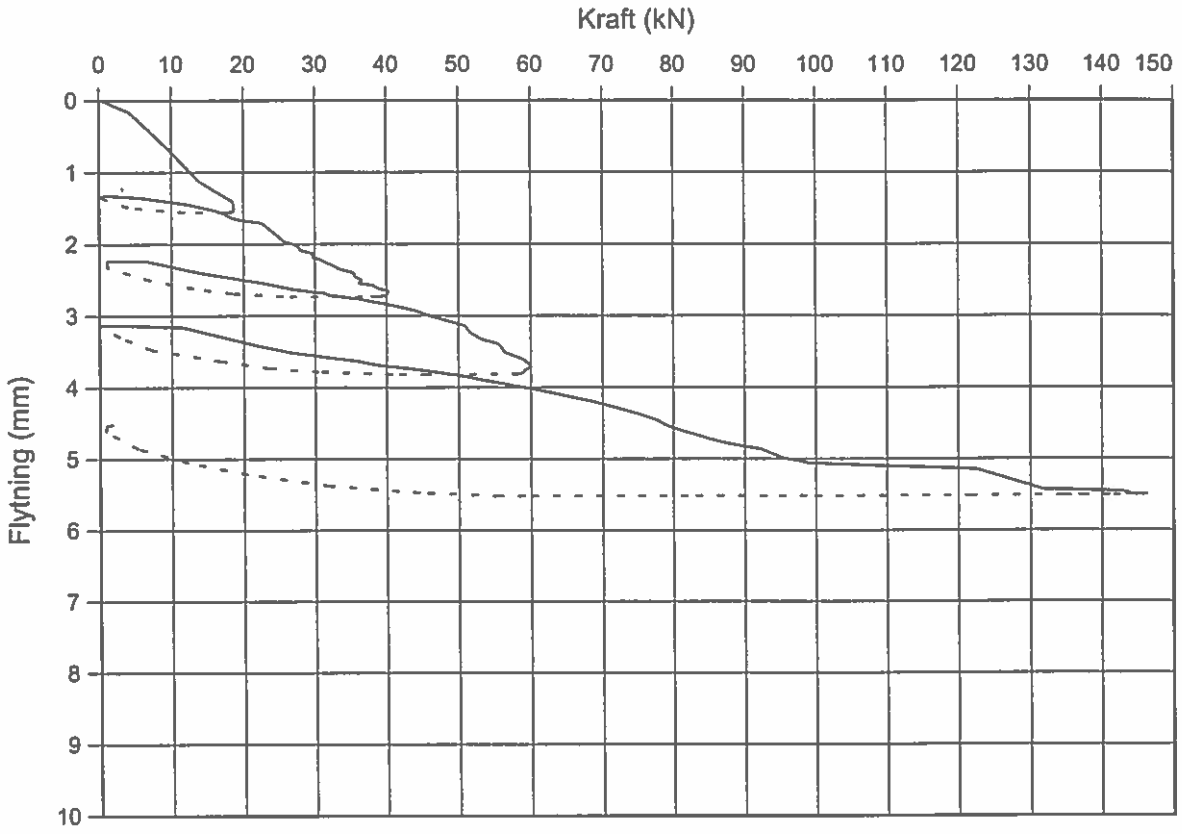

Fundament	: L-	Udført af	: BON-LEJ
Pladediameter	: 600 mm	Dato	: 2002-08-26

CEO Geoteknisk Institut

Projekt : 22741.50.1 Rødsand

Udført	: bon	Dato: 26-08-02	Emne : Belastningsforsøg L-03		
Kontrolleret	: HGR	Dato:			Side 1 / 1
Godkendt	: JBC	Dato:	Rapport: 1	Bilag 3	Rev.

Bilag 9

Bilag 10

Soil moisture and density measurements

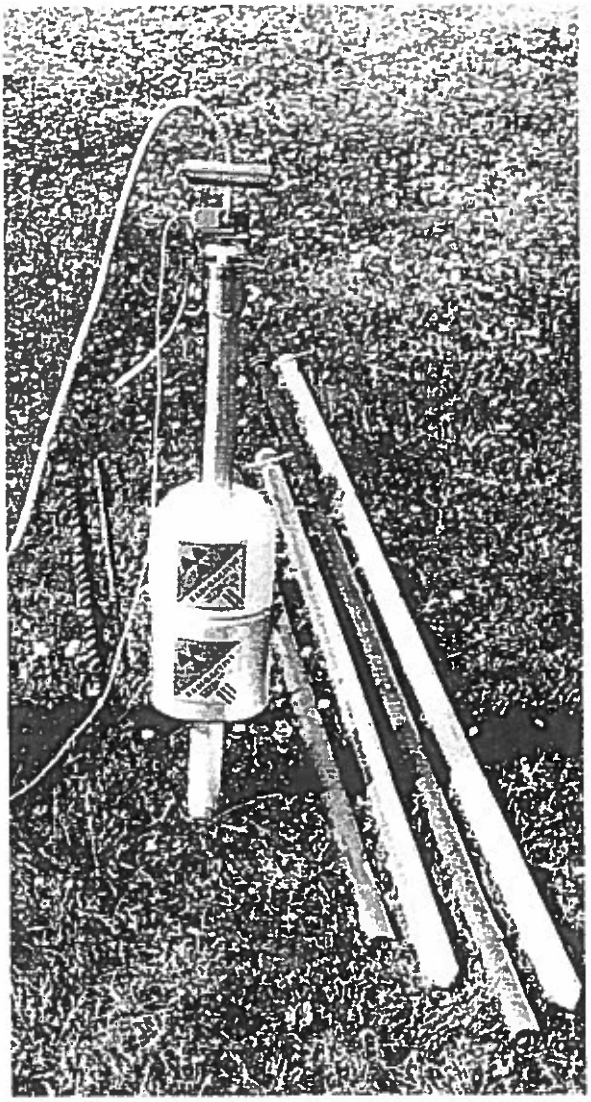

Agriculture

Determination of need for irrigation or drainage
Study of soil moisture/plant Growth relationships

Hydrology

Water balance measurements

Geology

Water balance measurements
Determination of porosity

Industry

Ask for special industry equipments

Description

Today the Depth Moisture/Density Probe is used in more than 40 countries. This is mostly because it is a very stable probe which measures with a very high accuracy. The combination of both moisture and density measurings in the same probe also makes it cheap to buy. The probe is portable and because the density part of the probe is easily detached, when not in use, it is quite handy. The density measurings are only made in newly drilled holes to find the dry density of the soil and as dry density normally not change from time to time the density which is once found normally will be the same for the rest of the time.

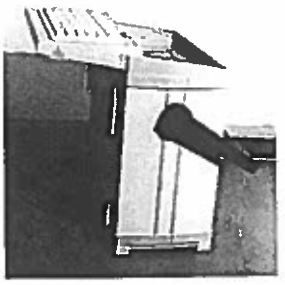

NUCLETRONICS ApS
Klintevej 526 • Magleby, DK 4791 Borre

Tel: +45 5581 2074
Fax: +45 5581 2274
Mobil: +45 2021 6559
E-mail: hub@nucle.dk

Method

Moisture measurements

Fast neutrons emitted from the neutron source penetrate into the surroundings of the probe. Neutrons rebound when hitting atoms. In collision with hydrogen atoms neutrons lose energy and they are slowed down. Hydrogen is a constituent of water. In soil and many other materials water is generally the only source of hydrogen. Some of the neutrons slowed down by hydrogen reach the lithium glass scintillator which emits light flashes when hit by a slow neutron. This light flashes are converted into electric pulses by the photomultiplier. The pulses are counted by the instrument. An increase in moisture content gives an increase in the number of slow neutrons scattered back into the scintillator and this gives an increase in the count rate.

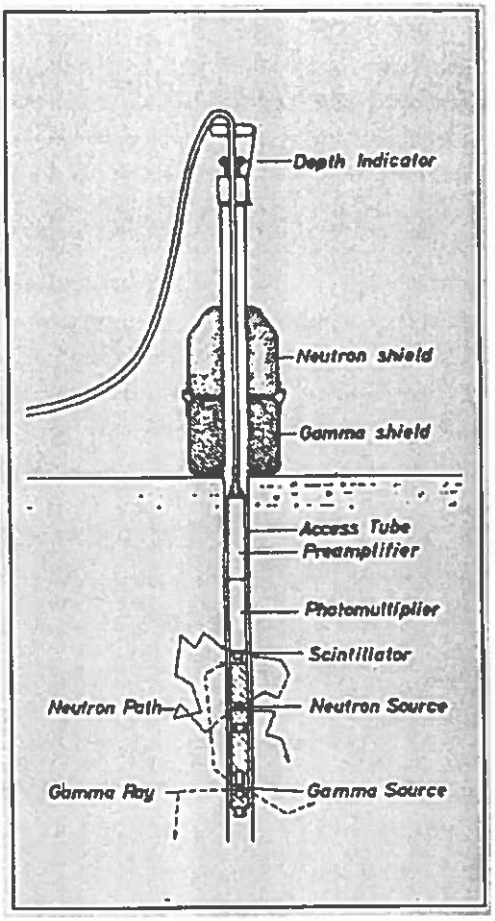

Density measurements

Gamma radiation emitted from the gamma source penetrates into the surroundings of the probe. Gamma radiation can either be scattered or absorbed when hittings atoms. Some of the gamma radiation scattered back from the material surrounding the probe hits the lithium glass scintillator and cause ligth flashes which are converted into electric pulses by the photomultiplier. An increase in soil density causes an increase in the absorption of gamma radiation and less gamma radiation reaches the scintillator. The intensity of the light flashes due to gamma radiation is much smaller than the intensity of ligth flashes due to neutrons.

The electric pulses from the photomultiplier have a pulse high proportional to the intensity of the ligth flashes. Thus, neutrons (due to moisture) give large electric pulses, while gamma radiation (giving information about density) gives small electic pulses. By means of a pulse height analyzer either the large or small pulses are counted.

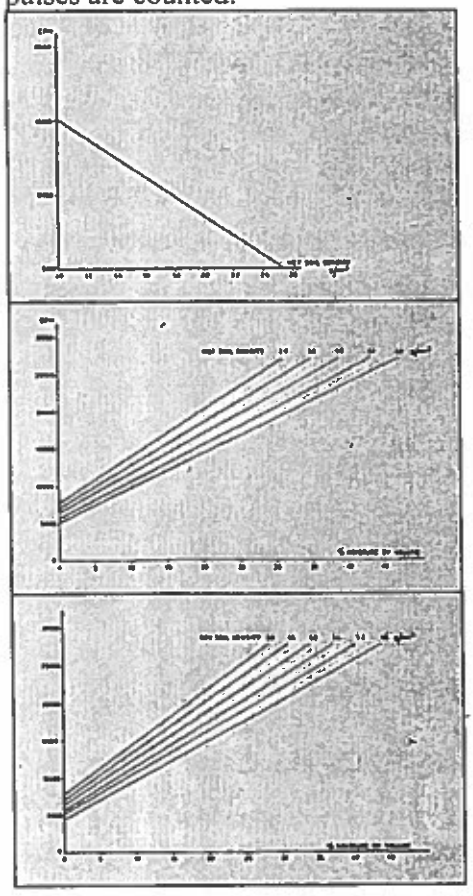

Calibration

Together with the probes, calibration curves are delivered for each probe so that the measurings can be made immediately after the equipment is received. No time is needed to make calibration curves for each measuring purpose.

As it appears from the calibration curves the calibration depends to some extent on soil density. This is an inherent of the neutron method for moisture measurements. The error is not very significant if only moisture changes have to be measured, but if high accuracy is required or absolute measurements are needed, it is necessary to take soil density into consideration. This is done in a very simple way with the equipment. The first time a measurement takes place in an access tube, both moisture and wet density are measured with the combined probe.

From the moisture calibration curve with wet density as parameter the moisture volume fraction is determined. By subtracting this from the wet density the dry density is obtained. In most natural soils dry density does not change with time and moisture variations.

The moisture probe has been specially designed to give the highest possible resolution for moisture variations with depth, alinear calibration curve over a large range of moisture contens, an excellent sensitivity and a comparatively small influence of soil composition and density.

Operation

Insertion of access tubes

Particularly in cases where long-term measurements or measurements of a moisture/density profile are to be made, aluminium access tubes, 45 mm in diameter are used. Depending on the type of soil they are driven into the ground or inserted into a bore hole. Access tubes, equipment for insertion and removal of access tubes and hand drilling equipment with soil auger for aluminium tubes can be supplied.

Specifications

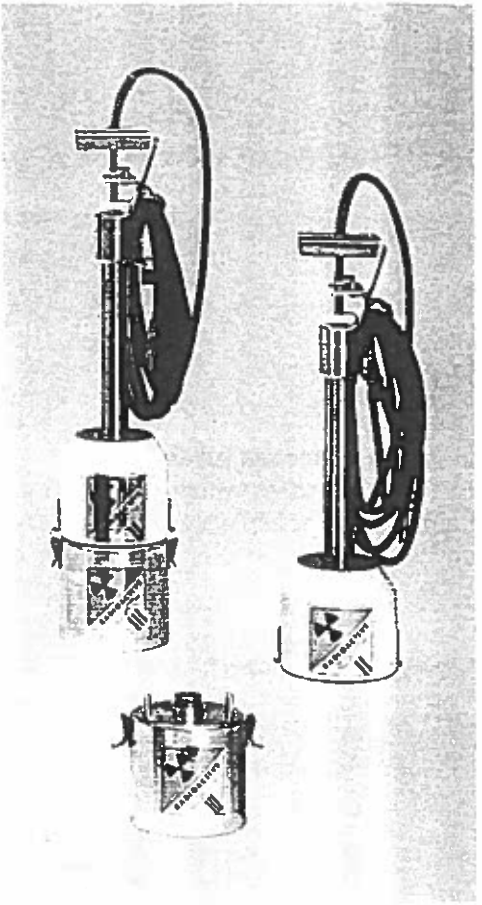

Moisture Probe for Depth Measurements

Source: 1110 MBq Americium-241/Beryllium, halflife 460 years
Detector: Glass Scintillator, containing lithium, enriched 96% in Li-6
Max. temperature: 50 dgrees C - Range: 0-100% Moisture
Sensitivity: About 700 counts per minute per % moisture by volume
Dimensions: Probe diameter: 38 mm, length: 440 mm
Shield and Transport Container height: 600 mm, max diam.: 170 mm
Weight: Transport Container and Probe: 8,7 Kg Supplied Complete with 6 m cable with plug, instruction manual, individual Calibration curve. Other cable length optional.

Gamma Source Unit for Density Measurements

Source: 37MBq Caesium-137, halflife 30 years
Dimensions: diameter: 38 mm, length for combined moisture and density: 580 mm
Gamma Source Shield and Transport Container diam.: 170 mm height: 155 mm
Weight: Gamma Source Unit and Shield Container: 8.6 Kg
Supplied Complete with individual calibration curve. This unit is optional.

Accessories

Standard Access Tubes Aluminium tube with conical aluminium head and rubber stopper, diameter 42 mm internal 45 mm external
Standard lengths: 2 and 3 m. Other lengths optional
Device for driving access tubes into soil: Steel tube fitting into the access tube with sleeve holding the open end of the access tube and handle
Device for withdrawal of access tubes after use: Expansion bolt with eye
Hand Drilling Equipment with Soil Auger for Aluminium tube.

Radiation safety

The tables gives the maximum radiation dose rate in µSv per hour at any point at a given distance from the surface of (1)the unshielded probe and (2)the transportcontainer with the probe. The dose rate values have been determined by adding the separately measured dose rates for fast neutrons, slow neutrons and gamma radiation. When in use the moisture probe is either in its shield or in soil. Thus, even in full time work with the equipment the actual dose rates received are without any difficulty kept far below 300 µSv per week which is the maximum permissible average dose rate according to the international Commission on Radiological Protection.

Gamma source unit for density measurements

	Distance from surface in cm					
Maximum dose rate in µSv per hour	0	10	25	50	75	100
Unshielded unit	2200	200	30	10	5	2
Shield Con. with Gamma Source Unit	200	50	10	3	2	1

Moisture Probe

	Distance from surface in cm					
Maximum dose rate in µSv per hour	0	10	25	50	75	100
Unshielded probe	1650	130	70	15	5	3
Shield Container With Probe	90	45	15	3	1	0

Densitetsmålinger udført d. 22/8 inden komprimering af 2.7 m stenpude ved lystbådehavn i Gedser

dybde	Rør 1		Rør 2		Rør 3		Rør 4		Rør 5		gennemsnit
m	tælletal	densitet	tælletal	densitet	tælletal	densitet	tælletal	densitet	tælletal	densitet	densitet
0,5	21844	1,892508	21684	1,900118	21455	1,910963	21431	1,912096	21324	1,917142	1,907
1	20991	1,932767	19863	1,984827	21220	1,922034	21194	1,923255	20519	1,954714	1,944
1,5	20543	1,953604	21155	1,925086	21158	1,924945	20522	1,954575	20737	1,944607	1,941
2	20838	1,939907	21207	1,922645	22428	1,864504	21712	1,898788	20430	1,958826	1,917
2,5	19616	1,996048	19757	1,989651	19410	2,005358	17298	2,098222	17714	2,080302	2,034
Gennemsnit		1,943		1,944		1,926		1,957		1,971	1,948

Densitetsmålinger udført d. 26/8 efter komprimering af 2.7 m stenpude ved lystbådehavn i Gedser

dybde	Rør 1		Rør 2		Rør 3		Rør 4		Rør 5		gennemsnit
m	tælletal	densitet	tælletal	densitet	tælletal	densitet	tælletal	densitet	tælletal	densitet	
0,5	18726	2,035947	18628	2,04029	19057	2,021206	18137	2,061894	18102	2,063424	2,045
1	18689	2,037588	17709	2,080518	18903	2,028079	18225	2,05804	18026	2,066742	2,054
1,5	18025	2,066786	17144	2,104809	20346	1,9627	18936	2,026608	18068	2,064909	2,045
2	19847	1,985556	18742	2,035237	16458	2,133851	17378	2,09479	16823	2,11846	2,074
Gennemsnit		2,031		2,065		2,036		2,060		2,078	2,054

Bilag 11

Densitetsmålinger i testpit ved Gedser

Geometrisk opmåling

	Topkote	Bundkote	Lagtykkelse	Middel diameter	Volumen	Ammet vægt	Kornandel	Vandmættet densitet	Tørdensitet	Komprimeringsgrad
	m	m	m	m	m3	tons	%	T/m3	T/m3	%
Før komprimering	0,05	-2,77	2,82	15,873	558,029325	950	62,58895191	2,076529973	1,70241949	81,29988
Efter komprimering	-0,44	-2,81	2,37	15,889	469,928038	950	74,32301924	2,278355931	2,02158612	96,54184

Ved vibrationsindstampning er målt en tørdensitet på 2,094 t/m3, som danner grundlag for beregning af komprimeringsgrad
Krav til komprimering af SG i vejbygning ved en vibrationsindstampning er 95%
Vægt af indfyldt stenmateriale er bestemt ved amning af skib

Følsomhedsanalyse på vægtmålet

Max. Hulrumsprocent på 40% efter udlægning

	Topkote	Bundkote	Lagtykkelse	Middel diameter	Volumen	Ammet vægt	Kornandel	Vandmættet densitet	Tørdensitet	Komprimeringsgrad
	m	m	m	m	m3	tons	%	T/m3	T/m3	%
Før komprimering	0,05	-2,77	2,82	15,873	558,029325	911	60,01951072	2,032335584	1,63253069	77,96231
Efter komprimering	-0,44	-2,81	2,37	15,889	469,928038	911	71,27186372	2,225876056	1,93859469	92,57854

Min. Hulrumsprocent på 35% efter udlægning

	Topkote	Bundkote	Lagtykkelse	Middel diameter	Volumen	Ammet vægt	Kornandel	Vandmættet densitet	Tørdensitet	Komprimeringsgrad
	m	m	m	m	m3	tons	%	T/m3	T/m3	%
Før komprimering	0,05	-2,77	2,82	15,873	558,029325	987	65,02662688	2,118457982	1,76872425	84,4663
Efter komprimering	-0,44	-2,81	2,37	15,889	469,928038	987	77,21770526	2,32814453	2,10032158	100,3019

Denne analyse sandsynliggør at den ammede mængde på 950 tons er korrekt, og at den højst sandsynligt ligger mellem 911 og 987 tons.

Bilag 12

Research at DTU on Liquefaction around Marine Structures

B. Mutlu Sumer and Jørgen Fredsøe

DTU, MEK, Coastal and River Engineering (formerly ISVA)

Outline

1. Liquefaction processes under waves. A brief description!
2. Research on wave-induced liquefaction at DTU, MEK, Vandbygning (Coastal and River Engineering Section; formerly ISVA)
3. LIMAS (Liquefaction Around Marine Structures), a European-Union FP5 project that we are coordinating!

Liquefaction processes under waves. Definition

- Soft marine soils under high waves may undergo a process
- in which the soil grains become completely free, and
- the water-sediment mixture, as a whole, acts like a fluid!
- This process is called liquefaction.
- Under the liquefaction condition, obviously the soil fails!

Consequences. With the soil liquefied,

- Buried pipelines may float to the surface of the seabed;
- Pipelines laid on the seabed may sink in the soil;
- Large individual blocks (like those used for scour protection) may penetrate into the seabed;
- Sea mines may enter into the seabed and eventually disappear;
- Or, an indirect effect: As a result of the wave motion, structures may execute cyclic motions, resulting in local liquefaction around them, which may enhance scour, thus leading to the instability of the structures;
- Sometimes, we use wave-induced liquefaction to our end, to compact sand (as was done by LICengineering A/S in combination with soil replacement in an engineering exercise!)

Waves (for those who are not terribly familiar with waves)?

- In coastal areas, Wave height = O(1-2 m)
- In offshore areas, with water depth of 60-70 m, for example, wave height for 50-100 years return period = O(10-20 m) are not unusual!
- Wave period = O(5-15 s)!

Two kinds of wave liquefaction

- Liquefaction induced by the buildup of pore pressure, called the Residual Liquefaction
- Liquefaction induced by the upward-directed pressure gradient, called the Momentary Liquefaction

Residual Liquefaction

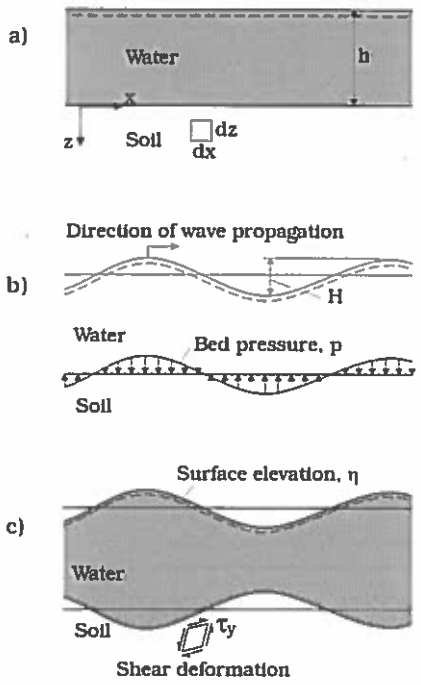

Residual Liquefaction

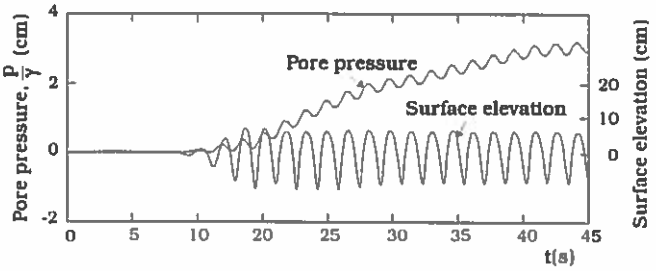

- The result of a lab experiment with a silt bottom; Two time series: (1) Surface elevation; and (2) Pressure time series
- Water depth = 42 cm, Wave height = 10 cm, Period = 1.6 s
- Pressure measured at depth 16.5 cm in the soil

Residual Liquefaction

- In this progressive buildup of the pore pressure, if the waves are high, the pressure may reach such levels that it will exceed the submerged weight of the soil above!
- In this case, the soil grains will become unbound and completely free, and the soil will begin to act like a liquid!
- This process is called the residual liquefaction!

Residual Liquefaction. A video film

- The video camera views the soil through the glass-side wall of the wave flume.
- Soil, Silt: d_{50} = 0.045 mm; Water depth = 40 cm; Wave height = 17 cm, Wave period = 1.6 s
- Will see a horizontal band in the middle of the screen. Do not take any account of this! It is silicon used to fill the gap between the side wall of the flume and the side wall of the silt box.

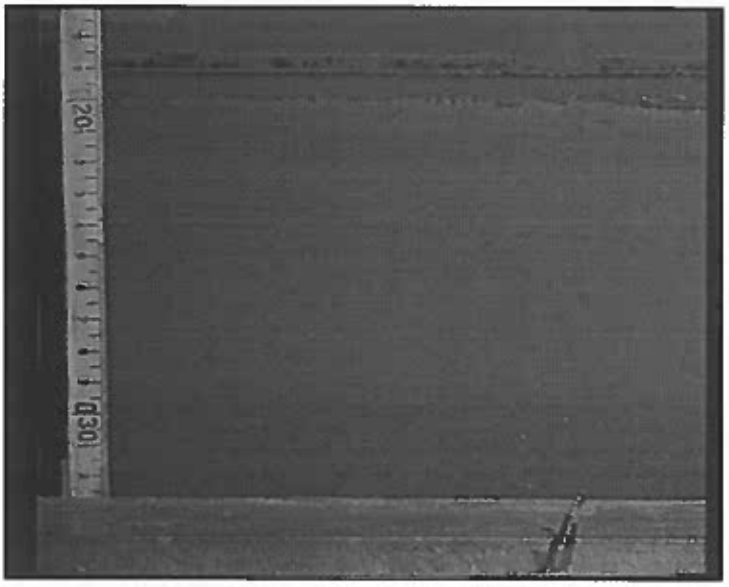

Momentary Liquefaction

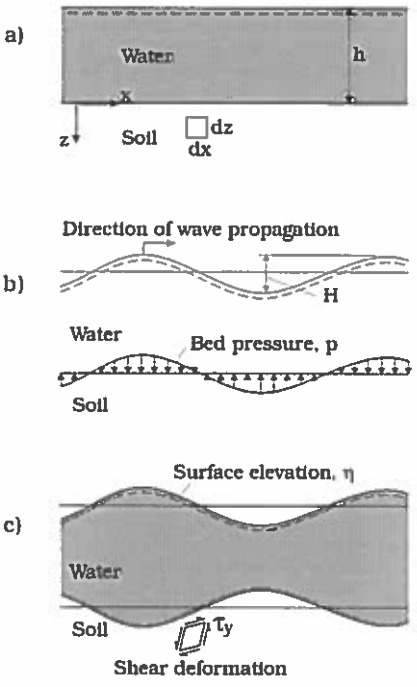

Momentary Liquefaction

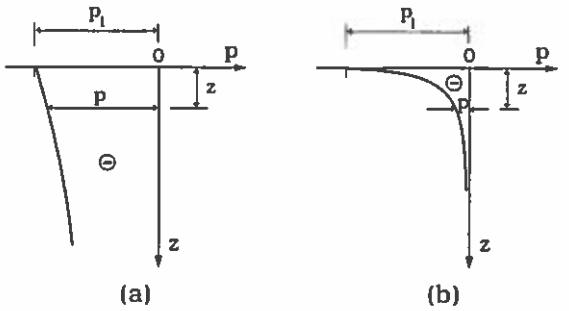

- Pressure distributions in the soil across the depth under the trough!
- This is for the following two situations:
- (a) The case of a saturated soil (there is no gas/air in the soil)!
- (b) The case of an unsaturated soil (there is gas/air in the soil)!

Momentary Liquefaction

- This upward-directed pressure gradient (which is under the wave trough) induces a lift force on the soil
- If this lift force exceeds the submerged weight, the soil will be liquefied!
- This process is called the momentary liquefaction!
- (Although there is also an upward-directed pressure-gradient force in the saturated case, this is apparently too small to cause liquefaction even under the highest waves!!)

Engineering practice

- Be it the residual liquefaction or the momentary liquefaction, the question in engineering practice boils down to the following:
- Given the soil;
- Given the waves (50 year, 100 year,..);
- Will there be any liquefaction risk for the soil supporting any structure (a pipeline, a gravity structure, a breakwater, a pier, a pile, a scour protection structure, etc.)?

To assess liquefaction

- This has stimulated research on the topic in the area of coastal engineering over the past 20 years or so!
- Our research on liquefaction does not go as far back as 20 years, though! Have started relatively recently.

Topics we study

- Sinking/flotation of pipelines and other objects in liquefied soil under waves
- Liquefaction around a buried pipeline under waves
- Influence of liquefaction (in partially/fully liquefied soil) on scour -- another failure mode of structures
- Liquefaction of soil under the rocking motion of a breakwater
- Mathematical modeling of liquefaction

Topic: Sinking/flotation of marine objects in liquefied soil

- Have studied sinking/floatation of marine objects in a silt bed under progressive waves in the lab.
- Marine objects: pipelines, spheres and cubes, the latter two simulating armour blocks/stones.
- Sumer, Fredsøe, Christensen and Lind: Coastal Engineering, vol. 38, 53-90, 1999.

Sinking/flotation… (contd.)

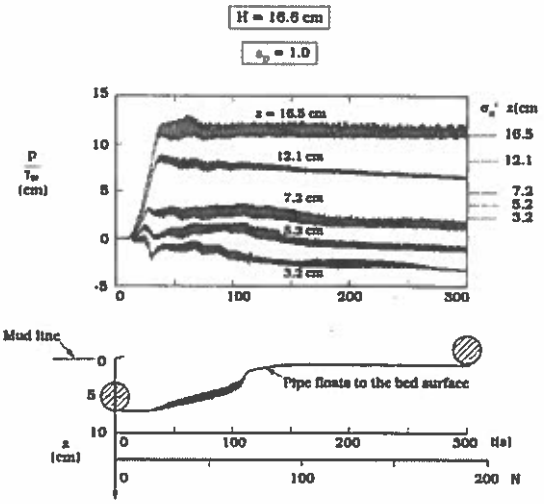

- Top panel: Pore-pressure time series at various depths. σ_0', the overburden pressure values at the depths where the pore pressure is measured.
- Bottom panel: Pipe displacement.
- Water depth = 42 cm; Wave height = 16.6 cm; Pipe buried; Pipe diameter = 4 cm; Pipe specific gravity = 1.0
- Liquefaction occurs when p reaches σ_0'
- The pipe begins to float towards the bed surface after the pore pressure reaches a substantial value!
- A similar picture when the pipe is heavier than the liquefied soil! But this time the pipe sinks in the soil

Topic: Liquefaction around a buried pipeline under waves

- A currently running project!

Test setup

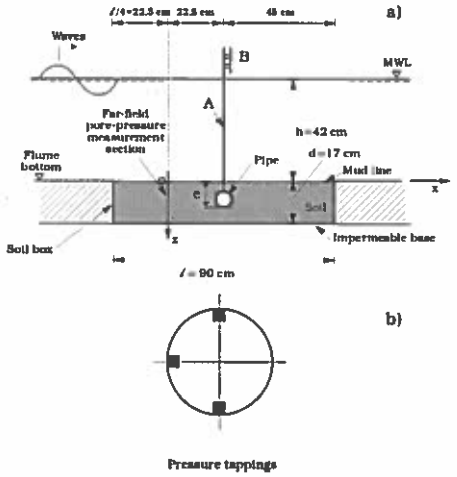

- Test setup is pretty much the same as in the 1999 work (Coastal Eng., 38, 53-90) (However, this time we also measure the pressure on the pipe!)
- Mount the pipe on a frame, fixed/free…
- Measure 4 quantities:
- p (far field); p (on the pipe); surface elevation; pipe displacement (when the pipe is not fixed)

Questions to be addressed:

- Does the liquefaction potential increase near the structure?
- Is the time scale of liquefaction influenced by the presence of the structure?
- Influence of the surface roughness? Slip condition, no-slip condition?
- Influence of various other parameters such as the structure size, the position of the structure, wave height, fixed structure versus free-to-sink structure

Topic: Influence of liquefaction on scour

- Influence of liquefaction (in partially and fully liquefied soils) on scour -- another failure mode of structures!
- This is also a currently running project
- Incidentally, scour is one of the major areas of our research at our department!

Commercial!

- Sumer, B.M. and Fredsøe, J. (2002). The Mechanics of Scour in the Marine Environment. World Scientific, xiv+536 p.
- A chapter on "impact of liquefaction"!

Topic: Liquefaction of soil under the rocking motion of a breakwater

- This, too, is a currently running project.
- A rectangular plate, partly buried in the soil, simulates the foundation of a caisson breakwater.
- The plate is oscillated around the horizontal symmetry axis, simulating the rocking motion of the breakwater
- Various effects such as Effect of the shape of the plate; Effect of sinking
- The research is only in its "infancy" at the moment!

Topic: Mathematical modeling

$$\frac{\partial P}{\partial t} = c_v \frac{\partial^2 P}{\partial z^2} + f(\tau) \qquad (1)$$

$$f(\tau) = \frac{\sigma_0'}{T}\left(\frac{1}{\alpha}\frac{\tau}{\sigma_0'}\right)^{-\beta} \qquad (2)$$

$\tau = Amplitude\ of\ \tau_y$

$$G\nabla^2 u + \frac{G}{1-2\nu}\frac{\partial \varepsilon}{\partial x} = \frac{\partial p}{\partial x} \qquad (3)$$

$$G\nabla^2 w + \frac{G}{1-2\nu}\frac{\partial \varepsilon}{\partial z} = \frac{\partial p}{\partial z} \qquad (4)$$

$$\frac{k}{\gamma}\nabla^2 p = \frac{n}{K'}\frac{\partial p}{\partial t} + \frac{\partial \varepsilon}{\partial t} \qquad (5)$$

$$\varepsilon = \frac{\partial u}{\partial x} + \frac{\partial w}{\partial z} \qquad (6)$$

$$\tau_y = G\left(\frac{\partial u}{\partial z} + \frac{\partial w}{\partial x}\right) \qquad (7)$$

- We consider, for example, a 1-D situation (i.e., a progressive wave over a seabed with no structure present)
- Left panel: Equation describing the buildup of pore pressure, P = the accumulated pore pressure
- Right panel: Biot equations, Eqs. (3) and (4) describe the equilibrium conditions for a poro-elastic material (the soil) and Eq. (5), the storage equation, describes the continuity for the pore water, incorporated with Darcy's law
- Procedure: **(1)** Determine P, from Eq. (1); **(2)** To this end, determine τ and therefore τ_y from Biot's equations; **(3)** Compare P with σ_0'; **(4)** If $P > \sigma_0'$, liquefaction occurs!

Our capabilities

- Given the wave climate (water depth, wave height, wave period)
- Given the soil properties (soil depth, Poisson's ratio, lateral earth pressure coefficient, specific weight, relative density, coefficient of consolidation, coefficient of permeability, shear modulus, bulk modulus, degree of saturation, porosity)
- We can make assessments whether or not there is any risk of liquefaction due to buildup of pore pressure
- For infinitely large soil depths, or for finite soil depths!
- Our capabilities also cover the momentary liquefaction as well!

Liquefaction Around Marine Structures (LIMAS)

- A European Union financed three-year (2001-2004) research program under the Frame Programme 5
- Is undertaken by a consortium with 10 members from 7 different countries

LIMAS Consortium

- DTU, MEK, Coastal and River Engineering Section (Coordinator)
- Ecole Nationale en Génie des Technologies, Industrielles Université de Pau, France
- Technische Universitat Braunschweig, LWI, Germany
- Laboratoire Sols, Solides, Structures Domaine Universitaire, Grenoble, France
- LICengineering A/S, Denmark
- NTNU, Department of Geotechnical Engineering, Norway
- GEODELFT, The Netherlands
- HR, Wallingford Ltd, UK
- University of Cambridge, Department of Engineering, UK
- Institute of Hydroengineering, Polish Academy of Sciences, Gdansk

LIMAS Objectives

- To investigate the potential risks for failure of marine structures due to liquefaction; and
- To prepare and disseminate practical guidelines, to be developed from the present research programme and also taking into consideration all state-of-the-art knowledge.

LIMAS Tasks

- Task 1. Liquefaction/Structure/Scour
- Task 2. Related processes and implementation

LIMAS Task 1. Liquefaction/Structure/Scour

- WP 1. Liquefaction around a structure due to buildup of pore pressure under waves
- WP 2. Fluid-Soil-Structure interaction in liquefaction around coastal structures
- WP 3. Processes to lead to liquefaction in the bed below caisson breakwaters. Large-scale experiments
- WP 4. Field study of liquefaction and scour
- WP 5. Stability of slender cylindrical structures on a liquefied bed, and scour around structures in fully or partially liquefied soil

LIMAS Task 2.
Related processes and implementation

- WP 6. Bearing capacity of sand during partially drained conditions caused by impulsive loads
- WP 7. Development of a soil sampler for investigation of real gas content in pore water
- WP 8. Impact of earthquake-induced liquefaction on marine structures
- WP 9. Formulation of guidelines for design and maintenance
- WP 10. Mathematical modelling for simulation of pore pressure generation/liquefaction due to earthquakes, and with special reference to the effects of the 1999 Kocaeli (Turkey) earthquake with regard to marine structures

LIMAS Web Site

- Detailed information from the LIMAS flyer
- http://www.isva.dtu.dk/limas/limas.html

LIMAS Publication List
(Copied from LIMAS Web Site at http://www.isva.dtu.dk/limas/limas.html)

***Books*:**

B.M. Sumer and J. Fredsøe: The Mechanics of Scour in the Marine Environment. World Scientific, 552 pp., 2002.

***Peer-reviewed Articles*:**

Authors	Date	Title	Journal/Conference	Reference
L. Cheng, B.M. Sumer and J. Fredsøe	2001	Solutions of pore pressure buildup due to progressive waves	International Journal of Numerical and Analytical Methods in Geomechanics	Vol. 25, issue 9, pp. 885-907.
D. Branque P. Foray S. Labanieh	2001	Experimental study of the interaction between seabed and pipelines submitted to the wave action	Revue Française de Géotechnique (in French)	N° 97, 4th trimester 2001, pp.61-78
J. S. Damgaard and A. Palmer	2001	Pipeline stability on a mobile and liquefied seabed: A discussion of magnitudes and engineering implications	Offshore Mechanics and Arctic Engineering 2001, OMAE '01	OMAE '01, Rio De Janeiro, 4 to 7 June 2001, ASME
D. Branque P. Foray S. Labanieh	2002	Wave-induced interaction between soil and flexible pipelines resting on the seabed	Int. Conference of Physical Modelling in Geotechnics, St John, Newfoundland, Canada	July 2002, Balkema Publishers pp.271-276
B.M. Sumer, A. Kaya and N.-E. Ottesen Hansen	2002	Impact of liquefaction on coastal structures in the 1999 Kocaeli, Turkey Earthquake	12th International Offshore and Polar Engineering Conference, KitaKyushu, Japan, May 26-31, 2002.	Proceedings of ISOPE 2002, vol. II, pp. 504-511.
T.C. Teh, A.C. Palmer and J.S. Damgaard	2002	Experimental study of marine pipelines on unstable and liquefied seabed	Coastal Engineering	Submitted in July 2002

***Non-refereed literature*:**

Authors/Editors	Date	Title	Event	Reference	Type
M. Long (University College Dublin) & R. Sandven (NTNU, Trondheim)	Sep 2001	Development of a soil sampler for gassy soils. Report on literature review of published work on sampling and behaviour of gassy soils.		LIMAS EVK3-CT-2000-00038. Obtainable from Rolf Sandven, NTNU	Report

B.M. Sumer, N.-E. Ottesen Hansen and A. Kaya	2001	Visit Report. Visit to Turkey in conjunction with WP 8: Impact of Earthquake-Induced Liquefaction on Marine Structures, 1-9. July, 2001		Obtainable from ISVA, or can be downloaded from LIMAS' web site, 14p.	Report
A. Kaya	2001	Impact of Liquefaction on Marine Structures in the 1999 Kocaeli, Turkey Earthquake		Internal Report, ISVA, December 2001, 67 p. Obtainable from ISVA	Report
B.M. Sumer	2002	Wave-induced liquefaction	Workshop on Wave- and Seismic-Induced Liquefaction and its Implications for Marine Structures, 16-18 Sept., 2002, Istanbul, Turkey.	Book of Abstracts, pp. 7-8	Extended abstract
M.B. de Groot and P. Meijers	2002	Wave-induced liquefaction versus seismic-induced liquefaction. Implications for engineering problems	,,	Book of Abstracts, pp. 9-10	Extended abstract
B.M Sumer, J. Fredsøe and C. Truelsen	2002	Liquefaction around a buried pipeline in a progressive wave	,,	Book of Abstracts, pp. 14-15	Extended abstract
D. Bonjean P. Foray H. Michallet M.Mory	2002	Fluid-Soil-Structure interaction in liquefaction around coastal structures.	,,	Book of Abstracts, pp. 11	Extended abstract
M. Kudella and H. Oumeraci	2002	Large Scale experiments on pore pressure generation underneath a caisson breakwater	,,	Book of Abstracts, pp. 11	Extended abstract
M. Mory D. Bonjean H. Michallet G. Valls-Benavides J.M. Barnoud P. Foray D. Rihouhey S. Abadie	2002	Observations of momentary liquefaction caused by breaking waves around a coastal structures	,,	Book of Abstracts	Extended abstract
T.C. Teh, A.C. Palmer and J.S. Damgaard	2002	Stability of pipelines on liquefied seabed	,,	Book of Abstracts, pp. 20	Extended abstract
S.L., Dunn, J. Damgaard, A. Chan and P.L.Vun	2002	Numerical modeling of liquefaction around a pipeline	,,	Book of Abstracts, pp. 21-22	Extended abstract
N.-E.O. Hansen	2002	Bearing capacity of sand during partially drained conditions caused by impulsive loads	,,	Book of Abstracts, pp. 14-15	Extended abstract

R. Sandvend and M. Long	2002	Development of a soil sampler for measurement of gas content in soils	,,	Book of Abstracts, pp. 25-27	Extended abstract
N.-E. O. Hansen	2002	Impact of liquefaction on marine structures in the 1999 Kocaeli Earthquake	,,	Book of Abstracts, pp. 32-33	Extended abstract
B.M. Sumer	2002	Field Visit. Visit to Erathquake-Stricken Areas, 18.September, 2002	4th LIMAS Workshop, Istanbul, Turkey	Obtainable from ISVA, or can be downloaded from LIMAS web site, 11p.	Report
H. Oumeraci and M. Kudella	2002	Liquefaction Around Marine Structures – Progress Report of Work Package 3		Internal Report	Report
B.M. Sumer	2002	Field Visit. Visit to Erathquake-Stricken Areas, 18.September, 2002	4th LIMAS Workshop, Istanbul, Turkey	Obtainable from ISVA, or can be downloaded from LIMAS web site, 11p.	Report

***Others (Videos, etc.)*:**

- B.M. Sumer and F. Hatipoglu: Soil Liquefaction Under a Progressive Wave, Video, 2002.
- T.C.Teh, A. Palmer and J. Damgaard: Free Movement/Burial of a Initially-Bottom-Seated-Horizontal Pipe in a Liquefied Soil Under a Progressive Wave, Video, 2002.
- M. de Groot: Wave induced versus seismic induced liquefaction, 4th LIMAS Workshop, Istanbul, Turkey, Power Point Presentation, posted on the LIMAS Web site, 2002.
- B.M. Sumer: Wave-induced liquefaction. General Lecture, 4th LIMAS Workshop, Istanbul, Turkey, Power Point Presentation, posted on the LIMAS Web site, 2002.
- Bonjean, P. Foray, H. Michallet and M. Mory: Wave-induced liquefaction at soil-structure interface. 4th LIMAS Workshop, Istanbul, Turkey, Power Point Presentation, posted on the LIMAS Web site, 2002.

Reviewed 12.December, 2002

LIMAS

Liquefaction Around Marine Structures

This FP-5 research program is partially funded by the European Commission Directorate General XII for Science, Research and Development

Contract No.

EVK3-CT-2000-00038

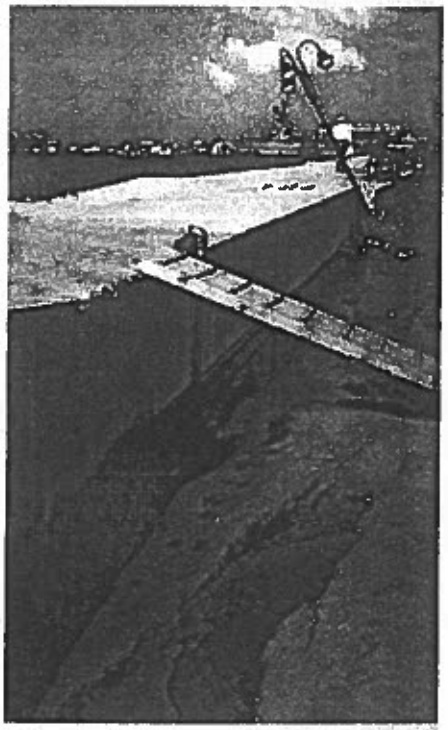

Project Coordinator

B. Mutlu Sumer

MEK

Technical University of Denmark
Department of Mechanical Engrg.
Coastal and River Engrg. Section
Build. 115, 2800 Lyngby, Denmark
sumer@isva.dtu.dk

Responsible EU Scientific Officer

Christos Fragakis

Christos.Fragakis@cec.eu.int

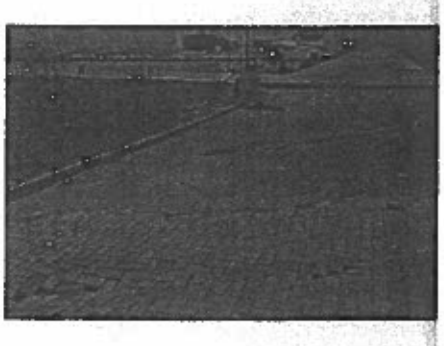

Duration

1. May, 2001 - 30. April, 2004

Liquefaction Around Marine Structure (LIMAS)

LIMAS is funded by the Commision of the European Union Directorate General XII under contract EVK3-CT-2000-00038 (2001-2004) within the framework of EU Fifth Framework Programme with specific programme: Energy, Environment and Sustainable Development, Key Action 3 "Sustainable Marine Ecosystems".

Summary of the research programme

Title of project Liquefaction Around Marine Structures (LIMAS).

Problems to be solved
Marine structures such as breakwaters, seawalls, pile structures, sea barriers, pipelines, and armouring systems are used to protect coastal communities against flooding and erosion.

Liquefaction of soil supporting these structure is one of the failure modes of the structures. Some such failures have been catastrophic in the past.

Liquefaction is induced by waves, seismic action, and impulsive loads (such as sudden blasting, wave slamming, and ship impact).

While a substantial amount of knowledge has accumulated on flow and morphological processes around marine structures in the last decade or so, comparatively little is known about the impact of liquefaction on these structures. The topic has been very little covered in recent EU research which has substantially advanced the design of coastal structures, but not of their foundations with regard to soil liquefaction.

This is basically what has motivated the present consortium to carry out this work.

It is important to design and construct these structures in such a way that reliable, economic and environmentally compatible and well functioning coastal protection can be achieved. This requires a comprehensive knowledge of the soil / foundation behaviour which supports them. This latter issue is essentially what the present work addresses. Incomplete knowledge results in damage or failure of these structures, leading to unreliable or uneconomic protection measures against flooding and erosion.

The benefits that will be gained from the project may be summarized as follows: (1) It will be ensured that the European coastal areas are protected with reliable, economic and environmentally compatible and well functioning coastal structures, which is essential and of strategic importance for the Community; (2) Coastal intervention options will be enhanced (an important issue with regard to "sustainability"); (3) The guidelines (the key product of the project) will help increase the long term integrity of the coastal structures (in addition to their safety) which will certainly help manage the sustainable use of the ocean (This will also contribute to improving the quality of life, health and safety); (4) Properly designed structures (by the implementation and exploitation of the RTD results of the project) will protect coastal communities (including the tourist resorts) against flooding and erosion better, and this will undoubtedly help improve the quality of life and safety of European citizens; (5)

The analysis of the risk of liquefaction around coastal structures will be a useful tool for local communities in the preparation of plans of risk prevention, in contingency plans such as disaster prevention plans with regard to earthquakes; (6) Failures of structures due to soil / foundation problems will be avoided by designing the structures properly, therefore the interruption of services will be avoided, benefiting the European Union industry and society, and obviously, this, too, will contribute to improving the quality of life; (7) Finally, upgrading of existing structures to withstand larger loads, or to alternative use, will be made on a safer basis.

Scientific objectives and approach

The objectives of the present project are two-fold: (1) To investigate potential risks for failure of structures due to liquefaction; and (2) Prepare and disseminate practical guidelines (guidance for design and maintenance), to be developed from the present research and also taking into consideration all state-of-the-art knowledge.

The work is organized in two tasks: Task 1. Liquefaction / Structure / Scour; and Task 2. Related processes and implementation.

Task 1 consists of five workpackages (WP):

- WP1. Liquefaction around a structure due to buildup of pore pressure under waves;
- WP2. Fluid-Soil-Structure interaction in liquefaction around coastal structures
- WP3. Investigation of processes susceptible to lead to liquefaction in the bed below caisson breakwaters. Large-Scale facility experiments;
- WP4. Field study of liquefaction and scour around coastal structures; and
- WP5. Stability of slender cylindrical structures on a liquefied bed, and scour around structures in fully or partially liquefied soil

.

Task 2, on the other hand, consists of four workpackages:

- WP6. Bearing capacity of sand during partially drained conditions caused by impulsive loads;
- WP7. Development of a soil sampler for investigation of real gas content in pore water;
- WP8. Impact of earthquake-induced liquefaction on marine structures; and
- WP9. Formulation of guidelines for design and maintenance.

Laboratory studies (WP1, WP2, WP5, WP6, WP7), large-scale laboratory studies (WP3), theoretical and numerical methods (WP4, WP5, WP6, WP8), and field investigations (WP4, WP7) will be adopted to achieve the previously mentioned objectives.

Web address:

http://www.isva.dtu.dk/limas/limas.html

List of partners

- **ISVA,** Technical University of Denmark, Department of Mechanical Engrg.,Coastal and River Engrg. Section, Building 115, 2800 Lyngby, Denmark. Contact person : B. Mutlu Sumer (Coordinator of LIMAS) (sumer@isva.dtu.dk)

- **UPPA,** Ecole Nationale en Génie des Technologies Industrielles Université de Pau et des Pays de l'Adour BP 576, 64012 PAU Cédex, France. Contact person: Mathieu Mory (mathieu.mory@univ-pau.fr)

- **LWI,** Technische Universitat Braunschweig Leichtweiss Institut fur Wasserbau Beethovenstrasse 51 a DE-38106 Braunschweig, Germany. Contact person: Hocine Oumeraci (H.Oumeraci@tu-bs.de)

- **INPG,** Laboratoire Sols, Solides, Structures Domaine Universitaire BP 53 38041 Grenoble Cedex France. Contact person: Pierre Foray (pierre.foray@hmg.inpg.fr)

- **LICENG,** LICengineering A/S Ehlersvej 24 2900 Hellerup, Denmark. Contact person: Niels-Erik Ottesen Hansen (neoh@liceng.dk)

- **NTNU,** Institutt for Geoteknikk Høgskoleringen 7 7491 Trondheim, Norway. Contact person: Rolf Sandven (rolf.sandven@bygg.ntnu.no)

- **GEODELFT,** GeoDelft, Stieltjesweg 2 2628 CK Delft, The Netherlands. Contact person : Maarten B. de Groot (Leader of Task 2) (M.B.deGroot@delftgeot.nl)

- **HR,** HR Wallingford Ltd. Howbery Park Wallingford, Oxon OX10 8 BA, United Kingdom. Contact person: Jesper S. Damgaard (Leader of Task 1) (jsd@hrwallingford.co.uk)

- **UCAM-DENG,** University of Cambridge, Department of Engineering, Trumpington Street, Cambridge CB2 1PZ, United Kingdom. Contact person: Andrew Palmer (acp24@eng.cam.ac.uk)

- Participants (http://www.isva.dtu.dk/limas/public/staff.htm)
- Fifth Framework Programme (FP-5) (http://www.cordis.lu/fp5/home.html)
- Abstracts (http://www.isva.dtu.dk/limas/public/abstracts.html)
- News (http://www.isva.dtu.dk/limas/public/LIMAS_news.html)
- List of Limas Publications (http://www.isva.dtu.dk/limas/public/LIMASpubl.htm)
- Project Server / Data Base (http://www.isva.dtu.dk/limas/public/projektDB.html)

The 9th (1999) International Offshore and Polar Engineering Conference,
ISOPE-99, Brest, France, May 30-June 4, 1999.

A RANDOM-WALK MODEL FOR PORE PRESSURE ACCUMULATION IN MARINE SOILS

B. Mutlu Sumer[1] and Nian-Sheng Cheng[2]
Technical University of Denmark, Department of Hydrodynamics and Water Resources (ISVA),
Building 115, 2800 Lyngby, Denmark

[1] Corresponding author, email: sumer@isva.dtu.dk
[2] Present address: Civil and Structural Engineering, Nanyang Technological University, Nanyang Avenue, Singapore 63798

ABSTRACT

A numerical random-walk model has been developed for the pore-water pressure. The model is based on the analogy between the variation of the pore pressure and the diffusion process of any passive quantity such as concentration. The pore pressure in the former process is analogous to the concentration in the latter. In the simulation, particles are released in the soil, and followed as they travel through the statistical field variables. The model has been validated (1) against the Terzaghi consolidation process, and (2) against the process where the pore pressure builds up under progressive waves. The model will apparently enable the researcher to handle complex geometries (such as a pipeline buried in a soil) relatively easily. Early results with regard to the latter example, namely the buildup of pore pressure around a buried pipeline subject to a progressive wave, are encouraging.

KEY WORDS: Buried pipelines, liquefaction, numerical model, pressure buildup, random walk, silt, soil, waves

NOMENCLATURE

a_i = coefficients;
c = factor;
c_v = consolidation coefficient;
$f(z)$ = source term;
$F(z)$ = integral of $f(z)$ over z and t;
h = water depth;
H = wave height;
k_0 = coefficient of the lateral earth pressure;
p = excess pore pressure, or accumulated pore pressure;
p_b = maximum value of the bed pressure;
t = time;
t' = dummy variable of integration;
T = wave period;
z = downward distance from the soil surface;
z' = dummy variable of integration;
Δz = depth increment;
Δt = time increment;
L = wave length;
N = number of particles released at the depth increment where cF is maximum;
d = depth of soil;
m = range variable;
n = number of particles at depth increment at time t;
N_f = number of cycles to cause liquefaction;
α = empirical constant in the Seed equation;
β = empirical constant in the Seed equation;
γ = specific weight of water;
γ' = submerged specific weight of soil in water;
λ = wave number;
ν = Poisson's ratio of the soil;
ξ = dummy variable of integration;
σ_0' = overburden pressure; and
τ = maximum value of the cyclic shear stress in the soil.

INTRODUCTION

The consolidation process is encountered in various marine engineering problems. Likewise, the process in which the excess pore pressure builds up under cyclic loading (such as the buildup of pore pressure under earthquakes, and that under wave action) is also encountered in marine engineering practice. Basically, the excess pore-water pressure in these processes is governed by the diffusion equation.

A simple alternative to solving the diffusion equation is the Lagrangian simulation of the diffusion process by a random-walk model. This method has been developed over the last decades (Bugliarello 1971, and Sullivan 1971), and is now a powerful numerical tool used in the numerical treatment of diffusion of mass in flow environments.

The random-walk model has been subsequently implemented for flow calculations in which the vorticity-transport equation is solved by means of a Lagrangian random-walk model. The models developed for this purpose are commonly known as the discrete vortex models (Chorin 1973, 1978, and Stansby and Dixon 1983). A recent review can be found in Sumer and Fredsøe (1997).

The advantages of this Lagrangian method over the other methods are: (1) the method is relatively stable; (2) the numerical diffusion problems associated with the concentration-gradient terms in Eulerian schemes (or the vorticity-gradient terms in the case of the vorticity-transport equation) are to a large degree avoided (Stansby & Isaacson, 1987); and (3) it can be implemented fairly easily for complex geometries, such as a buried pipeline confined by the water-soil interface above, and by an impermeable base below (see the definition sketch in Fig. 7).

Although random-walk simulations of the previously mentioned processes have been studied quite extensively, no study is yet available investigating the random-walk simulation of the excess pore pressure in soils.

The purpose of the present study is to investigate the latter in conjunction with the process in which the pore pressure accumulates under a progressive wave, thereby demonstrating the applicability of this Lagrangian random-walk model to the prediction of the excess pore pressure in marine soils. The model has been implemented subsequently for the prediction of the buildup of pore pressure around a buried pipeline subject to a progressive wave.

PORE-PRESSURE BUILDUP UNDER A PROGRESSIVE WAVE

Process

When the soil is exposed to a progressive wave (Fig. 1), it will undergo periodic, elastic, shear deformation. This will gradually rearrange the soil grains at the expense of the pore volume. The latter effect will compress the pore water, and lead to a gradual buildup of pore pressure in the case of an undrained loading of soil (Seed and Rahman, 1978).

Basic equations and analytical solution

The accumulated pore pressure, p, in the aforementioned process can be shown to satisfy the following equation

$$\frac{\partial p}{\partial t} = c_v \frac{\partial^2 p}{\partial z^2} + f(z, t) \qquad (1)$$

in which t is time, z is the vertical distance from the soil surface measured downwards (Fig. 1), c_v is the consolidation coefficient, and $f(z, t)$ is a source term (representing the total amount of excess pressure generated per unit time and per unit volume of soil), and may be given by

$$f(z, t) = \frac{\sigma'_0}{N_l T} \qquad (2)$$

in a linear approximation. Here, T is the wave period, and σ'_0 is the overburden pressure value, which can be taken as (McDougal et al., 1989)

$$\sigma'_0 = \gamma' z \frac{1+2k_0}{3} \qquad (3)$$

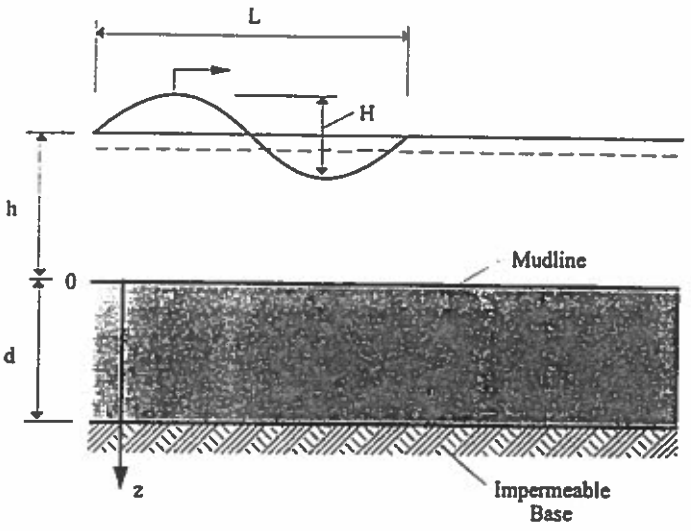

Fig. 1. Definition sketch.

in which γ' is the submerged specific weight of soil in water, and k_0 is the coefficient of the lateral earth pressure. The quantity N_l in Eq. 2 is the number of cycles to cause liquefaction, which may be given by the following empirical equation (Peacock and Seed 1968, and Alba, Seed and Chan 1976)

$$N_l = \left(\frac{1}{\alpha} \frac{\tau}{\sigma'_0}\right)^{1/\beta} \qquad (4)$$

in which τ is the maximum value of the cyclic shear stress in the soil induced by waves, and α and β are empirical constants, and depend basically on the relative density of the soil. Seed and Rahman (1978) was the first to adopt the model in Eq. 1 to describe the buildup of pressure under a progressive wave. Spierenburg (1987) and McDougal et al. (1989) have subsequently adopted similar approaches.

The maximum value of the shear stress, τ, in Eq. 4 may be given by (McDougal et al., 1989)

$$\tau = p_b \lambda a_1 \times \\ \times [a_2 \sinh(\lambda z) + a_3 z \cosh(\lambda z) + a_4 z \sinh(\lambda z)] \qquad (5)$$

in which

$$a_1 = 1 / [(2(1-\nu)a'_3 - \lambda)((1-2\nu)(3-4\nu)\sinh^2(\lambda d) - \lambda^2 d^2)]$$
$$a_2 = 2(1-2\nu)(\nu-1) - \lambda^2 d^2$$
$$a_3 = \lambda[(3-4\nu)\cosh^2(\lambda d) - (1-2\nu)]$$
$$a'_3 = a_3 / [(1-2\nu)(3-4\nu)\sinh^2(\lambda d) - \lambda^2 d^2]$$
$$a_4 = \lambda [\lambda d - (3-4\nu)\cosh(\lambda d)\sinh(\lambda d)]$$

in which d is the soil depth (Fig. 1). The quantity p_b in Eq. 5 is the maximum value of the bed pressure,

$$p_b = \gamma \frac{H}{2} \frac{1}{\cosh(\lambda h)} \qquad (6)$$

in which H is the wave height, h is the water depth, and λ is the wave number, namely $\lambda = 2\pi/L$, L being the wave length. The quantity ν is the Poisson ratio for the soil.

The solution to Eq. 1 with f given by Eq. 2, and τ by Eq. 5, is to be sought under the following initial and boundary conditions:

$$t = 0;\ 0 \le z \le d:\ p = 0$$
$$0 < t < \infty;\ z = 0:\ p = 0$$
$$0 < t < \infty;\ z = d:\ \partial p/\partial z = 0$$

The solution is (Weinberger 1965, p.131)

$$p(z,t) = \sum_{m=1}^{\infty} \frac{2}{\pi} \sin[(m-\frac{1}{2})(\pi/d)z] \times$$
$$\times \left[\int_0^{tc_v(\pi/d)^2} \left[\int_0^{\pi} \exp[-\frac{1}{4}(2m-1)^2\ [tc_v(\pi/d)^2 - t']\right] \times\right.$$
$$\left. \times \sin[(m-\frac{1}{2})\xi]\ g(\xi)\ d\xi\right]\ dt' \ ] \qquad (7)$$

in which $g(\xi)$ is

$$g(\xi) = \frac{1}{c_v}(\frac{d}{\pi})^2 \frac{1}{T}\gamma' \frac{1+2k_0}{3}\xi \frac{d}{\pi}[\frac{1}{\alpha}\frac{3}{1+2k_0}\frac{\tau}{\gamma'\xi(d/\pi)}]^{-1/\beta} \qquad (8)$$

RANDOM-WALK SIMULATION OF THE PORE-PRESSURE BUILDUP UNDER A PROGRESSIVE WAVE

Random-Walk simulation

As seen from Eq. 1, the excess pore pressure satisfies the diffusion equation, meaning that there is an analogy between the diffusion of any passive quantity such as concentration (or temperature in the case of heat transfer) and the spreading of the excess pore pressure. As mentioned previously, a simple alternative to solving the diffusion equation is the Lagrangian simulation of the diffusion process by a random-walk model.

In this simulation, particles are released in the soil, and followed as they move. (Note that, as will be indicated later in the section, the particle concentration, C, here simulates the excess pore pressure). Each particle moves in small steps. Each small step is selected randomly from a Gaussian distribution, as will be detailed in the following paragraphs. At the boundaries, the particles are reflected, or absorbed, depending on the boundary condition. The particle concentration is then determined across the soil depth at desired times.

The procedure used in the simulation is as follows:

(1) Divide the soil depth into small increments the size, Δz.

(2) Select the small time increment, Δt, to advance the simulation in time. (Δt is taken as $\Delta t = 0.7T$ in the simulation. The influence of Δt on the results will be discussed later in the paper).

(3) Calculate

$$F(z) = [\int_z^{z+\Delta z} f(z)\ dz]\ \Delta t \qquad (9)$$

for each increment $[z, z+\Delta z]$ where $f(z)$ is given by Eq. 2. The quantity $F(z)$ is the total amount of pore pressure generated over the depth increment $[z, z+\Delta z]$, and over the time increment Δt.

By the diffusion analogy, this is the number of the particles which need to be released from the depth increment $[z, z+\Delta z]$ over the time interval Δt.

(4) Multiply $F(z)$ by a factor, c, so that the maximum value of the product $cF(z)$ over the depth is, for example, $N = \text{Max}[cF(z)] = 500$. (Here, c is a dummy factor, and employed for convenience, to achieve the simulation of even the smallest pore pressure with a reasonably large number of particles. The actual value of c is unimportant, as will be seen later in item 9. However, N should be sufficiently large to give reliable ensemble averages, as will be discussed later in the paper).

(5) Release $cF(z)$ particles from each depth increment $[z, z+\Delta z]$.

(6) Move each particle upwards or downwards over the time interval, Δt, during which the particle takes a random step. Select this random step from a Gaussian process with a standard deviation set equal to

$$(2c_v\ \Delta t)^{1/2} \qquad (10)$$

(7) At the soil surface ($z = 0$), use the absorbing boundary condition, simulating the dissipating pore pressure, $p=0$, there; namely, absorb the particles (do not return them back to the soil) when they "impinge" this boundary.

(8) At the impermeable base ($z = d$), use the reflecting boundary condition, simulating that the pressure gradient with respect to z is zero; namely, reflect the particles back into the soil when they "impinge" this boundary.

(9) "Freeze" the process at the end of the time step Δt, and count the number of particles in each depth increment $[z, z+\Delta z]$. Let n be the number of particles at each $[z, z+\Delta z]$. Divide n by the product of $c\ \Delta z$. This will give the concentration of particles at that point. By the diffusion analogy, the latter quantity should be equivalent to the excess pore pressure, p (the accumulated pressure) at this point, and at time $0+\Delta t$:

$$p = \frac{n}{c\ \Delta z} \qquad (11)$$

(10) To advance the simulation from time $0+\Delta t$ to time $0+2\Delta t$, add the number of new particles, $F(z)$ (see Eq. 9), to the existing number of particles at the end of the previous time step, namely n/c, for each depth increment $[z, z+\Delta z]$.

(11) Replace $F(z)$ in Item 4 above with $F(z)+(n/c)$, and repeat the exercise between Steps 4-9.

(12) Repeat Steps 10-11, to advance the simulation in time until the accumulated pressure attains its equilibrium value.

Validation of the model against the Terzaghi consolidation process

The present random-walk model has been validated first against the Terzaghi consolidation process, namely the process represented by Eq. 1 without the source term (Terzaghi, 1948, p. 273). This enabled us to investigate the influence of various input parameters such as the influence of the number of particles, the influence of the small depth increment (Δz), and the influence of the small time increment (Δt). This exercise indicated that the random-walk results were in excellent agreement with the familiar analytical solution (Terzaghi, 1948, p. 274) when N (the number of particles released at the depth increment where cF is maximum) is larger than approximately 500, and $\Delta t\, c_v / d^2 = 0.0005$. Fig. 2 shows the effect of N. The quantity p_{cal} in the figure is the pressure calculated from the random-walk simulation, and p_{theor} is that from the Terzaghi solution. As seen, the simulation results converge to the theoretical value when $N \geq 500$, indicating that the sample size should be large enough (in the present case larger than approximately 500) to give reliable ensemble averages. The Δz increment, on the other hand, appeared not to have a very significant influence on the end results as long as it was sufficiently small; no significant difference between the simulation results was observed when $\Delta z/d$ was 0.1 and 0.02, the results in both cases being in very good agreement with the analytical solution.

Validation of the model against the analytical solution for the buildup of pore pressure under a progressive wave

The random-walk simulation for the case where the pore pressure builds up under a progressive wave was carried out for the following set of input parameters: Wave height, H = 0.166 m; Wave period, T = 1.6 s; Water depth, h = 0.42 m; Wave number, λ =2.17 m^{-1}; Specific weight of water, γ = 9.8 kN/m^3; Soil depth, d = 0.17 m; Submerged specific weight of soil in water, γ' = 10.73 kN/m^3; Coefficient of lateral earth pressure, k_0 = 0.41; Consolidation coefficient, c_v = 0.0000128 m^2/s; α and β constants in the Seed equation (Eq. 4), α = 0.48, and β = -0.29. This set of input parameters corresponds to a laboratory test, which will be discussed later in the paper.

Fig. 3 displays the result of the simulation, and compares it with the analytical solution given in Eq. 7 for time t/T = 30 (i.e., after 30 waves). In the simulation, $\Delta z\, d$ =0.02, Δt = 0.7T, and the number of particles was taken as N = 500 (see Item 4 above). The agreement between the random-walk simulation and the analytical solution is very good. Obviously, the model results may differ from the analytical solution when the system parameters are not properly chosen. This will be examined more closely in the following paragraphs.

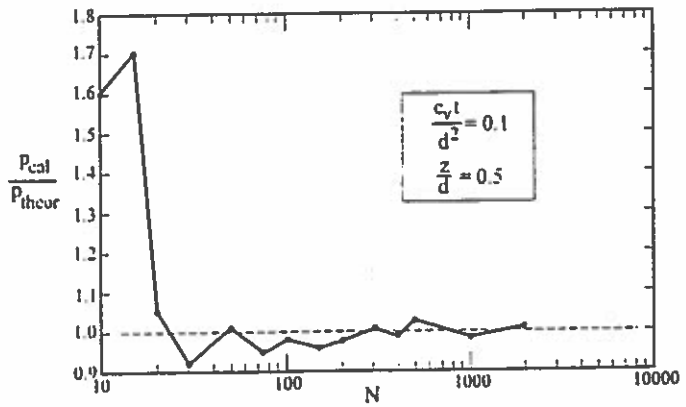

Fig. 2. Influence of the number of particles on the simulation results for the Terzaghi consolidation process. $\Delta z/d$ = 0.02, $\Delta t\, c_v / d^2$ = 0.0005.

The influence of Δz on the results was investigated in the simulations. Simulation runs were made with $\Delta z/d$ = 0.1, 0.033, 0.014, and 0.01. It was found that the results even with $\Delta z/d$ = 0.1 were as good as those in Fig. 3, similar to the Terzaghi case.

The influence of Δt was also investigated in the study. Simulation runs were made with Δt = T, 0.7T, 0.5T, 0.1T, 0.01T, and 0.001T. Apparently, Δt = 0.7T gave the best agreement with the analytical solution. We shall return to this issue later in the paper.

The effect of the number of particles released at each increment was also investigated in the simulations. It was found that the results converged to those predicted by the analytical solution when N was larger than approximately 500, similar to the previously mentioned Terzaghi case.

Figs. 4 and 5 display the time development of the accumulated pressure at three different z positions. In Fig. 4, Δt = 0.1T, while in Fig. 5, Δt =0.7T.

First of all, the agreement between the random-walk results and the analytical solution (Eq. 7) is excellent when Δt =0.7T (Fig. 5). It is interesting to note that this value of Δt, when normalized with c_v, and d corresponds to $\Delta t\, c_v / d^2$ = 0.0005, precisely the same value as in the simulation of the Terzaghi consolidation process found in conjunction with the influence of the time step Δt on the end results.

Secondly, the figures show that the pore pressure progressively builds up, and eventually reaches an equilibrium state where the pressure attains a constant value. We shall return to this point later in the section.

Thirdly, Fig. 5 also displays the overburden values σ'_0, normalized by γ, calculated from Eq. 3. When compared with the overburden values indicated in the figure, the pressures at all the three depths apparently exceed their corresponding overburden values (after about 300-500 waves), meaning that liquefaction occurs at these depths after 300-500 waves. In reality, once the pressure attains its overburden value, the soil will be liquefied, and the pressure will remain at this value. Therefore, the random-walk simulation for times larger than that for the onset of liquefaction will obviously not represent the actual physical process, as indicated in Fig. 5.

Fig. 6 displays the vertical distribution of the accumulated pore pressure in the equilibrium state obtained from the solution given in Eq. 7 and from the random-walk simulation. The figure also includes the results obtained from a laboratory experiment conducted at the Technical University of Denmark,

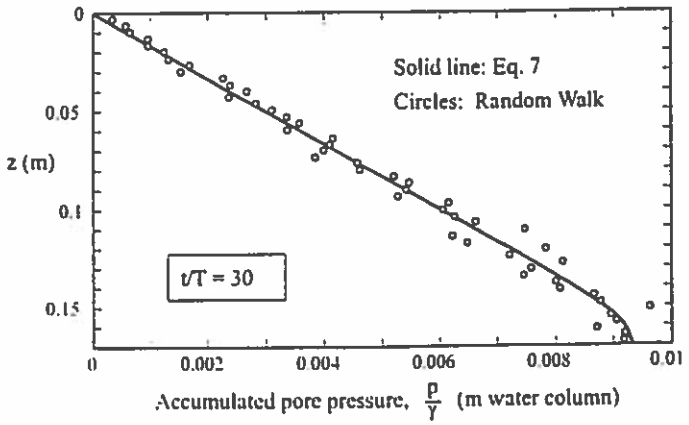

Fig. 3. Pore pressure accumulation after t/T = 30 waves. Comparison of the random-walk simulation and the analytical solution (Eq. 15). For the input parameters, see the text. $\Delta z/d$ = 0.02, Δt = 0.7T, and N = 500.

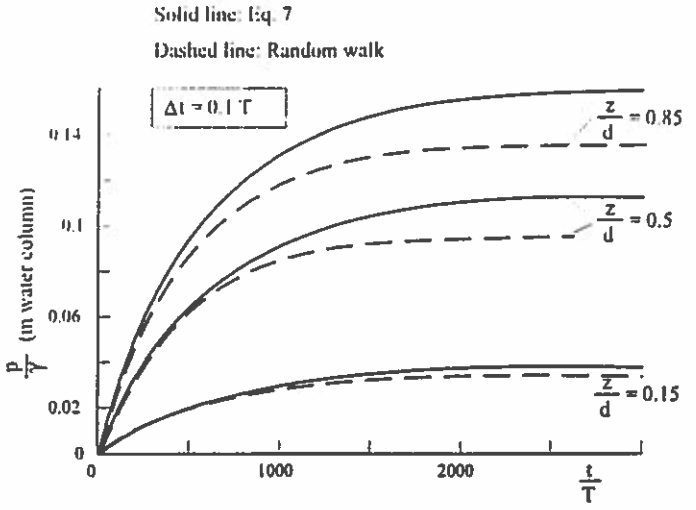

Fig. 4. Time development of pressure accumulation. $\Delta z/d = 0.02$, $\Delta t/T = 0.1$, and $N = 500$.

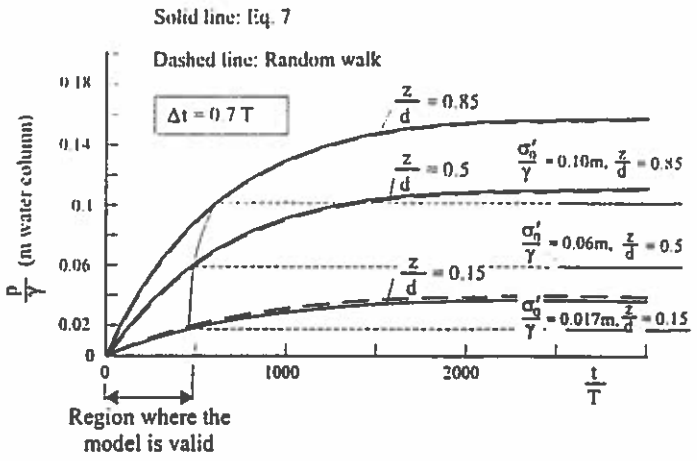

Fig. 5. Time development of pressure accumulation. $\Delta z/d = 0.02$, $\Delta t/T = 0.7$ (or alternatively, $\Delta t\, c_v/d^2 = 0.0005$), and $N = 500$.

Department of Hydrodynamics and Water Resources (ISVA). These experiments were conducted in a wave flume, 0.6 m in width, 0.8 m in depth and 26.5 m in length. The soil (silt) was placed in a box, $d = 0.17$ m in depth, and 0.9 m in length, and about 0.6 m in width. The surface of the soil in the box (after 3 hours of consolidation) was flush with the bottom of the flume. The grain size was $d_{50} = 0.045$ mm. The pore-water pressure across the soil depth was measured with Rosemount, model 1151 DP Alpaline pressure transducers at four points across the depth. The soil and wave properties are the same as those given in the beginning of this subsection.

As seen, the measured equilibrium-state pressures are somewhat smaller than the corresponding pressures obtained from the random-walk simulation and the analytical solution. This is explained as follows. Once the accumulated pore pressure reaches its overburden value, the soil is liquefied, and the pore pressure from this moment onwards remains at this overburden value, as has been pointed out in the preceding paragraphs in conjunction with Fig. 5. The measured pore-pressure distribution in Fig. 6 (the crosses) actually represents this distribution, as can be deduced from Fig. 5.

The fact that the simulation overestimates pressure buildup beyond liquefaction is actually not a problem when implementing the model to assess liquefaction potential. In this context, the following procedure is to be followed:

(1) Advance the simulation in time, and calculate the pore pressure, p.

(2) Check if p has reached the overburden value. If yes, stop the simulation. At this point liquefaction occurs.

(3) If no, check if p has attained its steady-state value. If yes, stop the simulation. There is no liquefaction potential.

(4) If no, return to item (1).

APPLICATION OF THE MODEL TO BUILDUP OF PORE PRESSURE AROUND A BURIED PIPELINE

The random-walk model described in the preceding section has been implemented for the prediction of the buildup of pore pressure around a buried pipeline (Magda, Sumer and Fredsøe, 1998). The latter work is only in the initial stage, and some early results will be presented in the following paragraphs.

The random-walk simulation was carried out for the same set of input parameters as that in the example in the preceding section. The pipe ($D = 8$ cm) is buried in the soil at a depth of $e = 14.5$ cm (see the definition sketch in Fig. 7).

Eq. 1 in this 2-D case will read

$$\frac{\partial p}{\partial t} = c_v \left(\frac{\partial^2 p}{\partial x^2} + \frac{\partial^2 p}{\partial z^2}\right) + f(x, z, t) \qquad (12)$$

The source term in Eq. 1 was taken as

$$f(x, z, t) = \frac{\sigma'_0}{N_l T} \left(\frac{t}{N_l T}\right)^s \qquad (13)$$

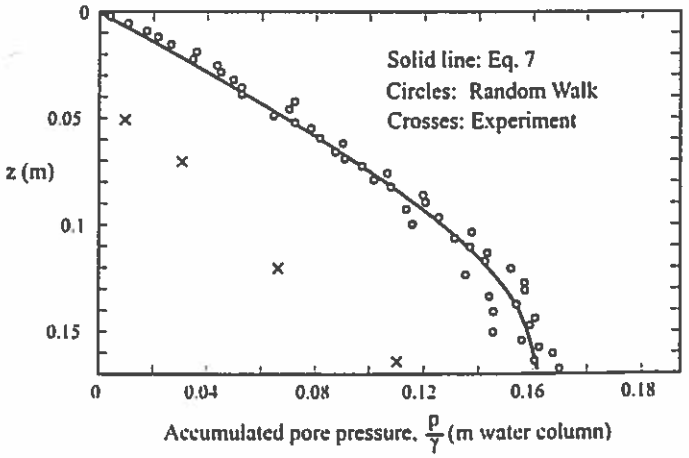

Fig. 6. Pore pressure accumulation. Equilibrium state. $\Delta z/d = 0.02$, $\Delta t/T = 0.7$, and $N = 500$.

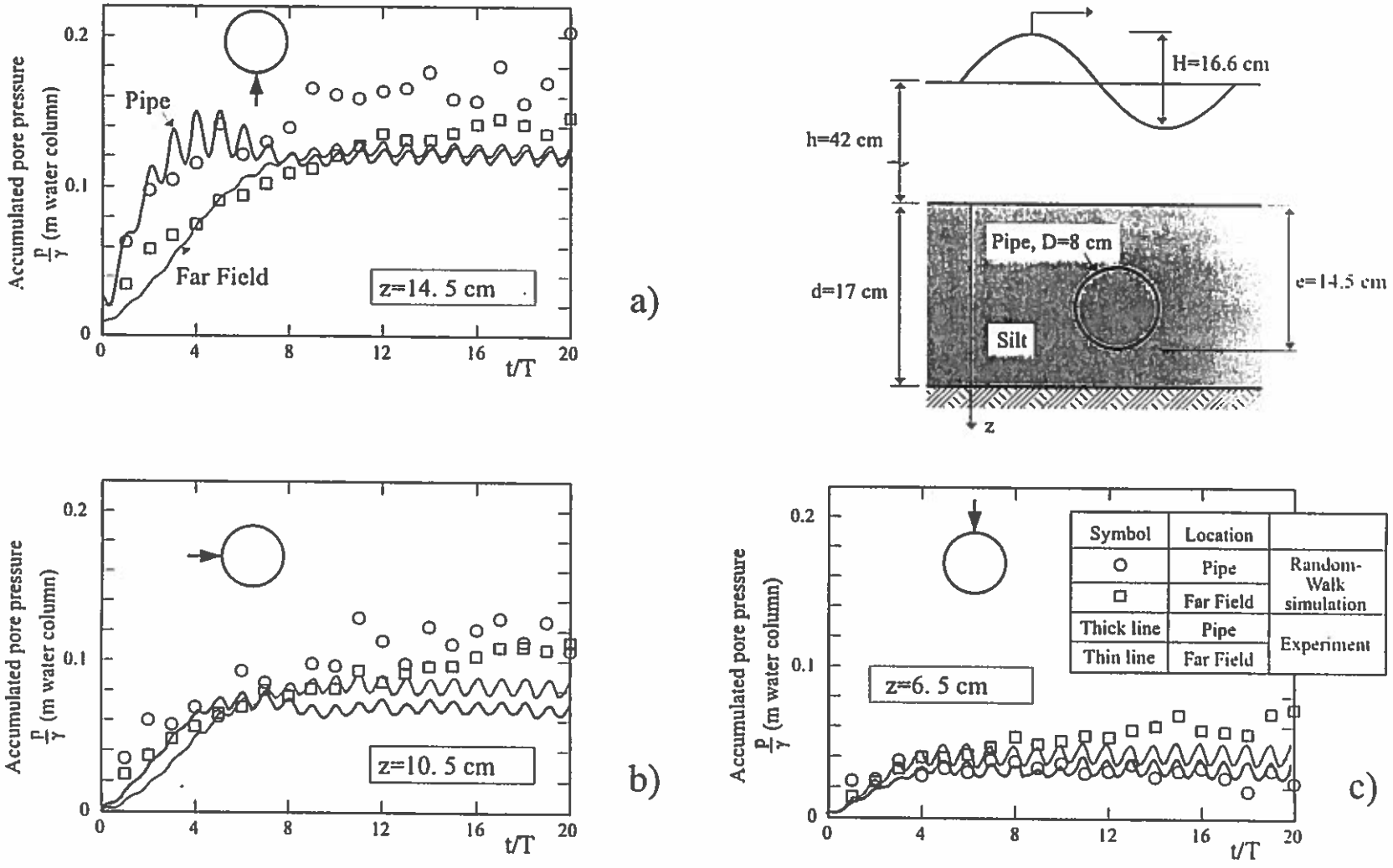

Fig. 7. Buildup of pore pressure around a buried pipeline. H = 16.6 cm, T = 1.6 s, N = 500, $\Delta t/T$ = 1. Symbols: Random-walk simulation. Lines: Experiment.

in which s is a shape factor, and was chosen as s = -0.82. The quantity σ_0' was calculated from Eq. 3, and N_l was calculated from Eq. 4. The maximum value of the shear stress in the soil, τ, needed to calculate N_l, was computed from the 2-D finite-element solution of the equations of equilibrium and the storage equation, as described in Magda (1996, 1997).

At the impermeable base ($z = d$), and at the pipe surface, the reflecting boundary conditions were used, while at the surface of the soil ($z = 0$), the absorbing boundary condition was used. The results are plotted in Fig. 7 in the form of time series at three different depths, z =14.5 cm, z = 10.5 cm, and z = 6.5 cm, and at each depth at two different locations, one in the far-field, and the other at the pipe surface. The figure includes also the results obtained from a laboratory experiment conducted at ISVA. These experiments were carried out in the same wave flume as that described in the preceding paragraph in conjunction with Fig. 6, with the same wave and soil parameters.

The model seems to give the general behaviour of the buildup of pore pressure satisfactorily. It picks up well the experimentally observed larger pressures (larger than the pressures in the far-field at the same depths) both at the bottom of the pipe, and at the midway between the bottom and the top of the pipe (Figs. 7 a and b). Likewise, it picks up the slightly smaller pressures at the top of the pipe (Fig. 7 c).

The model describes the process only for the time period during which the soil is in the no-liquefaction regime. Once the liquefaction is set in, the process of spreading of the pressure will change radically. Therefore, beyond the onset of liquefaction (i.e., beyond the point where the experimentally determined pressure time series attend their asymptotic values in Fig. 7), the simulated time series will begin to deviate from the experiments.

CONCLUSIONS

(1) A random-walk model is given for the prediction of pore pressure and pore-pressure buildup in marine soils.

(2) The model has been validated against two cases where the analytical solutions are known, namely (a) the Terzaghi consolidation case; and (b) the case of the buildup of pore pressure under a progressive wave.

(3) The influence of various parameters for the implementation of the model (such as the small time increment, the depth increment, and the number of particles for the simulation) has been investigated. The influence of the time increment and that of the number of particles was found to be significant.

(4) The model has been implemented for the prediction of the buildup of pore pressure around a buried pipeline exposed to a progressive wave. Early results are encouraging.

ACKNOWLEDGEMENT

This study was partially funded by the Commission of the European Communities, Directorate-General XII for Science, Research and Development Program Marine Science and Technology (MAST III) Contract No.MAS3-CT97-0097, Scour Around Coastal Structures (SCARCOST). The ISVA experiment without the model pipeline was conducted by Mr. Steffen Christensen (M.Sc.), and that with the model pipeline was conducted by Mr. Christoffer Truelsen (M.Sc.) and Mr. Jacob Larsen (M.Sc.). The senior author acknowledges greatly the discussions with Professor Jørgen Fredsøe.

REFERENCES

Alba, P. D., Seed, H. B. & Chan, C. K. (1976): "Sand liquefaction in large-scale simple shear tests". J. of the Geotechnical Engineering Division, ASCE, vol. 102, No. GT9, 909-927.

Bugliarello, G. (1971): "Some examples of stochastic modelling for mass and momentum transfer". In: Stochastic Hydraulics (Ed. Chao-Lin Chiu), Proc. 1st Int. Symp. on Stochastic Hyd., Univ. of Pittsburgh, Penn., USA, May 31- June 2, 1971, pp. 39-55.

Chorin, A. J. (1973): "Numerical study of slightly viscous flow". J. Fluid Mech., vol. 57, part 4, pp. 785-796.

Chorin, A. J. (1978): "Vortex sheet approximation of boundary layers". J. Computational Physics, vol. 27, pp.428-442.

Magda, W. (1996): "Wave-induced uplift force acting on a submarine buried pipeline: Finite element formulation and verification of computations". Computers and Geotechnics, vol. 19, No. 1, 47-73.

Magda, W. (1997): "Wave-induced uplift force on a submarine pipeline buried in a compressible seabed". Ocean Eng., vol. 24, 551-576.

Magda, W. Sumer, B.M. & Fredsøe, J. (1998): Pore Pressure Buildup Around a Buried Pipeline Under Progressive Surface Waves. Internal Report, Technical University of Denmark, Department of Hydrodynamics and Water Resources (ISVA), August 1998, 107 p.

McDougal, W. G., Tsai, Y. T., Liu, P. L-F. & Clukey, E. C. (1989): "Wave-Induced pore water pressure accumulation in marine soils". Trans. ASME, J. Offshore Mechanics and Arctic Engineering, vol. 111, pp.1-11.

Peacock, W. H. & Seed, H. B. (1968): "Sand liquefaction under cyclic loading simple shear conditions". J. Soil Mechanics and Foundations Engineering, vol. 94, No. SM3, pp. 689-708.

Seed, H.B., Martin, P.O. & Lysmer, J. (1975): The Generation and Dissipation of Pore Water Pressures During Soil liquefaction. Report No. EERC 75-26, College of Engineering, University of California, Berkeley, Calif.

Seed, H. B. & Rahman, M. S. (1978): "Wave-Induced pore pressure in relation to ocean floor stability of cohesionless soil". Marine Geotechnology, 3, No. 2, 123-150.

Spierenburg, S. E. J. (1987): Seabed Response to Water Waves. Ph. D. dissertation, Delft University of Technology, The Netherlands.

Stansby, P. K. & Dixon, A. G. (1983): "Simulation of flows around cylinders by a Lagrangian vortex scheme". Appl. Ocean Res. vol. 5, 3, pp. 167-178.

Stansby, P. K. & Isaacson, M. (1987): "Recent developments in offshore hydrodynamics: workshop report". Appl. Ocean Res., vol. 9, 3, pp.118-127.

Sullivan, P. J. (1971): "Longitudinal dispersion within a two-dimensional shear flow". J. Fluid Mech., vol. 49, pp. 551-576.

Sumer, B.M. and Fredsøe, J. (1997): Hydrodynamics Around Cylindrical Structures. World Scientific, xviii+530 p.

Terzaghi, K. (1948): Theoretical Soil Mechanics. London: Chapman and Hall, John Wiley and Sons, Inc., NY.

Weinberger, H. F. (1965): A First Course in Partial Differential Equations with Complex Variables and Transform Methods. Xerox College Publishing, Lexington, Massachusetts.

INTERNATIONAL NAVIGATION ASSOCIATION

SEISMIC DESIGN GUIDELINES FOR PORT STRUCTURES

Report of Working Group No. 34
of the
Maritime Navigation Commission

INTERNATIONAL NAVIGATION
ASSOCIATION

ASSOCIATION INTERNATIONALE
DE NAVIGATION

2001

TABLE OF CONTENTS

1. INTRODUCTION

The occurrence of a large earthquake near a major city may be a rare event but its societal and economic impact can be so devastating that it is a matter of national interest. The earthquake disasters at Los Angeles, USA, in 1994 (61 fatalities and 30 billion US dollars); Kobe, Japan, in 1995 (over 6,400 fatalities and 100 billion US dollars); Kocaeli, Turkey, in 1999 (over 15,000 fatalities and 20 billion US dollars); Athens, Greece, in 1999 (143 fatalities and 2 billion US dollars); and Taiwan in 1999 (over 2,300 fatalities and 9 billion US dollars) are recent examples. Although seismic activity varies depending on coastal regions as reflected in the zones shown in Fig. 1.1, earthquake disasters have repeatedly occurred not only in the seismically active regions in the world but also in areas within low seismicity regions, such as in regions 1 or 2 in the figure. Mitigating the outcome of earthquake disasters is a matter of worldwide interest.

In order to mitigate hazards and losses due to earthquakes, seismic design methodologies have been developed and implemented in design practice in many regions since the early twentieth century, often in the form of codes and standards. Most of these methodologies are based on a force-balance approach, in which structures are designed to resist a prescribed level of seismic force specified as a fraction of gravity. These methodologies have contributed to the acceptable seismic performance of port structures, particularly when the earthquake motions are more or less within the prescribed design level. Earthquake disasters, however, have continued to occur. These disasters are caused either by strong earthquake motions, often in the near field of seismic source areas, or by moderate earthquake motions in the regions where the damage due to ground failures has not been anticipated or considered in the seismic design.

The objectives of the seismic design guidelines for port structures presented in this report are to address the limitations present in conventional design, and establish the framework for a new design approach. In particular, the guidelines are intended to be:

- performance-based, allowing a certain degree of damage depending on the specific functions and response characteristics of a port structure and probability of earthquake occurrence in the region,
- user-friendly, offering design engineers a choice of analysis methods, which range from simple to sophisticated, for evaluating the seismic performance of structures, and
- general enough to be useful throughout the world, where the required functions of port structures, economic and social environment, and seismic activities may differ from region to region.

The expected users of the guidelines are design engineers, port authorities, and specialists in earthquake engineering. The applicability of the guidelines will reflect regional standards of practice. If a region has no seismic codes or standards for designing port structures, the guidelines may be used as a basis to develop a new seismic design methodology, or codes applicable to that particular region. If a region has already developed seismic codes, standards, or established design practice, then the guidelines may be used to supplement these design and analysis procedures. It is not the intent of the authors to claim that these guidelines should be used instead of the existing codes or standards or established design practice in the region of interest. It is anticipated, however, that the guidelines will, with continual modification and upgrading, be recognized as a new and useful basis for mitigating seismic disasters in port areas. It is hoped that the guidelines may eventually be accepted worldwide as recommended seismic design provisions.

Earthquake engineering demands background knowledge in several disciplines. Although this background knowledge is not a pre-requisite to understanding the guidelines, readers may find it useful to have reference textbooks readily available. Pertinent examples include Kramer (1996) on geotechnical earthquake engineering and Tsinker (1997) on design practice for port structures.

This summary report provides an overview of the seismic design guidelines. The complete guidelines document will be available in a book published separately through Balkema in 2001. Highlights of the book "Seismic Design Guidelines for Port Structures" will include the following Technical Commentaries (TC):

TC1: Existing Codes and Guidelines
TC2: Case Histories
TC3: Earthquake Motion
TC4: Geotechnical Characterization
TC5: Structural Design Aspects of Pile-Deck Systems
TC6: Remediation of Liquefiable Soils
TC7: Analysis Methods
TC8: Examples of Seismic Performance Evaluations

LIMAS

Liquefaction Around Marine Structures
Dansk Vandbygningsteknisk Selskab 20 March 2003

IMPACT OF LIQUEFACTION ON COASTAL STRUCTURES IN THE 1999 KOCAELI, TURKEY EARTHQUAKE

By

B. Mutlu Sumer, Abidin Kaya

And Niels-Erik Ottesen Hansen

LIMAS

Liquefaction Around Marine Structures
Dansk Vandbygningsteknisk Selskab 20 March 2003

- **BACKGROUND**
- **WHAT HAEEPEND**
- **LIQUEFACTION DAMAGE ON THE MARINE STRUCTURE**
- **LESSONS LEARNED**

LIMAS

Liquefaction Around Marine Structures
Dansk Vandbygningsteknisk Selskab 20 March 2003

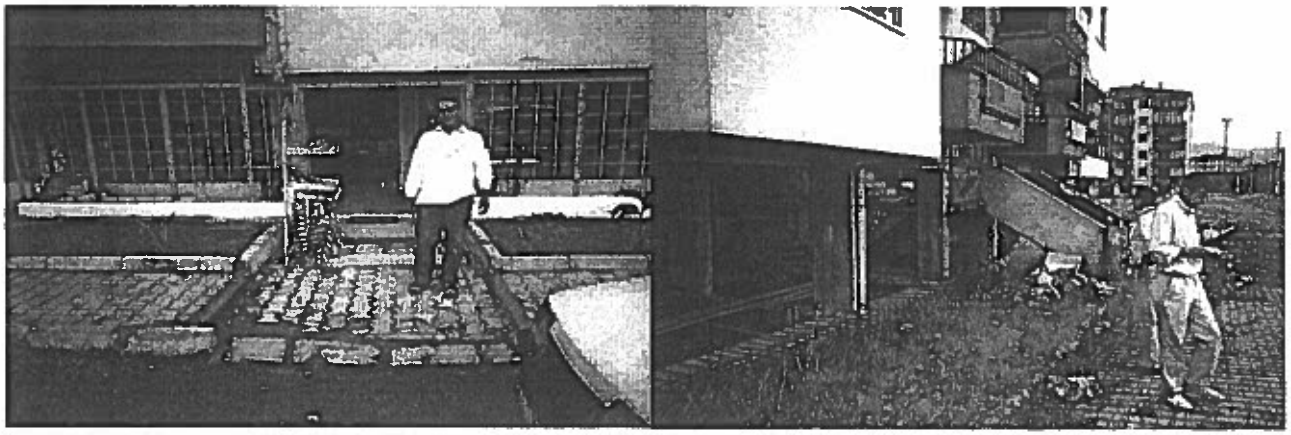

LIMAS

Liquefaction Around Marine Structures
Dansk Vandbygningsteknisk Selskab 20 March 2003

LIMAS

Liquefaction Around Marine Structures
Dansk Vandbygningsteknisk Selskab 20 March 2003

LIMAS

Liquefaction Around Marine Structures
Dansk Vandbygningsteknisk Selskab 20 March 2003

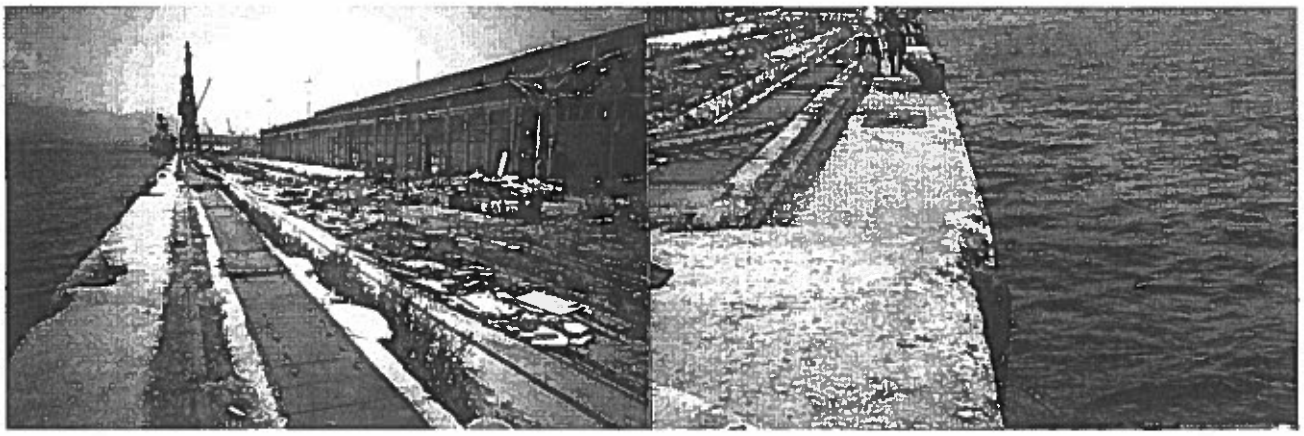

LIMAS

Liquefaction Around Marine Structures
Dansk Vandbygningsteknisk Selskab 20 March 2003

LIMAS

Liquefaction Around Marine Structures
Dansk Vandbygningsteknisk Selskab 20 March 2003

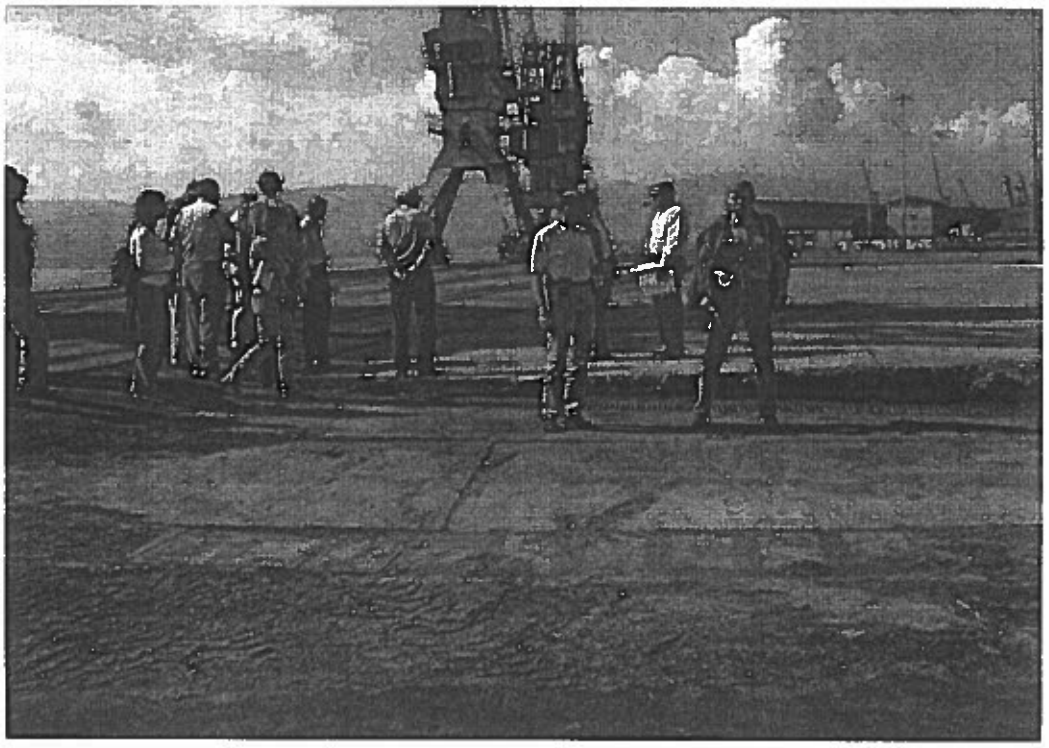

LIMAS

Liquefaction Around Marine Structures
Dansk Vandbygningsteknisk Selskab 20 March 2003

LIMAS

Liquefaction Around Marine Structures
Dansk Vandbygningsteknisk Selskab 20 March 2003

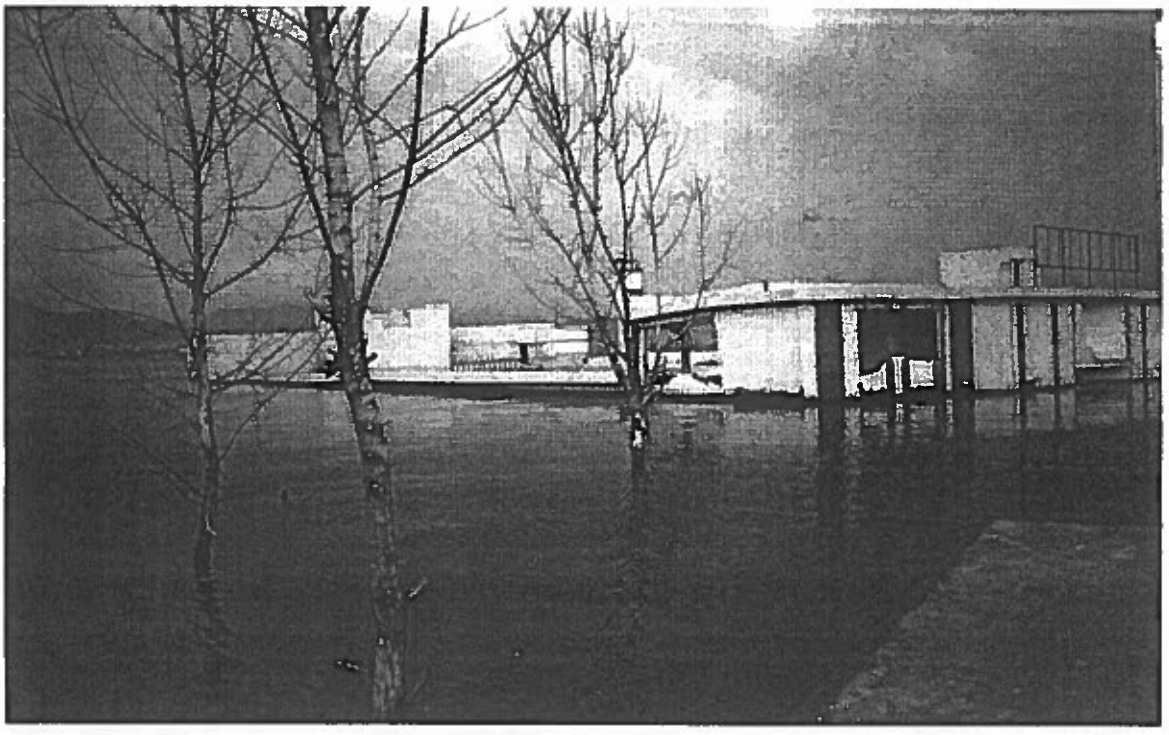

LIMAS

Liquefaction Around Marine Structures
Dansk Vandbygningsteknisk Selskab 20 March 2003

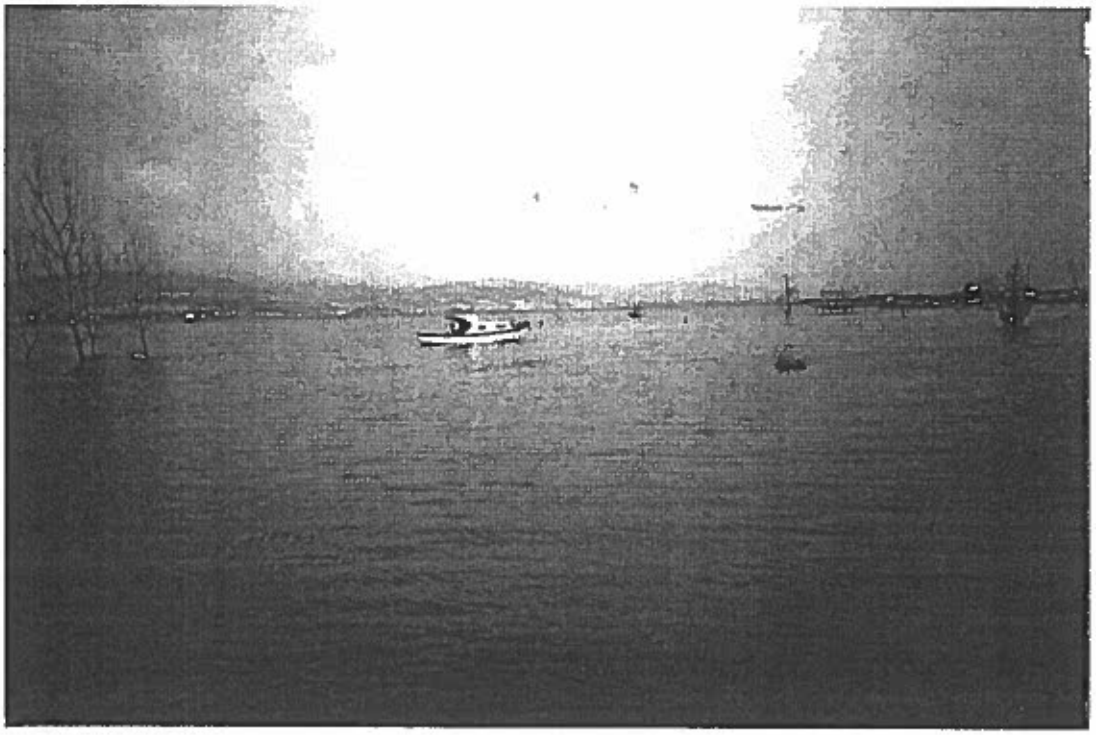

LIMAS

Liquefaction Around Marine Structures
Dansk Vandbygningsteknisk Selskab 20 March 2003

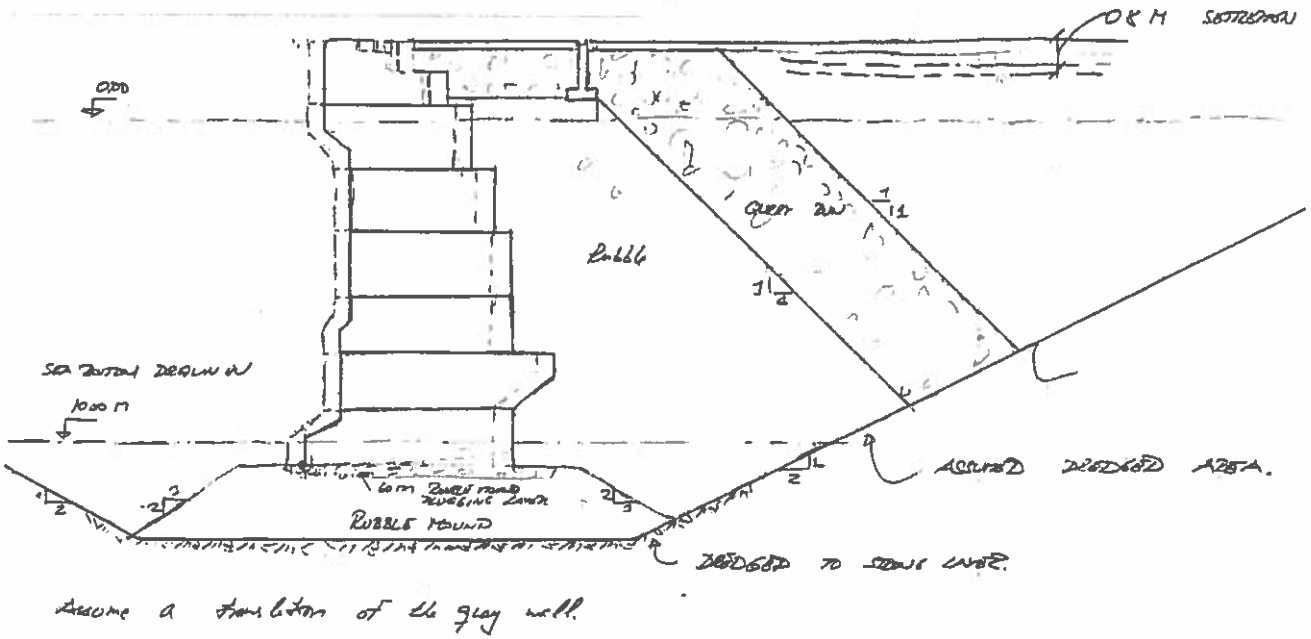

Assume a thickness of the quay wall.

LIMAS

Liquefaction Around Marine Structures
Dansk Vandbygningsteknisk Selskab 20 March 2003

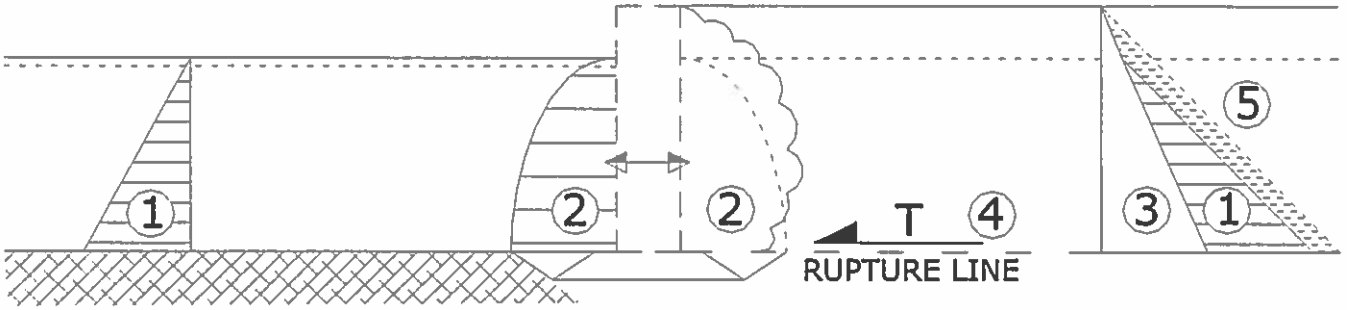

1. HYDROSTATIC PRESSURE
2. HYDRODYNAMIC MASS
3. LATERAL SOIL PRESSURE (ACTIVE)
4. FRICTIONAL FORCE
5. ADDITIONAL WATER PRESURE FROM LIQUEFACTION

SAFETY:	ASEISMIC
SLIDING	~2.2
OVERTURNING	~2.4
SAFETY:	SEISMIC
SLIDING	?
OVERTURNING	

LIMAS

Liquefaction Around Marine Structures
Dansk Vandbygningsteknisk Selskab 20 March 2003

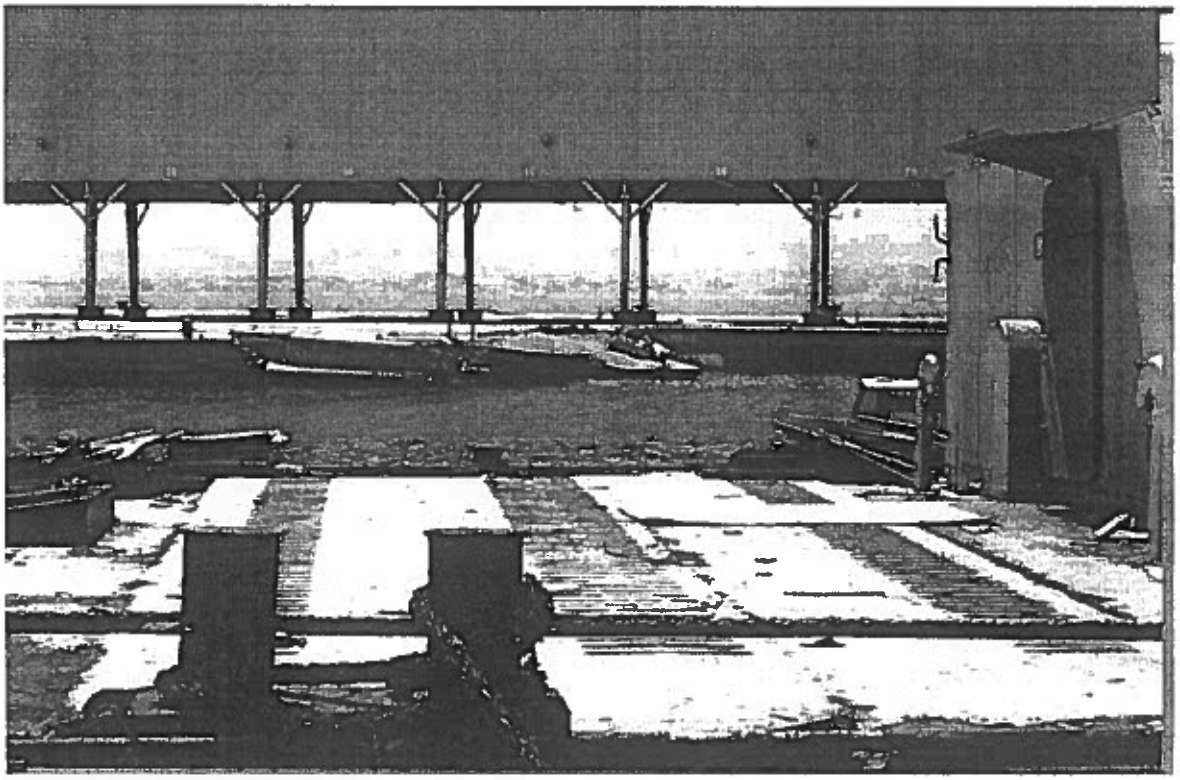

LIMAS

Liquefaction Around Marine Structures Dansk Vandbygningsteknisk Selskab 20 March 2003

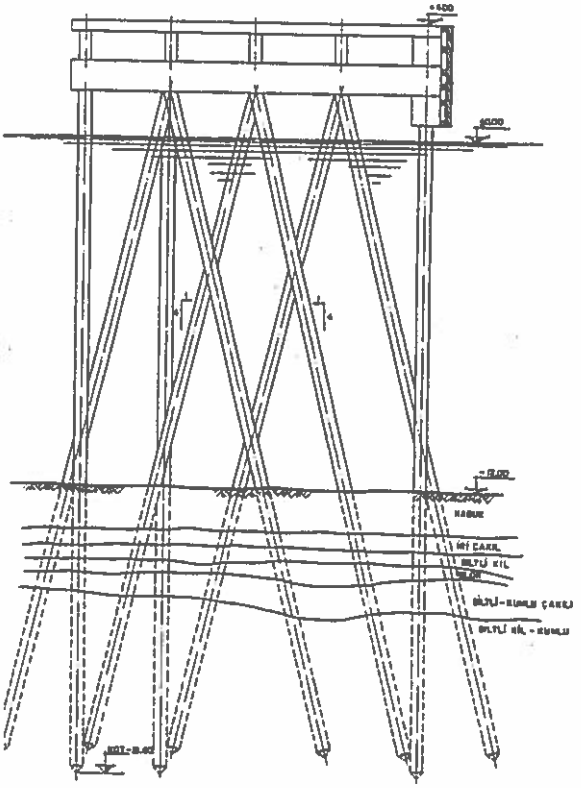

B/0-30 ÇALIŞMA PLATFORMU YAN GÖRÜNÜŞ 1/100

LIMAS

Liquefaction Around Marine Structures Dansk Vandbygningsteknisk Selskab 20 March 2003

LIMAS

Liquefaction Around Marine Structures
Dansk Vandbygningsteknisk Selskab 20 March 2003

LIMAS

Liquefaction Around Marine Structures
Dansk Vandbygningsteknisk Selskab 20 March 2003

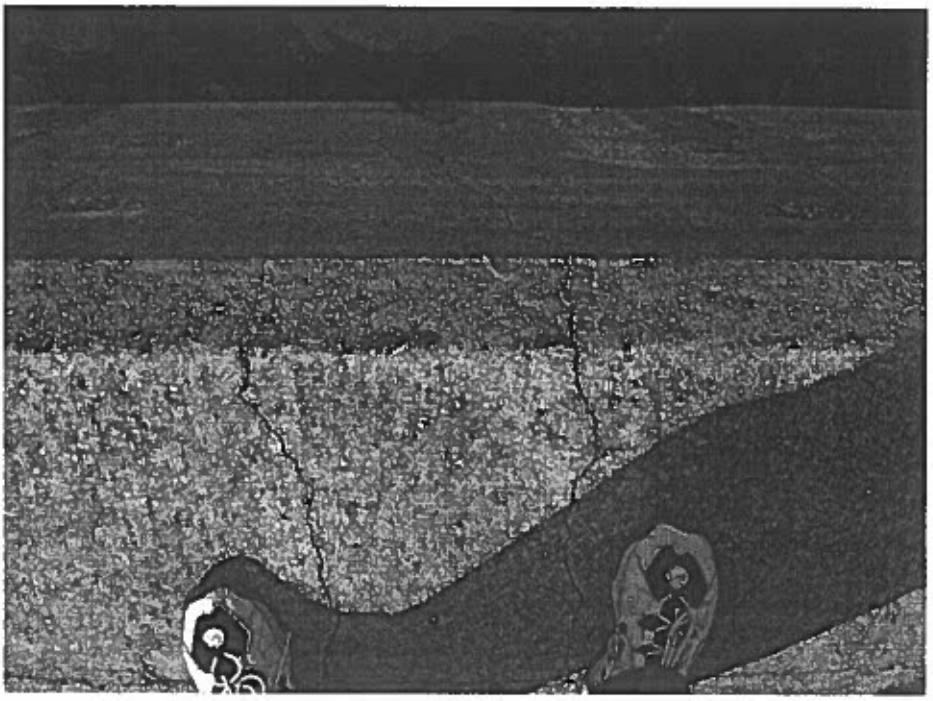

LIMAS

Liquefaction Around Marine Structures
Dansk Vandbygningsteknisk Selskab 20 March 2003

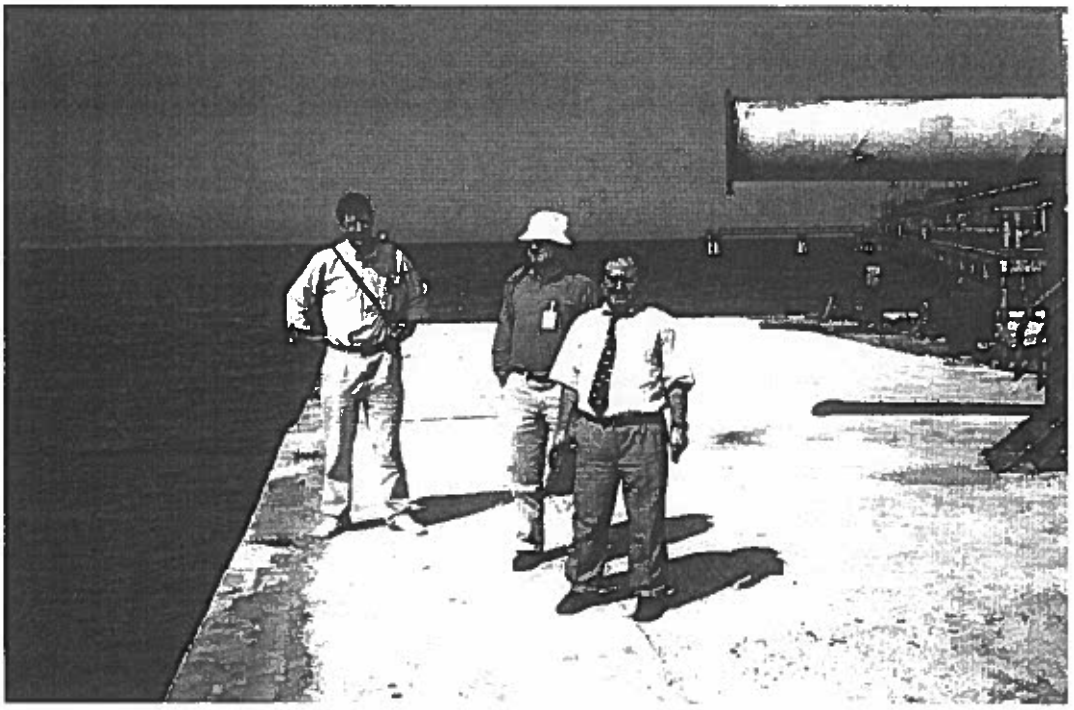

LIMAS

Liquefaction Around Marine Structures
Dansk Vandbygningsteknisk Selskab 20 March 2003

LIMAS

Liquefaction Around Marine Structures
Dansk Vandbygningsteknisk Selskab 20 March 2003

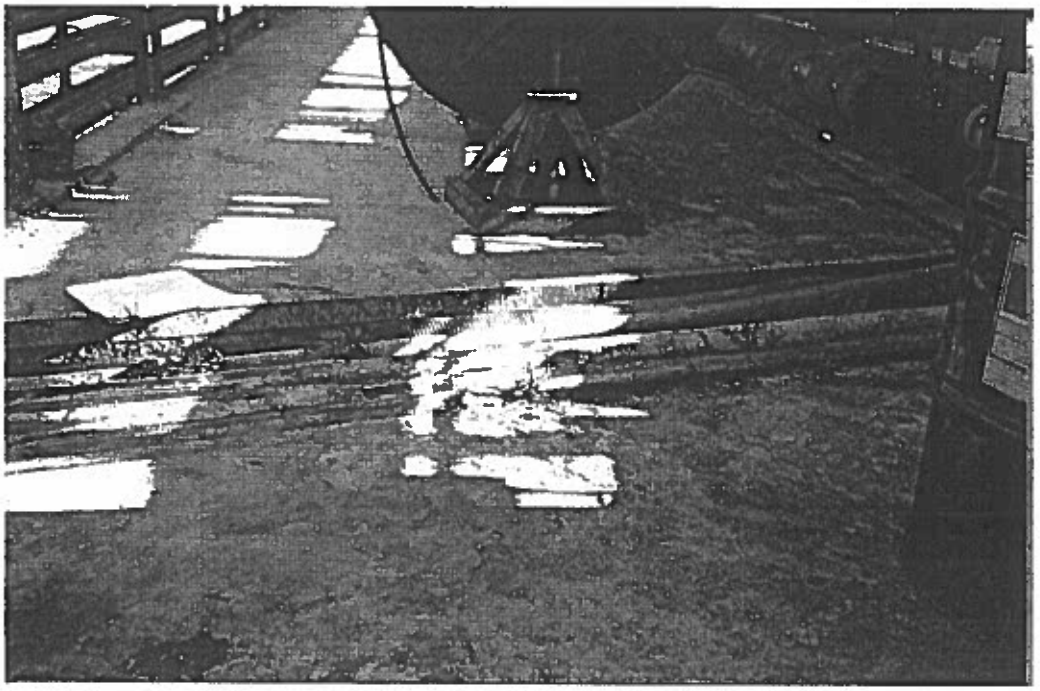

LIMAS

Liquefaction Around Marine Structures
Dansk Vandbygningsteknisk Selskab 20 March 2003

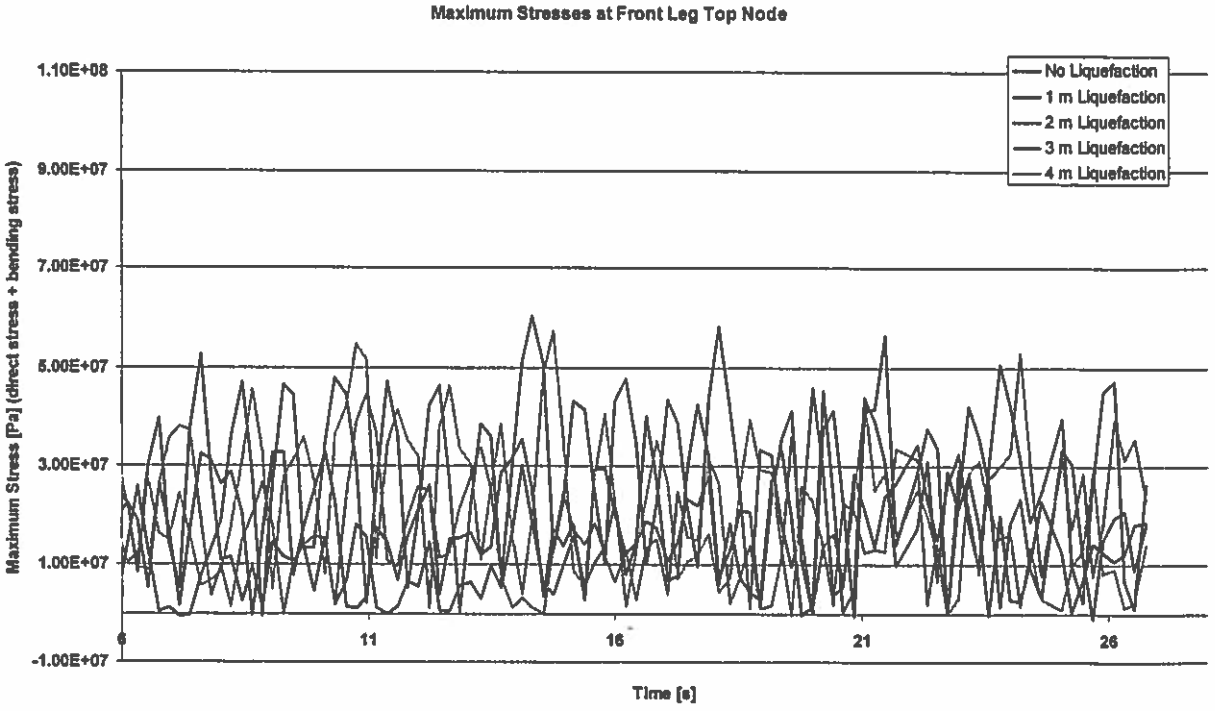

LIMAS

Liquefaction Around Marine Structures
Dansk Vandbygningsteknisk Selskab 20 March 2003

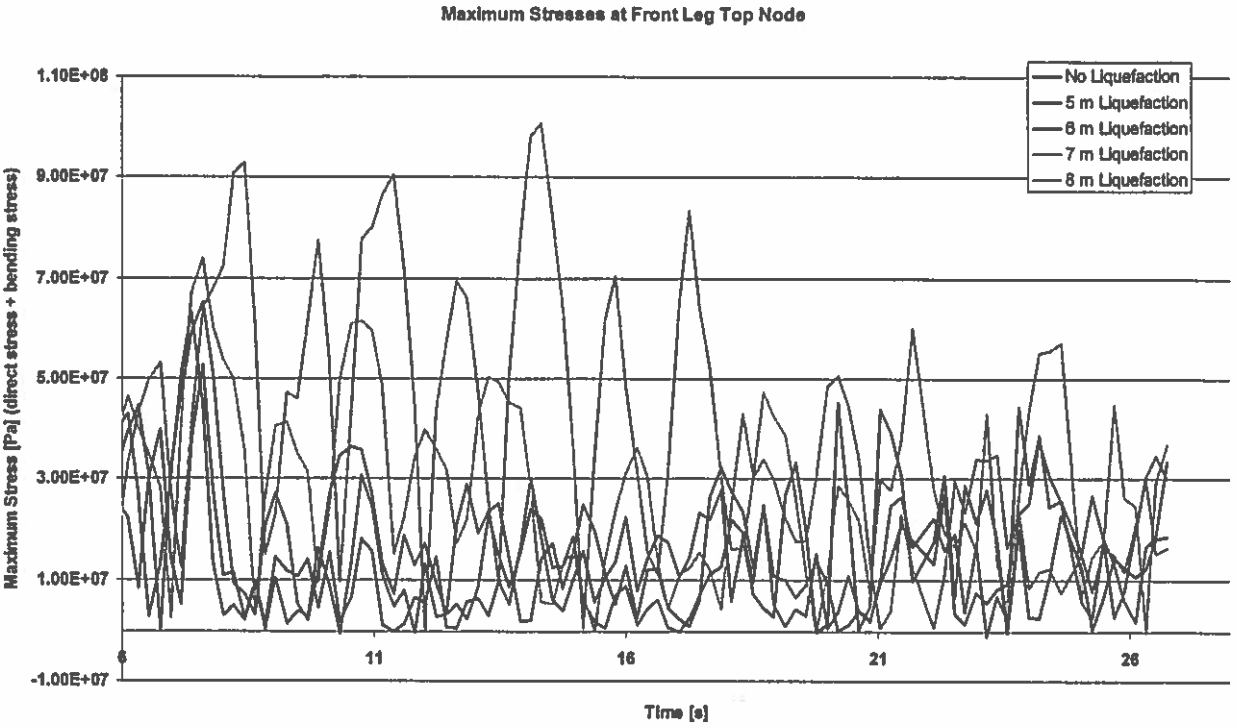

LIMAS

Liquefaction Around Marine Structures
Dansk Vandbygningsteknisk Selskab 20 March 2003

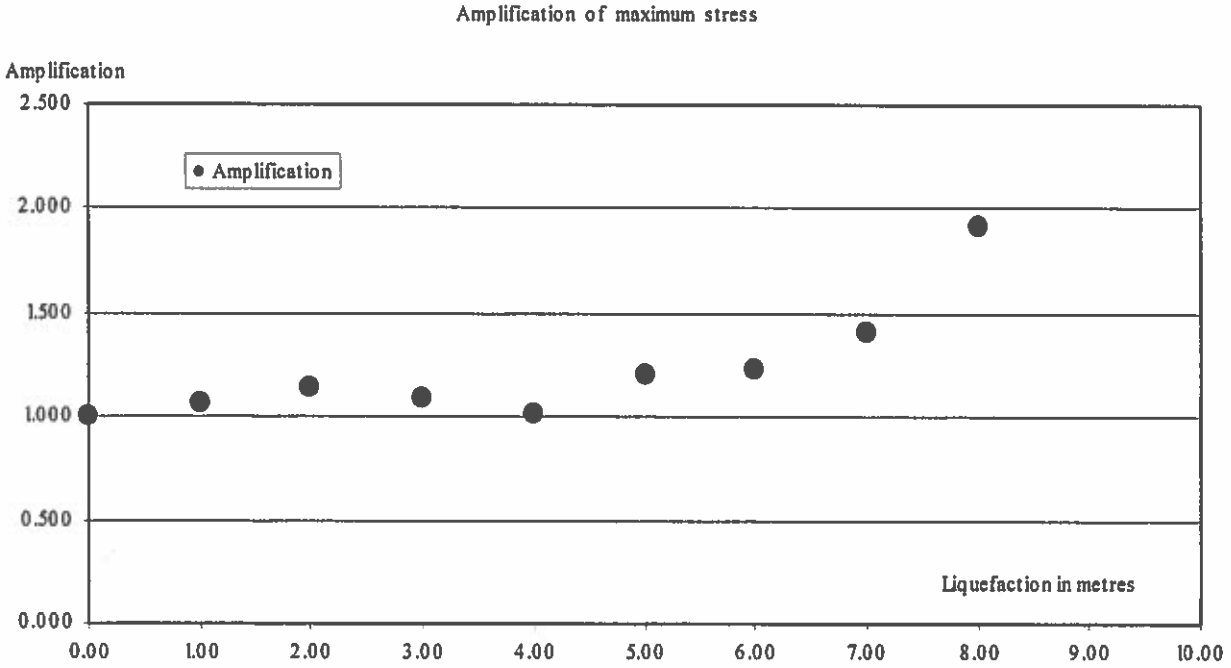

LIMAS

Liquefaction Around Marine Structures
Dansk Vandbygningsteknisk Selskab 20 March 2003

CONCLUSIONS:

PILE SUPPORTED PIERS MAY HAVE EXPERIENCED ADDITIONAL LOADING DUE TO REDUCTION IN EFFECTIVE STRESSES.

PILED STRUCTURES WITH SHORT CONCRETE PILES COLLAPSED. PILED STEEL STRUCTURES WERE MORE RESILIENT.

DAMAGE TO QUAY WALL STRUCTURES SMALL. OUTWARD MOVEMENTS OBSERVED o (0.1m – 1m).

NOT COMPACTED BACKFILL SETTLED o (1m).

SPACE FRAME STRUCTURES OF GOOD QUALITY MAINTAINED INTEGRITY UNDER LIQUEFACTION INDUCED SETTLEMENTS.

IMPACT OF LIQUEFACTION ON COASTAL STRUCTURES IN THE 1999 KOCAELI, TURKEY EARTHQUAKE

B. Mutlu Sumer[1], Abidin Kaya[2] and Niels-Erik Ottesen Hansen[3]
[1]Technical University of Denmark, Department of Mechanical Engineering
Coastal and River Engineering Section, Building 115, 2800 Lyngby, Denmark
[2]Same address as above. On leave from Dokuz Eylul University, Izmir, Turkey
[3]LICengineering A/S, Ehlersvej 24, 2900 Hellerup, Denmark

ABSTRACT

An inventory is presented of the damage to marine structures caused by liquefaction in the 17.August, 1999 Kocaeli, Turkey earthquake. The inventory includes twenty-four coastal structures. The observations show that backfills behind quay walls and sheet-piled structures were almost invariably liquefied; quay walls and sheet-piled structures were displaced seaward; storage tanks near the shoreline were tilted; there were cases where the seabed settled, and structures settled and collapsed; the observations also show that the rubble-mound breakwaters survived the earthquake with very little or no damage.

KEY WORDS: Coastal structures; earthquake; Kocaeli (Turkey) earthquake liquefaction; pore pressure; quay walls; tsunami; waves.

INTRODUCTION

Liquefaction is a process in which shear strength of soil goes to zero due to developed excessive large pore pressures, and the soil behaves like viscous liquid producing excessive deformations or movements as a result of transit or repeated loads (NRC, 1985; Youd and Idriss, 2001).

The transit/repeated loads may be induced by effects such as earthquakes; shocks (the shock effects may be caused by a sudden failure of a slope, or blasting effects); surface waves; rocking motions that structures may execute under cyclic loadings (rocking motion of vertical-wall breakwaters under waves, for example) and so on.

Strength loss and large deformations of such soils can result in failures such as flow slides, slope instabilities, and increased bending forces on piles and other embedded structures (Chaney and Pamukcu, 1991, Hyodo, et al. 1999). With the soil liquefied, buried structures (such as pipelines) may float to the surface; large individual blocks (like those used for scour protection at

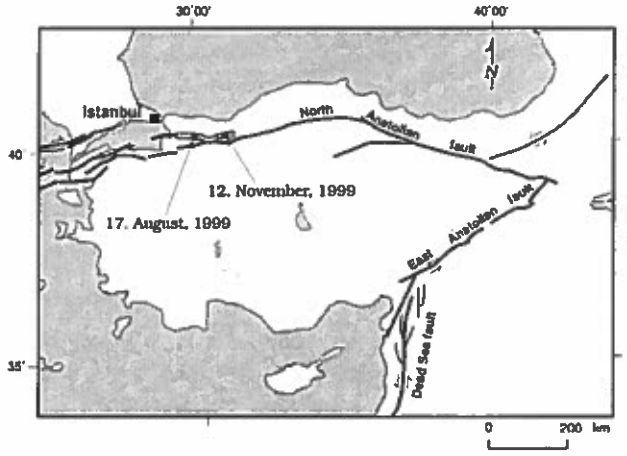

Fig. 1. The North Anatolian Fault. Adapted from Lettis et al. (2000 a).

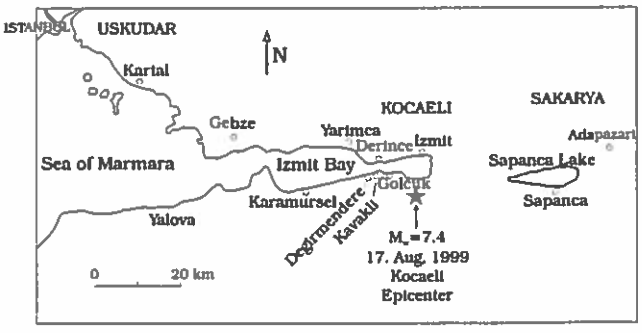

Fig. 2. Map of the area stricken by the 17. August, 1999 Kocaeli, Turkey earthquake.

marine structures) may sink in the seabed; sea mines may sink in the seabed and eventually disappear. Sand boils, ground fissures and/or lateral spreads are the field evidence of marine liquefaction (Youd and Idriss, 2001).

In 1999, Turkey experienced two earthquakes: (1) The 17.August, 1999 Kocaeli Earthquake, and (2) The 12.November, 1999 Duzce Earthquake. Both occurred on the North Anatolian Fault in the North Western Turkey (Fig. 1). The Kocaeli earthquake, which had a magnitude of M_w = 7.4 with its epicentre located rather close to the south east corner of the Izmit Bay (Figs. 2 and 3) and lasted 42 s with the largest horizontal acceleration of 0.407*g* (Safak et al., 2000), caused extensive damage to marine structures along the coast of the Izmit Bay.

Boulanger et al. (2000) discuss the damage to and the performance of the marine structures in the Kocaeli Earthquake in the special volume of the journal Earthquake Spectra (2000) dedicated to the this earthquake. Gunbak, Muyesser and Yuksel (2000) give an "inventory" of the damage inflicted over more than 20 marine structures while Yuksel et al. (2000, 2001) further elaborate on the effects of the Kocaeli Earthquake on the majority of the marine structures and coastal areas in the region.

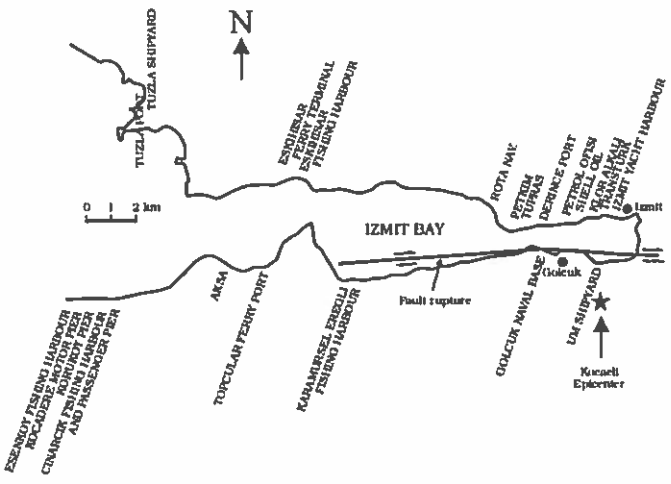

Fig. 3. Partial layout of coastal structures along the coastline of the Izmit Bay. Site of seabed settlements extend on the Northern coast from Rota Nav. to Izmit. Adapted from Gunbak et al. (2000), Yuksel et al. (2000, 2001).

The purpose of the present paper is to summarize the early results of a study where the focus is the impact of liquefaction on coastal structures in the 17.August, 1999 Kocaeli earthquake. The data compiled is mainly from Boulanger et al. (2000), Gunbak et al. (2000), Yuksel et al. (2000, 2001) and from a field visit of the authors, which took place 1-9.July, 2001.

INVENTORY OF THE DAMAGE CAUSED BY SEISMIC-INDUCED LIQUEFACTION, AND ANALYSIS

Table 1 lists an "inventory" of the damage to coastal structures along the coastline of the Izmit Bay (Table 1 is given at the end of the paper). The data has been compiled mainly from Boulanger et al. (2000), Gunbak et al. (2000), Yuksel et al. (2000, 2001) and during a visit by the present authors made on 1 thru 9.July, 2001, as mentioned previously. The names of the coastal facilities given in Column 2 in Table 1 are indicated in Fig. 3.

The following observations can be made from Table 1.

1. Almost invariably, backfill areas behind quay walls and sheet-piled structures failed due to liquefaction, as in Tuzla Port (Row 1, Table 1), Tuzla Shipyard (Row 2 C), Eskihisar Ferry Terminal (Row 3 A and B), Derince Port (Row 8 A and B), Shell Oil Facility (Row 11), Izmit Yacht Harbour (Row 14), UM Shipyard (Row 15), Golcuk Naval Base (Row 16 B), Karamursel Eregli Fishing Harbour (Row 17 B), Topcular Ferry Pier (Row 18), Cinarcik Fishing Harbour (Row 20) and Esenkoy Fishing Harbour (Row 24 B) although, in some cases, the failure in the backfill areas may have been influenced by other factors as well. From the table, the settlement in the backfill areas varies from O(10 cm) to O(1 m) in which the symbol O indicates the order of magnitude. The magnitude of the settlement generally decreases with the distance from the epicenter of the earthquake (Table 1 and Fig. 3), as anticipated. One of the implications of this kind of failure is that rail foundations for cranes present in the area settle unevenly, leading to tilting of (and eventually damage to) cranes, as revealed clearly in the case of Derince Port (see photographs in Boulanger et al., 2000, Yuksel et al., 2000).

2. Quay walls and sheet-piled structures were displaced seaward, as in Tuzla Port (Row 1 in Table 1), Tuzla Shipyard (Row 2 C), Derince Port (Row 8 A), Izmit Yacht Harbour (Row 14), Golcuk Naval base (Row 16 B), the displacements being in the range from O(10 cm) to O(1 m).

3. Storage tanks near the shoreline tilted due to liquefaction, as in Petrol Ofisi facilities (Row 10 C in Table 1), Klor Alkali facilities (Row 12) and Transturk facilities (Row 13).

4. There are cases where the seabed settled, as in Rota Navigation Trade Pier (Row 5 in Table 1), Tupras Refinery (Row 7), Petrol Ofisi facilities (Row 10 A) and Shell Oil Piers (Row 11), the settlement being in the range O(10 cm)-O(1 m). However, it is not clear if these settlements are caused by liquefaction (and therefore by the resulting consolidation) or by other processes such as slope instability, surface rupture, etc, or a combination of those processes.

5. There are also cases where structures settled, as in Petkim facilities (Row 6 in Table 1) and Petrol Ofisi facilities (Row

10 A), or they settled and eventually collapsed below water as in Shell Oil Piers (Row 11), Transturk facilities (Row 13), UM Shipyard (Row 15) and Aksa facilities (Row 19). Again, it is not quite clear if these settlements (and collapses) are caused by liquefaction or by other processes such as slope instability, surface rupture, etc, or a combination of those processes.

6. It is interesting to notice that although a large reclamation area settled in front of the 95.000-ton capacity silos in Derince Port TMO facilities (Row 9, Table 1), these silos survived the earthquake. Likewise, the 510-ton shipyard crane also survived the earthquake despite the large settlement of the area adjacent to this structure in UM Shipyard (Row 15). These structures survived the earthquake largely because of their foundations; both the TMO silos and the UM crane are supported on piles penetrating into the stiff soil, and therefore avoided any problem caused by liquefaction/weakening of the soil in the top layers due to pressure buildup. It is also interesting to note that the new pier in Petrol Ofisi facilities (Row 10 B in Table 1) has also survived the earthquake while the neighbouring old pier has not. This may also be attributed to the fact that the piles in this case, too, penetrated into the stiff soil.

7. The rubble-mound breakwaters survived the earthquake with practically no damage or very little damage, as in Tuzla Shipyard (Row 2 A in Table 1), Eskihisar Fishing Harbour (Row 4 A), Karamursel Eregli Fishing Harbour (Row 17 A), Cinarcik Fishing Harbour (Row 20) and Esenkoy Fishing Harbour (Row 24). However, it is not known if the seabed at these locations experienced liquefaction/weakening due to buildup of pore pressure.

DISCUSSION

Liquefaction of seabed

As mentioned previously, although the settlement of the seabed has been observed along the North coast of Izmit Bay at Rota Navigation Trade Pier, Tupras Refinery, Petrol Ofisi facilities and Shell Oil Piers (Fig. 3 and Rows 5, 7, 10 A, 11 in Table 1), it is not clear if these settlements are caused by liquefaction (and therefore by the resulting consolidation) or by other processes such as slope instability, surface rupture, etc., or a combination of those processes. This subsection discusses the possibility of liquefaction/weakening of the seabed by the shaking caused by the 17.August, 1999 earthquake.

Table 2 depicts a partial list of the earthquakes experienced in the vicinity of Sea of Marmara and North Anatolian Fault. Note the magnitudes of these past earthquakes (namely up to M_w = 7.1) before the 17.August, 1999 Kocaeli Earthquake occurred.

Now, given that the soil had been heavily shaken by the previous earthquakes (Table 2), we expect that there was not much "room" for the rearrangement of soil grains and therefore for buildup of pore pressure and hence for the resulting liquefaction/weakening of the seabed when the 17.August, 1999 earthquake occurred.

However, there is clear evidence that the soil has been liquefied in areas such as that marked "Liquefaction Zone" in the map in Fig. 2.6b of the paper by Lettis et al. (2000 b), the area to the East of Naval Base in Golcuk (see Fig. 3 for the location). Although

1. the locations where the seabed settlements were observed are not as close to the earthquake epicentre as the previously mentioned "Liquefaction Zone", and also
2. the soil in these locations is essentially different from that in this "Liquefaction Zone" area,

Table 2. A partial list of earthquakes that occurred in the vicinity of Sea of Marmara and North Anatolian Fault[1] (Taymaz, 1999).

Date	Latitude	Longtitude	Magnit.
20.06.1943	40.70	30.38	$M = 6.3$
13.08.1951	40.95	32.57	$M_s = 6.7$
26.05.1957	40.66	30.89	$M_s = 7.0$
18.09.1963	40.90	29.20	$M_s = 6.4$
09.10.1964	40.30	28.23	$M_s = 6.9$
22.07 1967	40.67	30.69	$M_s = 7.1$
30.07.1967	40.72	30.52	$M_s = 5.6$
03.09.1968	41.81	32.39	$M_s = 6.6$
05.10.1977	41.02	33.57	$M_s = 5.8$
05.07.1983	40.33	27.23	$m_b = 5.5$
21.10.1983	40.54	30.05	$m_b = 5.1$
24.04.1988	40.77	28.73	$m_b = 5.0$
17.08.1999	40.709 (Kocaeli)	29.998	$M_w = 7.4$
13.09.1999	40.765 (Marmara)	30.072	$M_w = 5.9$
11.11.1999	40.804 (Duzce)	30.260	$M_w = 5.7$
12.11.1999	40.790 (Duzce)	31.070	$M_w = 7.1$

[1] Note that M_s is the surface wave magnitude, M_w the moment magnitude and m_b the body wave magnitude. The relationships between these magnitudes are that M_w and M_s are rather close to each other for M_w smaller than about 8, while m_b becomes increasingly smaller than M_w when M_w becomes larger than about 6, Kramer (1996, p. 49).

the possibility of the seabed liquefaction (or weakening) may not be entirely ruled out. One reason why the seabed may be liquefied (or weakened) by the shaking of the 17.August, 1999 earthquake may be that this latest earthquake had a magnitude, which is significantly larger than the previous ones (the amplitude of the ground motion being at least a factor of 2 larger in the M_w = 7.4 earthquake than, for example, the M_w = 7.1 earthquake). It may also be noted that the duration of the earthquake is also an influencing factor. Unlike the liquefaction in on-land areas, the seabed is also subject to waves, another effect to cause liquefaction. (The seabed liquefaction under waves may occur in two forms, the residual liquefaction and the momentary liquefaction, see for example, Sumer and Fredsøe, 2002, Chapter 10). Since the seabed has a long history of wave exposure, it may be expected that the soil is well consolidated under the action of waves, and hence, again there was not much

room for the accumulation of the pore pressure with the shaking of the 17.August, 1999 earthquake, similar to the effect of the long history of shaking due to the previous earthquakes. However, the wave statistics predicted from the wind data (with a 50-year significant wave height of O(1-2 m) and with a 50-year significant wave period of O(5 s) at Karamursel (Fig. 2) for water depths of O(20 m), Y. Yuksel, 2001, personal communication) implies that the waves will not induce any significant buildup of pore pressure or any significant effect of momentary liquefaction, and therefore the seabed may still have experienced liquefaction (or weakening) due to the shaking of the 17.August, 1999 earthquake.

Liquefaction of backfills

This subsection discusses two aspects of the backfill failure described in the preceding paragraphs:

1. the backfill material, and
2. the additional force exerted on the quay wall/sheet-piled structure.

As mentioned in the previous section, the backfills behind the quay walls and sheet-piled structures were almost invariably liquefied in the 17.August, 1999 earthquake. Although the backfill material varied from one case to another, it was typically hydraulically-placed sand from the seabed, as in the case of Derince Port.

A relevant question here is: Could the liquefaction failure have been avoided had the backfill material been replaced with a coarser material, a material which is sufficiently permeable so that all pore pressures developed in the backfill would dissipate as rapidly as they develop? Unfortunately, no data exists in conjunction with the 17.August, 1999 earthquake to reveal as to whether this is the case, and, if so, how coarse this material should be.

One of the implications of liquefaction (or a significant buildup of pore pressure) in the backfill is that the quay wall/sheet-piled structure undergoes an additional, seaward-directed horizontal (or almost horizontal) force caused by the accumulated pore pressure in the backfill behind the structure. This latter force contributes to the total horizontal force on the structure in the outward direction. In the liquefied state, the pressure acting on the wall is the hydrostatic pore pressure, $\gamma_w z$, plus the accumulated pore pressure, which is equal to the initial effective stress, the overburden-pressure value, $\sigma_0' = \gamma' z\ (1+2k_0)/3$ in which γ_w is the specific weight of water, z the depth measured downwards from the surface of the backfill, k_0 the coefficient of lateral earth pressure and γ' the submerged specific weight of the backfill material. (It may be noted that (1) the pressure on the wall in the "undisturbed" case is $\gamma_w z$ plus $k_0\gamma' z$; and (2) the initial effective stress has been taken as $\sigma_0' = \gamma' z\ (1+2k_0)/3$ rather than $\gamma' z$ in the above analysis on grounds that, this, when taken as $\sigma_0' = \gamma' z\ (1+2k_0)/3$, gives more realistic results for the liquefaction criterion, as observed in the works of McDougal et al., 1989, Jeng, 1997 and Sumer et al., 1999 in conjunction with liquefaction of soils under waves). From the preceding analysis, there is an additional force on the wall in the outward direction in the case of the liquefied backfill equal to $(1/2)\ \gamma' h^2\ (1-k_0)/3$ in which h is the height of the wall. This additional force obviously helps displace the structure seaward. As mentioned earlier, this kind of outward displacements of quay walls and sheet-piled structures have indeed been observed in the 17.August, 1999 earthquake, in Tuzla Port, Tuzla Shipyard, Derince Port, Izmit Yacht Harbour and Golcuk Naval Base (Rows 1, 2 C, 8 A, 14, 16 B in Table 1).

Remarks on the implication of tsunami for soil liquefaction

The 17.August, 1999 earthquake generated tsunami waves in the Izmit Bay. Yalciner et al. (2000), from their field surveys, concluded that a major tsunami was generated due to a large tectonic subsidence near and/or at the shoreline. This tsunami had a period shorter than 1 minute. It arrived at the Southern coasts one minute after the earthquake, and it arrived at the Northern coasts a few minutes after the earthquake. The sea receded first and subsequently rose and flooded the in-land areas with values of run-up heights of up to 2.5 m. Yalciner et al. also concluded that tsunami waves may have also been generated by sediment slumping in addition to tectonic subsidence.

Although no study is yet available, investigating the liquefaction of soil under tsunami waves near the shoreline, it may be expected that strong vertical (upward directed) pore-pressure gradients may be generated during a tsunami, particularly during the drawdown stage. This latter effect may help reduce the stiffness of the soil, eventually leading to liquefaction. However, how much this process has contributed to the observed settlements of the seabed and the observed settlements (and collapses) of the structures referred to in the preceding paragraphs (items 4 and 5 under Inventory of the Damage Caused by Seismic-Induced Liquefaction and Analysis) is unknown. Likewise, the contribution of the tsunamis to massive coast subsidences particularly at Kavakli and Degirmendere areas (reported in Bardet et al., 2000, see the map in Fig. 2 for these locations) is also unknown.

In the previous subsection, we have discussed the forces exerted on quay walls and sheet-piled structures by pore pressure, which tend to displace the structure in the seaward direction. Now, immediately after the earthquake, this force is equal to the undisturbed pore pressure force plus the accumulated pore pressure force, as described in the preceding subsection. With the water receded during the tsunami a few minutes after the earthquake, the hydrostatic pressure force on the wall at the sea side will decrease or completely vanish, and therefore the wall will undergo a relatively larger, seaward resultant pressure force. This effect may have played a significant role in the observed seaward displacements of quay walls and sheet-piled structures mentioned earlier.

CONCLUSIONS

1. Backfill areas behind quay walls and sheet-piled structures

failed due to liquefaction.

2. Quay walls and sheet-piled structures were displaced seaward. Liquefaction in backfill areas may have contributed to the seaward displacements of these structures.
3. Storage tanks near the shoreline were tilted due to liquefaction.
4. There are cases where the seabed settled, and there are also cases where structures settled and collapsed below water. It is not clear, however, whether these incidents are due to liquefaction, or due to other processes such as slope instability, surface rupture, etc, or due to a combination of these processes.
5. Two large structures (95.000-ton capacity silos and a 510-ton shipyard crane) and one newly constructed pier survived the earthquake despite the large settlement of the areas adjacent to these structures largely because of their foundations; namely these structures are supported on piles penetrating into the stiff soil.
6. The rubble-mound breakwaters survived the earthquake with practically no or very little damage.

ACKNOWLEDGEMENTS

This study has been partially funded by the European Commission Research Directorates' FP5 specific program "Energy, Environment and Sustainable Development" Contract No. EVK3-CT-2000-00038, Liquefaction Around Marine Structures (http://www.isva.dtu.dk/limas/public/limas2.html), LIMAS. We would like to thank Professors I. Avci, T. Durgunoglu, A.R. Gunbak, A. Onalp, A. Saglamer, A.C. Yalciner and Y. Yuksel for their advice and generous help.

REFERENCES

Bardet J.-P. et al. (2000). "Soil Liquefaction, Landslides, and Subsidences". Chapter 7, in 1999 Kocaeli, Turkey, Earthquake Reconnaissance Report, *Supplement A to Earthquake Spectra*, Volume 16, T.L. Youd, J.-P. Bardet, J.D. Bray, Eds., pp. 141-162.

Boulanger, R., Iai, S., Ansal, A., Cetin, K.O., Idriss, I.M., Sunman, B., Sunman, K. (2000). "Performance of Waterfront Structures". Chapter 13, in 1999 Kocaeli, Turkey, Earthquake Reconnaissance Report, *Supplement A to Earthquake Spectra*, Volume 16, T.L. Youd, J.-P. Bardet, J.D. Bray, Eds., pp. 295-310.

Chaney, R. C., and Pamukcu, S. (1991). "Earthquake Effects on Soil-Foundation Systems, Part II," in *Foundation Engineering Handbook*, H.-Y. Fang, Ed. pp. 623-672.

Earthquake Spectra (2000). Earthquake of August Reconnaissance Report, *Earthquake Spectra, Supplement* Volume 16.

Gunbak, A.R., Muyesser, O. and Yuksel, Y. (2000). "Damages Recorded at the Coastal and Port Structures around Izmit Bay under the 17th August, 1999 Earthquake", PIANC Buenos Aires Conference, 29.November, 2000, pp. 1-19.

Hyodo, M., Hyde, A. F.L., Yamamoto, Y., and Fujii, T. (1999) "Cyclic Shear Strength of Undisturbed and Remolded Marine Clays" *Soils and Foundation*, Vol. 39, 45-58.

Jeng, D.S. (1997): Wave-induced seabed instability in front of a breakwater. *Ocean Engng.*, Vol. 24, No. 10, 887-917.

Kaya, A. (2001). Impact of Liquefaction on Marine Structures in the 1999 Kocaeli, Turkey Earthquake. Internal Report, Dec. 2001, Tech. Univ. of Denmark, Coastal and River Eng. Section, Building 115, 2800 Lyngby.

Kramer, S.L. (1996). *Geotechnical Earthquake Engineering*. Prentice Hall, Upper Saddle River, New Jersey, xvii + 653.

Lettis W. et al. (2000 a). "Geology and seismicity". Earth Spectra, Chapter 1, in 1999 Kocaeli, Turkey, Earthquake Reconnaissance Report, *Supplement A to Earthquake Spectra*, Volume 16, T.L. Youd, J.-P. Bardet, J.D. Bray, Eds., pp.1-9.

Lettis W. et al. (2000 b). "Surface Fault Rupture". Earth Spectra, Chapter 2, in 1999 Kocaeli, Turkey, Earthquake Reconnaissance Report, *Supplement A to Earthquake Spectra*, Volume 16, T.L. Youd, J.-P. Bardet, J.D. Bray, Eds., pp.11-53.

McDougal, W.G., Tsai, Y.T., Liu, P.L-F. and Clukey, E.C. (1989). "Wave-induced pore water pressure accumulation in marine soils". *J. Offshore Mechanics and Arctic Engineering, ASME*, Vol. 111, 1-11.

NRC (1985). Liquefaction of Soils during Earthquakes, National Research Council Report CETS-EE-001, National Academic Press, Washington, D.C.

Safak E. et al. (2000). "Recorded Main Shock and Aftershock Motions". Chapter 5, in 1999 Kocaeli, Turkey, Earthquake Reconnaissance Report, *Supplement A to Earthquake Spectra*, Volume 16, T.L. Youd, J.-P. Bardet, J.D, pp. 97-112.

Sumer, B.M. and Fredsøe, J. (2002). *Mechanics of Scour in the Marine Environment*. World Scientific, ix + 536 p. In print.

Sumer, B.M., Fredsøe, J., Christensen, S. and Lind, M. T. (1999). "Sinking/Floatation of pipelines and other objects in liquefied soil under waves". *Coastal Engineering*, Vol. 38, 53-90.

Taymaz, T. (1999). "On the Seismotectonics of the Marmara Region: Source Charecteristics of 1999 Golcuk, Sapanca, Duzce Earthquakes," *Proc. of Int. Conf. On Earthquake and Risk in The Mediterranean Region*, Vol. 1, pp. 55-76.

Yalciner, A.C. et al. (2000). "Tsunami Waves in Izmit Bay", Chapter 3, in 1999 Kocaeli, Turkey, Earthquake Reconnaissance Report, *Supplement A to Earthquake Spectra*, Volume 16, T.L. Youd, J.-P. Bardet, J.D. Bray, Eds., pp. 55-62.

Youd, T. L., and Idriss, I.M. (2001). "Liquefaction Resistance of soils: Summary report from the 1999 NCEER and 1998 NCEER/NSF Workshops on Evaluation of Liquefaction Resistance Soils" *J. Geotech. And Geoenvir., ASCE*, Vol. 127, pp. 297-313.

Yuksel Y. et al. (2000). Effects of the Eastern Marmara Earthquake on Marine Structures and Coastal Areas. Report I, February 2000, Yildiz Technical University, Civil Engineering Faculty, Yildiz, Istanbul. In Turkish.

Yuksel, Y., Alpar, B., Yalciner, A., Cevik, E., Ozguven, O., and Celikoglu, Y. (2001). "Effects of the Eastern Marmara Earthquake on the Marine Structures and Coastal Areas". To appear in the *Proceedings of the Institution of Civil Eng. (ICE), Water and Marine Eng. Div.*, UK.

Table 1. "Inventory" of the damage to coastal structures caused by liquefaction in the 17. August, 1999 Kocaeli, Turkey earthquake.

No (1)	Name (2)	Structure (3)	Damage? (4)	Damage caused by liquefaction? (5)	Comments (6)	Reference (7)
1	Tuzla Port	Block-type quay wall with coarse limestone backfill	Yes	No?	• Quay wall was displaced seaward by O(40 cm). • Backfill settled by O(10 cm). No direct evidence of liquefaction (i.e., no sand boils)	Boulanger et al. (2000)
2	Tuzla Shipyard	A. Rubble-mound breakwater	No			Gunbak et al. (2000)
		B. Block-type breakwater	No			
		C. Block-type quay wall	Yes	Yes?	• The backfill area settled by O(20 cm). • Two rows of blocks between –1.7 m and –6 m depth moved seaward relative to neighboring blocks by O(20 cm).	
3	Eskihisar Ferry Terminal	A. Block-type quay wall	Yes	Yes?	• The backfill area settled by O(1-2 cm).	,,
		B. Sheet-piled structure	Yes	Yes?	• A sink hole of O(20 m^2) was observed behind the sheet piled structure	,,
4	Eskihisar Fishing Harbour	A. Rubble-mound breakwater	Very slight damage	No?		,,
		B. Block-type quay wall	,,	,,		
5	Rota Navigation Trade Pier	Pier supported on steel pipe piles	No		• Diver inspection showed O(70 cm) settlement of the seabed. No settlement of / damage to the piles.	,,
6	Petkim (Yarimca Petrochemical Complex)	Pier supported on reinforced-concrete piles, and two loading dolphins supported on reinforced concrete piles and two on steel-pipe piles	Yes	No?	• Reinforced concrete piles were damaged above the water surface. • The pier head experienced O(5-10 cm) sinking relative to the access trestle. Furthermore, lateral movements of O(40 cm) were also experienced.	Boulanger et al. (2000) and Visit by the present authors, 1-9. July, 2001
7	Tupras Refinery	Pier supported on steel pipe piles. The piles filled with concrete.	Yes	No	• Steel piles were buckled at/above the water surface. • Ground deformations and cracking along the shoreline were observed near the pier.	Boulanger et al. (2000) and Gunbak et al. (2000)
8	Derince Port	A. Block-type quay wall (Berths 6 through 8)	Yes	Yes	• The quay walls were displaced towards the sea by O(0.1-0.5m). • The backfill area settled by O(0.5-1 m). • There were very clear indications of liquefaction of the backfill area (and also in and around two warehouses located in this area), in the form of sand boils; Sand volcanoes the size O(30 cm) were observed very clearly.	Boulanger et al. (2000), Gunbak et al. (2000) and Visit by the present authors, 1-9. July, 2001
		B. Quay wall with steel-pile-supported deck and sheet-pile wall (Berths 3 through 5)	Yes	Yes?	• Minor damage at pile caps in some small number of piles. • The backfill area settled. No sand boils were observed, however.	
9	Derince Port, TMO Silos	Pile-supported, large, 95.000 ton capacity silos near the shoreline	Very minor	Yes?	• A large reclamation area in front of the silos settled (by O(1.5-3 m)). However, practically no damage occurred to the silos except there is a very minor damage at the top of the corner pile in the first row at the seaside.	Boulanger et al. (2000) and Visit by the present authors, 1-9. July, 2001

10	Petrol Ofisi	A. Old pier: Pier supported on reinforced concrete piles, the piles being almost entirely in the soft soil	Yes	No?	• The pier was tilted and displaced laterally (away from the new one), and one segment of the pier settled by O(7 cm). • The sea bottom settled. • Divers reportedly did not feel safe near the sea bottom because the sediment appeared unstable.	Boulanger et al. (2000) and Gunbak et al. (2000)
		B. New pier: Pier supported on reinforced concrete piles for the first 60 m, and on steel-pipe piles for the outer 100 m, constructed near the old pier and parallel to it, the piles penetrating into the stiff soil	Virtually none			
		C. Tanks near the shoreline	Yes	Yes?	• One of the two tanks, full at the time of the earthquake, tilted O(2-3%). • Ground cracking and deformations were visible in the fill between the tanks and the shoreline wall.	
11	Shell Oil Piers	Two piers supported on steel-pipe piles; 18 m by 12 m dolphin on steel piles; Fill area of 5 m by 57 m, encircled by reinforced concrete sheet piles	Yes	?	• The piers were extensively damaged and largely collapsed below water. • The fill area collapsed below water • The dolphin also collapsed below water. • A large rupture hole was observed in the seabed at the tip of the pier; this hole was later filled with sediment due to natural processes.	Boulanger et al. (2000), Gunbak et al. (2000) and Visit by the present authors, 1-9. July, 2001
12	Klor Alkali	Pier supported on reinforced concrete piles	Yes	Yes?	• The pier largely collapsed below water. • Storage tanks near the shoreline tilted.	Yuksel et al. (2000) and Kaya et al. (2001)
13	Transturk	Two piers supported on steel-pipe piles	Yes	?	• One of the piers largely collapsed below water. • The other pier remained intact. • One of the tanks closest to the shoreline was visibly tilted.	Boulanger et al. (2000)
14	Izmit Yacht Harbour (Public Marina)	Quay walls made up of 24 m long concrete segments supported on four row of piles, the inner three rows of piles being reinforced concrete and the outer row consisting of closely spaced concrete-infilled steel pipe piles	Yes	Yes?	• The backfill area adjacent to the shoreline section settled by as much as O(80 cm) due to liquefaction. • One segment of the wall was displaced towards the sea by O(10 to 30 cm). • Separation between neighboring segments of O(3 to 8 cm) was observed. • Piers extending perpendicular to the quay wall experienced a separation of O(3 cm) at the wall ends.	Boulanger et al. (2000), Gunbak et al. (2000) and Visit by the present authors, 1-9. July, 2001
15	UM Shipyard	Pier supported on steel pipe piles	Yes	Yes?	• The pier was completely damaged and collapsed below water. According to eyewitnesses, the collapse was gradual, implying that the failure was likely due to liquefaction, slope instability or both. • The fill area containing part of the ship yard on the shore settled over an area of O(50 m) and disappeared into the sea, the settlement being O(1 m) near the shoreline. • The 510-ton shipyard crane survived the earthquake with minor damage.	Boulanger et al. (2000), Gunbak et al. (2000) and Visit by the present authors, 1-9. July, 2001
16	Golcuk Naval Base	A. Seven piers supported on reinforced concrete piles	Yes	?	• Extensive damage due to surface rupture and ground failure, or a combination of both. Note that the fault rupture, involving as much as 5.5 m right-lateral slip and 2.5 m local vertical displacements (Earthquake Spectra, 2000, Chapter 2), ran through the Golcuk Naval Base, see Fig. 3.	Boulanger et al. (2000) and Gunbak et al. (2000)

		B. Sheet-piled quay wall	Yes	?	• Extensive seaward deformation of the sheet piling due to surface rupture and ground failure. • The backfill settled by O(1 m).	
		C. Dockyards	Yes	?	• Extensive damage due to surface rupture and ground failure, or a combination of both.	
17	Karamursel Eregli Fishing Harbour	A. Rubble-mound breakwater	Very slight damage	?	• A differential movement between the neighboring wave screens of O(10 cm).	Gunbak et al. (2000)
		B. Block-type quay wall	Yes	Yes?	• Crack between the crown wall and backfill of O(30 cm). • The backfill area settled by O(25 cm).	
18	Topcular Ferry Pier	Two piers supported on steel pipe piles	Yes	Yes?	• The fill area settled by O(15 cm).	,,
19	Aksa Piers and Dolphins	Two trestles supported on reinforced concrete piles and six dolphins supported on steel pipe piles	Yes	?	• One trestle was displaced laterally by O(25 cm). • The other trestle largely collapsed below water. • Four dolphins collapsed below water.	,,
20	Cinarcik Fishing Harbour	Rubble-mound breakwater		?	• Crack of width O(30 cm) along the breakwater crown wall near the backfill area. • Concrete slabs in the backfill area were separated (O(15 to 20 cm)) by swelling and sinking.	,,
21	Cinarcik Passenger Pier	Pier supported on steel piles	No			,,
22	Korukoy Pier	Pier supported on reinforced concrete piles	No			,,
23	Kocadere Motor Pier	?	No			,,
24	Esenkoy Fishing Harbour	A. Rubble-mound breakwater	Minor damage	?	• Cracks along the crown wall	,,
		B. Block-type quay walls	Yes	Yes?	• The backfill settled by O(3 cm)	

Danish Society of Hydraulic Engineering
Seminar on Dynamic Loads to Stone Bed Foundations – from Offshore Wind Turbines to Earthquake

20 March 2003. The Technical University of Denmark, Lyngby

SOIL REACTIONS IN SATURATED SAND TO IMPULSIVE LOADS

by

N.-E. Ottesen Hansen
LICengineering A/S

ABSTRACT

The decisive force scenarios in marine engineering are often impact loads such as ship impact or wave slamming. It is demonstrated that if the soil comprises saturated sand the ultimate reaction is decided by the interaction of soils rupture and pore water flow, both for compressive sand and for dilatant sand. Effective stresses and the pore pressure will contribute to the reaction.

A methodology has been developed based on the equilibrium theory as a practical method to analyse the problem. An example of a laterally loaded pile is used to demonstrate the effects. Even though realistic soils parameters will usually be difficult to obtain for a refined calculations, it is concluded that the dynamic soil reaction may be increased several times over the static values for normal saturated sands.

INTRODUCTION

It is common knowledge that the soil under impact loading normally will produce reactions, which exceed the static capacity. However, this fact has not been used often in engineering practice.

It has, however, been used for the ship impact protection of the Great Belt and the Øresund fixed links, Simonsen, 1993, Ottesen Hansen et al 1994, Simonsen and Ottesen Hansen 1998. An extensive series of tests both in laboratory but also in full scale showed that the dynamic reactions exceeded the static reactions with order of magnitudes. The results from these tests and analyses can be used on other problems.

In order to understand the physical mechanism some of the tests, made for the ship impact protection, are particularly illustrative, Ottesen Hansen, et al, 1994. A ship with cylinder bow with vertical sides was rammed horizontally into a submerged slope of sand of 1:6, Figure 1. The bow had a semi-circular shape with a radius of r = 378 mm. The bottom was flat. The sand was very uniform in gradation with a mean diameter of 0.125 mm, permeability coefficient $9 \cdot 10^{-5}$ m/s, and frictional angle of estimated 39^0. The ship was rammed with constant velocity and it was locked in the horizontal position such that it could not heave or pitch.

In Figures 2 and 3, respectively, the resulting horizontal forces and vertical forces for different impact velocities are presented as a function of horizontal position for a ship with cylindrical bow rammed into a slope of 1:6. The soil reactions are shown for tests in both dry sand and submerged slopes of different impact velocities.

The horizontal resisting force and the lifting force on the bow depends on the velocity. The force is 10-20 times larger than the resisting force for the identical tests performed out of water where the bow is rammed into the same slope of dry sand, Figure 2.

Therefore the porewater flow generated by the bow during the impact must have great influence on the reaction in the soil. The porewater flow creates strong effective stresses in the soil, which act on the hull both as normal stresses and as tangential stresses. It is then the question of how these effective stresses are generated. There seem to be two possible mechanisms to choose:

1. At the rupture the sand will dilatate and thereby create a large suction in the porewater in the rupture zone. This suction will result in corresponding larger effective stresses in the grain skeleton.

2. At the impact the sand will be compressed and porewater will be squeezed out in the compression zone creating an additional pore water flow. This porewater flow will build up large effective stresses in areas of the grain skeleton. In other areas liquefied zones will be formed.

Which of the two mechanisms were correct was decided by investigating the vertical lift on the ship bow. This lift must partly be caused by friction on the front and partly of the porewater pressure at the bottom of the model ship. From Figure 3 it can be seen that there was a relatively large lift on the bow. Consequently there must have been an excess pore pressure underneath the bow. This indicated that the impact follows the mechanism, 2, where the sand skeleton was compressed and the porewater squeezed out.

The pressure generated by the porewater was further demonstrated by establishing a vertical downwards directed porewater flow through the sand (originally made to compact the laboratory sand), Figure 4. This drainage reduced the initial pore pressure with depth. Figure 4 shows the difference between the lift on the ship bow with and without the additional vertical porewater flow. The important finding was that even though the initial pressure underneath the bottom of the model ship is reduced, still a lift was generated. This proves that excess pore pressures were generated by the impact.

Parallel with the beaching a method of analysis was developed for predicting the behaviour of a ship beaching on a sand slope. They included soil mechanics rupture calculations, Simonsen 1993. The methodology reasonably and successfully predicted the beaching behaviour of a trawler being sailed into a sand beach, Figure 5, Ottesen Hansen et al, 1994, Simonsen and Ottesen Hansen, 1998. It confirmed that both the "footprint" of the ship in the beach and the friction between keel and bow was reasonably correct.

The same behaviour of saturated sand was reported by Palmer, 1999, in connection with burying of marine pipelines in sand by ploughing. The soil reactions on ploughs were dependent on plough dragging speed, the higher dragging speed, the higher reaction. He advocated for the dilatation mechanism to be responsible for the increased resistance.

For cohesion material effects of dynamics have been considered by Ibsen and Jacobsen 1997.

The decisive loading for marine structures is often impact loading from ships or from wave slamming. Hence, the soil mechanics problems should also be solved using dynamic methods.

The already developed methods can be used to a certain degree. The reason is that they suffer from some drawbacks. The main drawback of the above method is that the interaction between dilatant and compression behaviour was not stringently represented. For foundation problems this is necessary. The implications will be considered in the following.

GOVERNING EQUATIONS

Sand is an elastic-plastic material, which may dilate or contract depending on the relative density. The order of magnitude for the Young Modulus of sand is $E_{sand} \sim 2\text{-}20 \cdot 10^7$ N/m^2, depending on surrounding pressure or previous over-consolidation.

Water, on the other hand, has an E modulus of $2 \cdot 10^9$ N/m^2 . Hence, it is far stiffer than the grain skeleton.

Loading a completely saturated sand volume impulsively will result in a changed pore pressure depending on the draining time and on how the sand behaves. The sand may contract or it may dilate. In both cases it will result in pore water movements.

In case of compression pore water will be squeezed out like water from a sponge. In case of dilatation the water volume will suck water from neighbouring soils volumes.

The process is illustrated for a deeper end of a vertical pile impulsively moved laterally, Figure 6. Hence, it can be seen that the following events take place at the impact:

1. The formation of a passive rupture zone.
2. A compression of the soils skeleton and squeezing out of the water.
3. A progressive development of the rupture changing the soils density in the process.

The effect no. 2 corresponds to the traditional consolidation process, whereas the effect no. 3 is a progressive process.

For dilatant sand the process is the same but with opposite sign. However, it starts by compression but ends with dilatation. In this case the porewater flow is reversed.

In order to analyse such problems and determine the passive pressure zones the traditional rupture theory has to be modified with the influence of the pore water flow.

The analytical equations valid for the process are the socalled Biot equations, Sumer and Fredsøe, 2002, coupled with a rupture criterion. In principle these equations can be used, but this is very cumbersome. Instead, an approximate rupture calculation is developed. As framework the equilibrium method developed by J. Brinch Hansen, 1953, has been further modified.

The equation for the shear stress, τ, in a circular rupture line with porewater flow has been given by Simonsen, 1993.:

$$\frac{\partial \tau}{\partial v} + 2\tan\varphi\tau + \gamma' r\sin(v+\varphi)\sin\varphi - \sin^2\varphi\, r\frac{\partial p}{\partial r} + \sin\varphi\cos\varphi\frac{\partial p}{\partial v} = \rho a_v r\sin\varphi\cos\varphi$$

in which p is the pore pressure in the rupture line. The definition sketch for the parameters is shown in Figure 7. The acceleration term on the right hand side can be neglected for practical problems. The equation is a modified from of the Kötter equation.

The interesting terms are contribution from the pore water flow. In order for the shear stress to grow $\frac{\partial \tau}{\partial v} < 0$ due to the sign convention.

$$\tan\varphi\frac{\partial p}{\partial r} - \frac{\partial p}{r\partial v} < 0$$

So either there should be a radial outwards flow $\left[\frac{\partial p}{\partial r} < 0\right]$, a clockwise flow or $\left[\frac{\partial p}{\partial v} > 0\right]$ or combinations of these flows in order to obtain increased reactions.

If the porewater flow does not observe the above criteria with respect to the rupture line the shear stress may vanish, i.e. liquefaction is formed in the rupture line.

The rupture lines are of course not simple circles. However, it has been shown by Brinch Hansen, 1953, that combining up to 4 consecutive rupture circles observing the boundary conditions, an upper bound approximate solution for the soils reaction can be found.

The complication in the present application is that the associated porewater flow has to be determined. The compression or dilatation of the soils skeleton at impact and the progressive movement of the rupture zones are a consolidation problem. It is calculated as follows:

- Assume a rupture zone.
- Determine the deformations inside the soils bodies or rupture zones by elastic theory or by knowledge to the sands stress/strain relationship.
- Perform consolidation analysis for the soils by means of the Biot-equations.
- Check whether the results fit the initial assumptions.
- Correct rupture zones.
- Repeat calculations.
- Repeat calculations until convergence is achieved.

THE STRESS/STRAIN RELATIONSHIP OF SAND

Stress/strain relationships for sands are presented in Figures 8, 9 and 10. It is seen that:

- Loose sand is compressive
- Dense sand is dilatant at low surrounding pressures, but can be more and more compressive for increasing surrounding pressure.

Hence, the behaviour will be highly dependent on the relative density of the sand.

LATERALLY LOADED PILE

As an example a laterally loaded Ø 1.3 m pile in 3 m of water is considered. The pile is placed in a frictional material with $\gamma' \equiv 10$ kN/m^3 and $\varphi = 35^0$ to a depth of 5.4 m, Fig. 11. The example has been given by Brinch Hansen, 1961. He determined the lateral capacity for a force acting 5 m above the sea bottom to 240 kN.

The calculations were made with the following soils pressure coefficient, determined by Brinch Hansen:

$$K \sim \frac{K^0 + K^{\infty}\alpha \cdot \frac{z}{D}}{1 + \alpha \cdot \frac{z}{D}}$$

$$\alpha \sim \frac{K^0}{K^{\infty} - K^0} \frac{K_0 \sin\varphi}{\sin(45^0 + \varphi/2)}$$

in which

$$K^0 = \exp\left[\left(\frac{\pi}{2} + \varphi\right)\tan\varphi\right]\cos\varphi \tan\left(\frac{\pi}{2} + \frac{\varphi}{2}\right) - \exp\left[-\left(\frac{\pi}{2} - \varphi\right)\tan\varphi\right]\cos\varphi \tan\left(\frac{\pi}{2} - \frac{\varphi}{2}\right)$$

$$K^{\infty} = \left[\exp[\pi(\tan\varphi)]\tan^2\left(\frac{\pi}{4} + \frac{\varphi}{2}\right) - 1\right](1.58 + 4.09\tan^4\varphi)(1 - \sin\varphi)$$

Now consider the example where the sand is dilatant, and a very strong impulsive force is applied forcing the tip to move with a velocity of 2 m/s.

Dilatant behaviour means that the porewater will have to flow towards the pile. Hence, the porewater pressure along the pile must be at a minimum. An upper value for the effect can be calculated in the event that the speed of the forcing of the top of the pile is so high that the pore pressure is lowered to the absolutely lowest value, which is the cavitation pressure for water –1 bar. This low porewater pressure can be achieved at the bottom of the pile and the pore pressure will vary linearly to the seabed. Since the total stresses shall remain constant this means that the effective stresses must increase corresponding to the original porewater pressure plus the new pressure with cavitation pressure at the bottom. The effective stress distribution remains the same but all the effective stresses are increased with a factor 4.4 (from 54 nN/m^2 to 238 kN/m^2 at the pile tip). Hence, the soil resistance increases with a factor 4.4 for this extreme condition. The total reaction can reach 1056 kN.

Now let us turn to the case where the sand is assumed to be loose. Assume $G \sim 2 \cdot 10^7$ N/m^2 and the permeability factor $k \equiv 10^{-4}$ m/s.

Further, making the very conservative assumption that the initial compression of the grain skeleton is made with a pressure corresponding to the steady state passive pressure the contribution from the porewater flow can be calculated using the methodology outlined in the previous chapter. The calculations have to be done numerically.

The results of the calculation are presented in Table 1:

z m	σ'_s kN/m^2	u m/s	σ'_m kN/m^2	P kN/m^2	σ kN/m^2	Increase factor
0	0	0.92	0	0	0	1
1.08	93	0.68	17	320	430	4.6
2.16	214	0.44	25	480	719	3.4
3.24	363	0.21	21	380	764	2.1
4.32	531	~0	0	0	531	1
5.60	718	-0.27	52	990	1760	2.5

Table 1 Soils pressure due to pore flow generated by rupture.

From the Table 1 it is realised that the resulting stresses acting on the pile are increased with a factor 2.5 in the bottom whereas the increase is around 3-5 in the upper part of the soil. The conditions around the point of rotation is not very well determined neither in the static calculation nor in the dynamic calculation. The increase in soil reaction to the load is around a factor 3 for the particular example.

DISCUSSION

It is remarkable to note that a dense sand assumption and a loose sand assumption results in a dynamic reaction of several time the static reaction of the soil.

Even though a very detailed set of soils parameters in principle will be necessary for a calculation and that these parameters in practice only can be obtained with large efforts it can be concluded that this background knowledge may not be so important after all. In practice the calculation whether a loose soil approximation or a dense soil approximation is used will result in dynamic reactions several times those of the static reactions. This will be sufficient for many practical engineering impact calculations.

ACKNOWLEDGEMENTS

The results are preliminary results of the EU Framework 5 project EVK3-CT-2000-00038 LIMAS (Liquefaction in Marine Structure) managed by Dr. Mutlu Sumer, ISVA, Technical University of Denmark.

The contribution is gratefully acknowledged. The project shall be completed mid 2004.

Part of the project will be experimental verification of the consolidation processes in order to verify the analytical means.

LIST OF PARAMETERS

a_v	:	Acceleration angular direction	u	:	Transverse velocity of pile
D	:	Diameter	v	:	Angle
D_r	:	Relative density of sand	z	:	Vertical coordinate
E	:	Young Modulus	α	:	Coefficient
g:	:	Gravitational acceleration	γ'	:	Effective weight of soil
G	:	Shear modulus	ε_q	:	Shear strain
k	:	Permeability coefficient	ε_v	:	Volume strain
K	:	Earth pressure coefficient	φ	:	Frictional angle
K_o	:	Coefficient horizontal pressure at rest	ρ	:	Density of water
K^{∞}	:	Earth pressure coefficient infinite depth	σ'	:	Effective soil stress
K^0	:	Earth pressure coefficient at soil surface	σ'_s	:	Steady state passive soil pressure
r	:	Radius of rupture circle	σ'_m	:	Effective soil stress generated by porewater flow
p	:	Porewater pressure	σ	:	Total stress on pile
			τ	:	Shear stress

REFERENCES

Aylin, A, and S. Krenk, 1999: Characteristic State Plasticity for granular Materials. Danish Center for Applied Mathematics and Mechanics, Report No. 619. Technical University of Denmark. May 1999.

Hansen, J. Brinch, 1953: Earth Pressure Calculation. The Danish Technical Press. The Institution of Danish Civil Engineers, Copenhagen, 1953.

Hansen, J. Brinch, 1961: The ultimate Resistance of rigid Piles against transversal Forces. Bulletin No. 12. The Danish Geotechnical Institute, Copenhagen. 1961.

Ibsen, L.B. and K. P. Jacobsen, 1997: Dynamic Bearing Capacity of Caisson Breakwaters subjected to impulsive loading. MAST III (PROVERBS) Workshop, Las Palmas, Spain 18-23 Feb. 1997.

Ottesen Hansen, N.-E., B.C. Simonsen and M.J. Sterndorff, 1994: The Soil Mechanics of Ship Beaching. Proceedings of the 24th International Conference on Coastal Engineering, Kobe, Japan, 1994.

Palmer, A.C: 1997: Speed Effects in cutting and ploughing. Geotechnique 49, No. 3, 285-294.

Simonsen, B.C. 1993: The Mechanics of Beaching (in Danish). M.Sc. Report. Department of Ocean Engineering. The Technical University of Denmark. August 1993.

Simonsen, B.C. and N.-E. Ottesen Hansen, 1998: Protection of Marine Structures by Artificial Islands. Ship Collision Analysis. Gluver/Olsen (eds.) 1998 Balkema, Rotterdam, ISBN 9054 10962 9.

Sumer, B.M. and J. Fredsøe, 2002: The Mechanics of Scour in the Marine Environment, Advanced Series on Ocean Engineering – Volume 7. World Scientific ISBN: 981-02-4930-6.

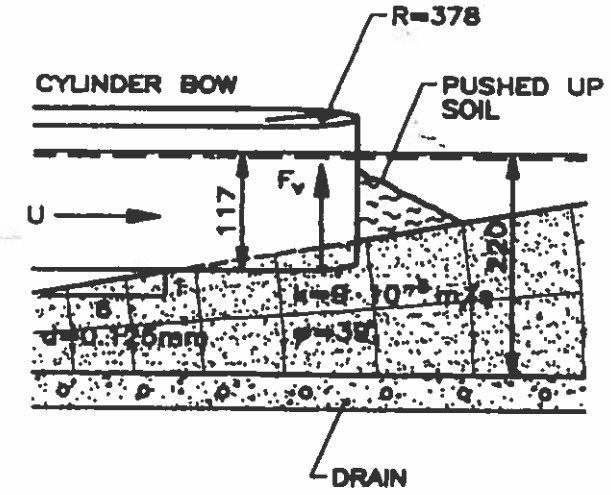

Fig. 1 Scale model test with cylinder bow beam rammed into sand slope. Lengths in mm.

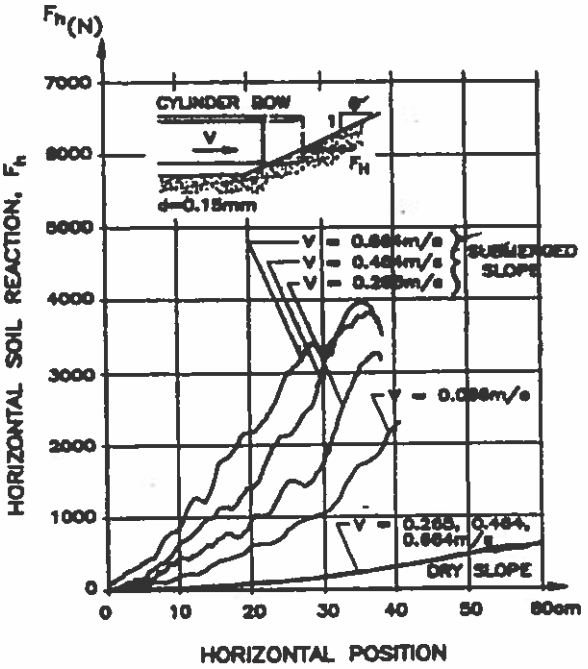

Fig. 2 Horizontal force on ship bow from test in Fig. 1.

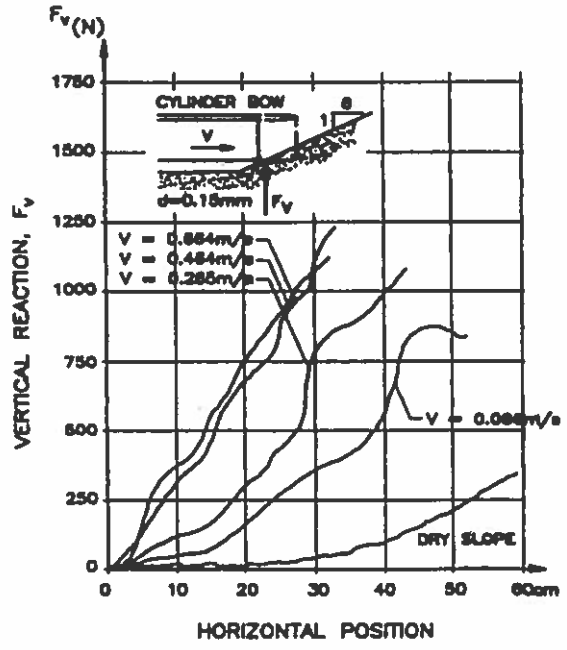

Fig. 3 Vertical force on curved part of ship bow from tests in Fig. 1.

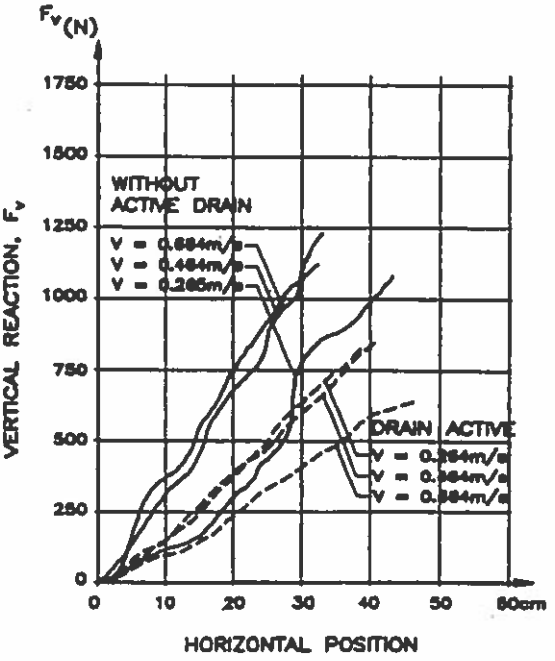

Fig. 4 Vertical force on curved part of ship bow from tests in Fig. 1 with a downward directed seepage in the sand slope.

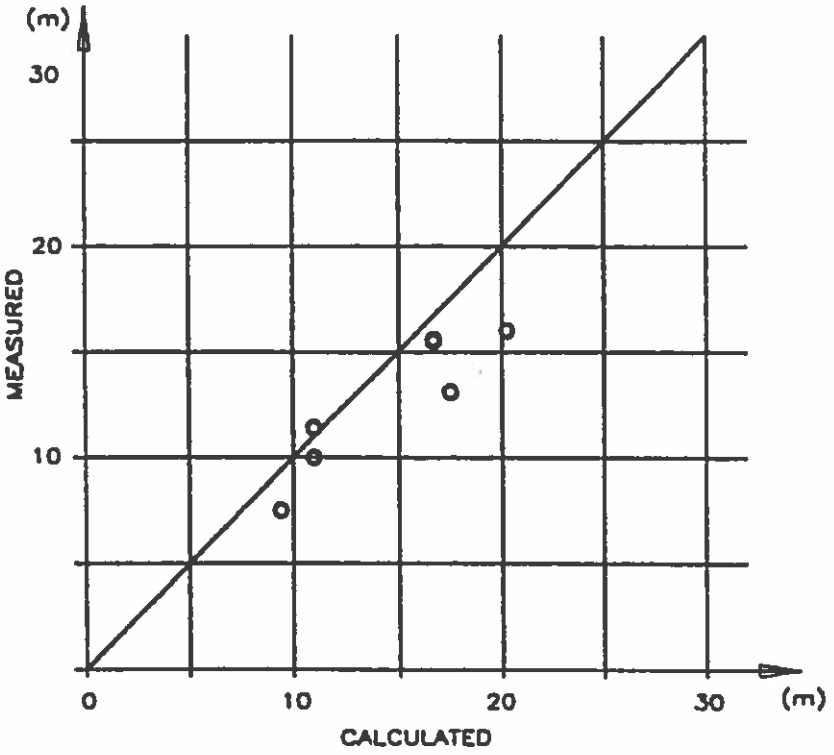

Fig. 5 Measured and predicted run-up distances (from point of contact) on a beach of a 300 DWT trawler being sailed into a beach.

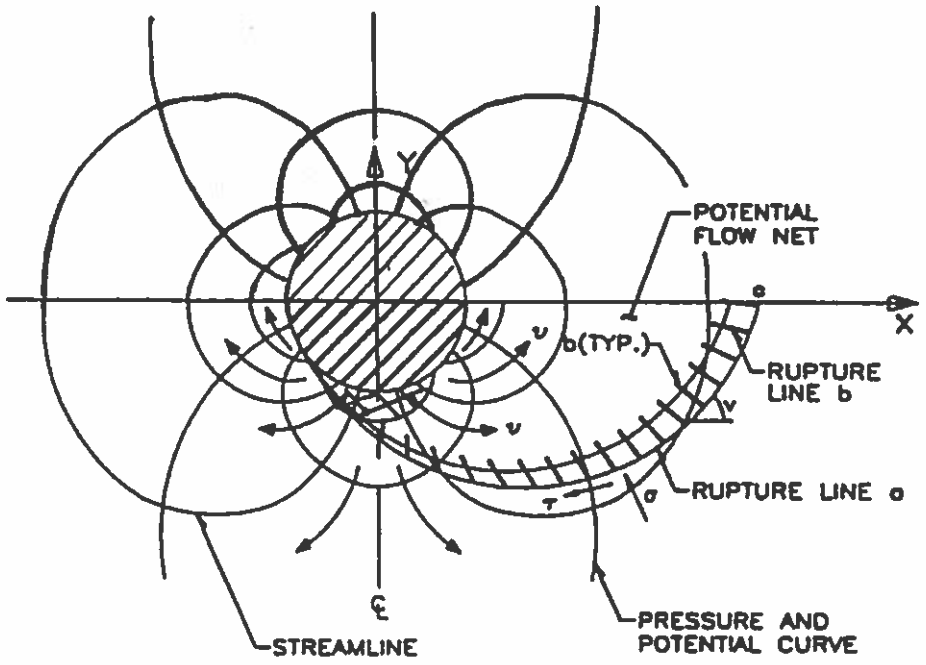

Fig. 6 Vertical pile in saturated sand moved laterally impulsively. Conditions far away from soil surface.

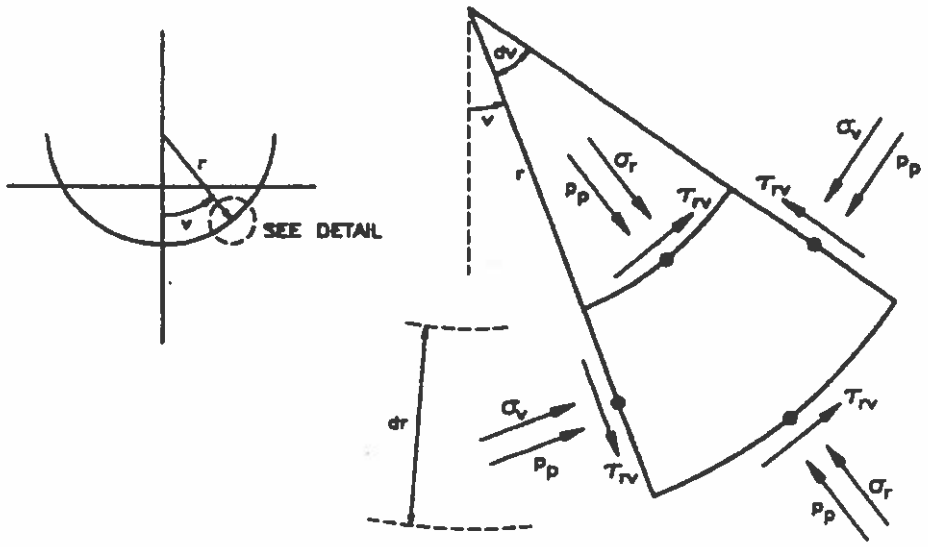

Fig. 7 Coordinate system for circular rupture line, Simonsen 1993.

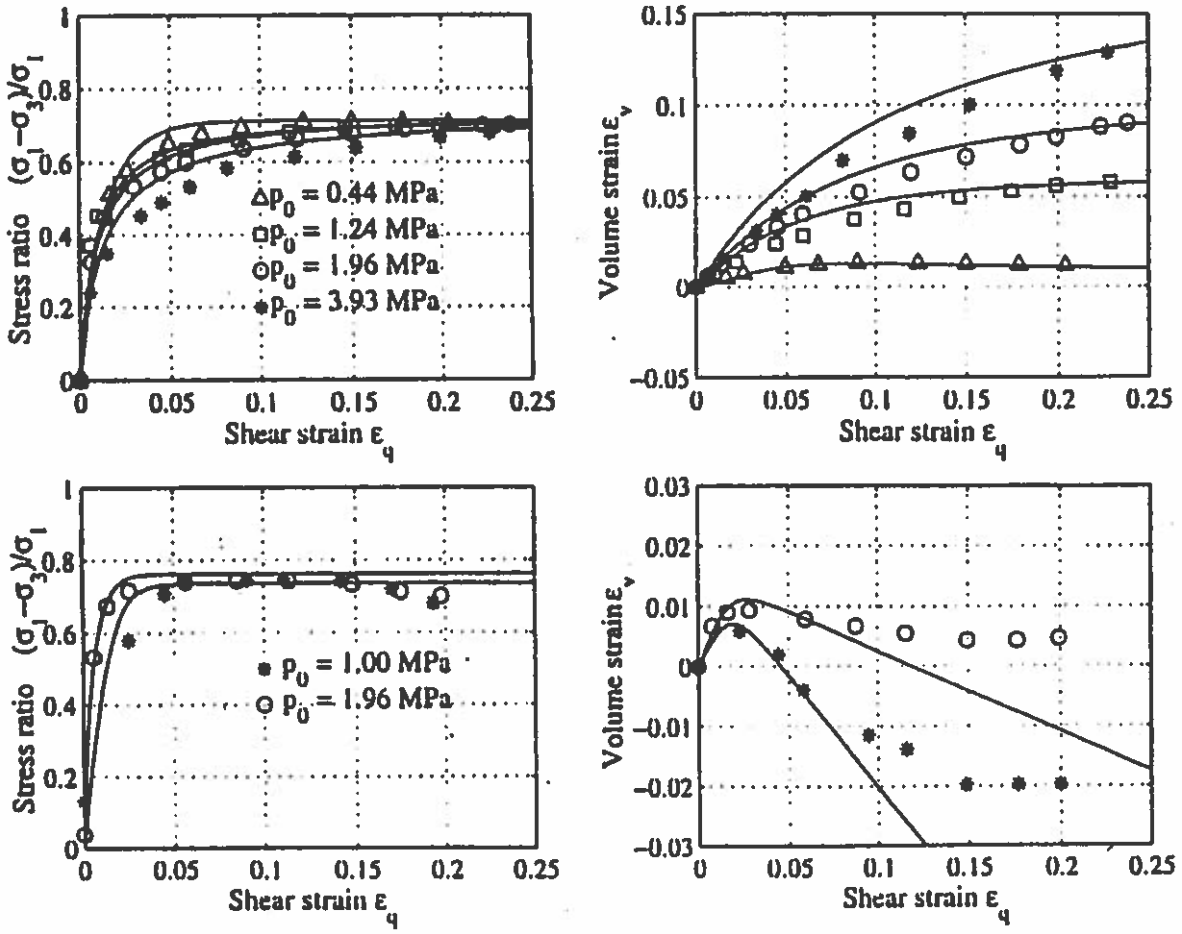

Fig. 8 Theoretical and experimental stress ratio and volumetric strain for loose (top) e = 0.87, G = 12-108 Mpa, and dense, (bottom), e = 0.61, G = 68-128 Mpa, Sacramento sand. Aylin and Krenk, 1999.

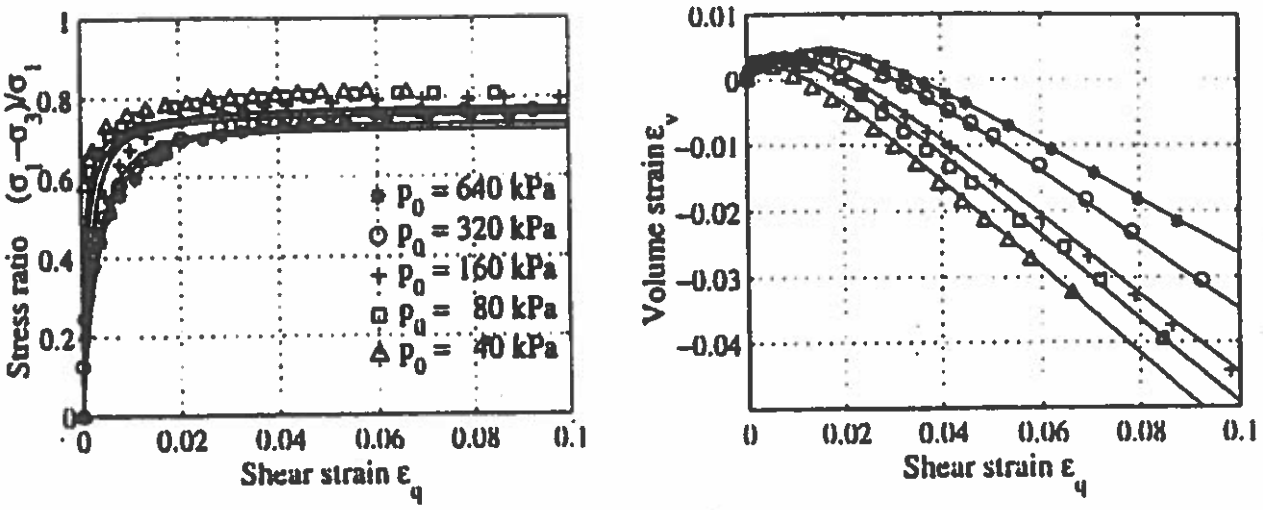

Fig. 9 Theoretical and experimental stress ratio and volumetric strain, Lund Sand, e = 0.57, G = 15-47 Mpa. Aylin and Krenk, 1999.

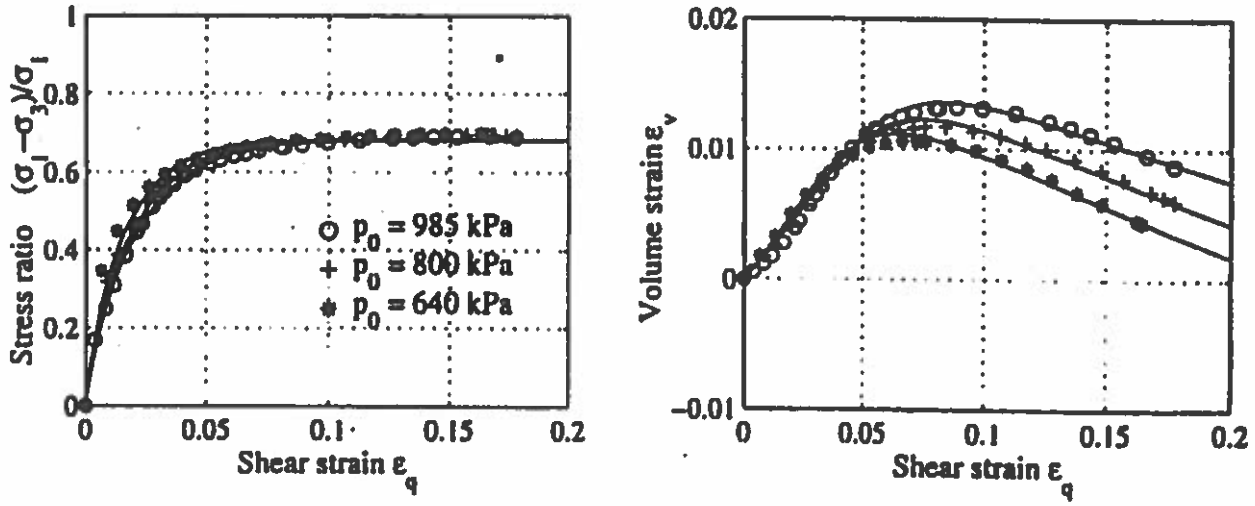

Fig. 10 Theoretical and experimental stress ratio and volumetric strain. Baskarp sand, e = 0.85, G = 12-14 Mpa. Aylin and Krenk, 1999.

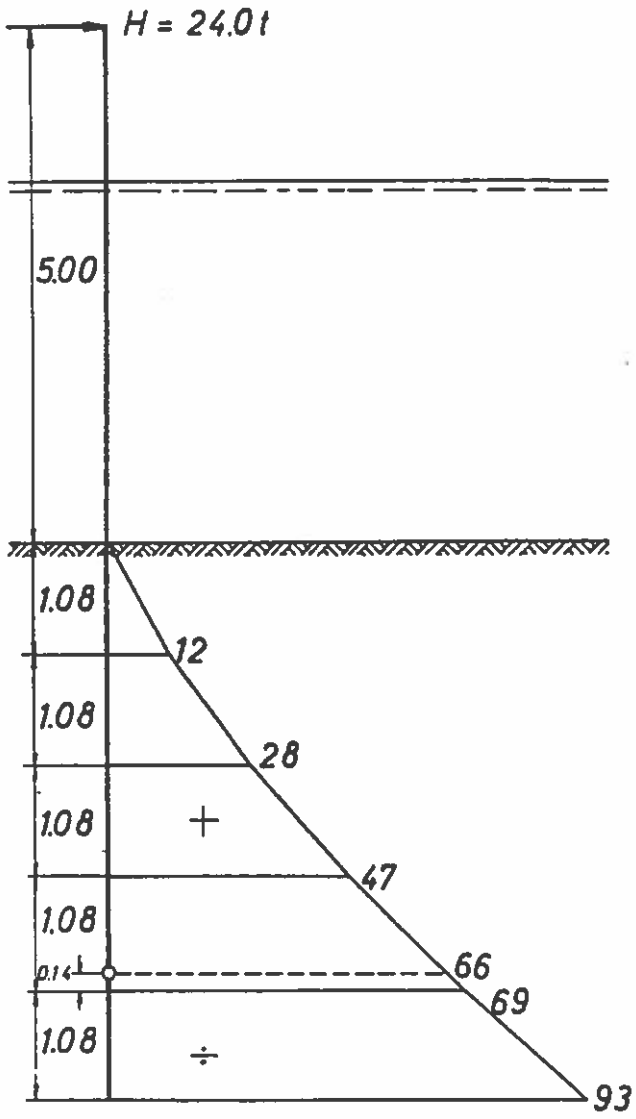

Fig. 11 Example of static loads laterally loaded pile. Pile diameter 1.3 m. Brinch Hansen, 1961.